

AMERICAN UNIVERSITY OF BEIRUT

EVALUATION OF DIFFERENT OSTEOTOMIES IN
SURGICALLY ASSISTED RAPID PALATAL EXPANSION: A
FINITE ELEMENT ANALYSIS STUDY

By
PERLA JALIL RIACHY

A thesis
submitted in partial fulfillment of the requirements
for the degree of Master of Science
to the Department of Dentofacial Medicine
of the Faculty of Medicine
at the American University of Beirut

Beirut, Lebanon
April 2023

AMERICAN UNIVERSITY OF BEIRUT

EVALUATION OF DIFFERENT OSTEOTOMIES IN
SURGICALLY ASSISTED RAPID PALATAL EXPANSION:
A FINITE ELEMENT ANALYSIS STUDY

By

PERLA JALIL RIACHY

Approved by:



Dr. Joseph G. Ghafari, Professor and Chairman
Department of Dentofacial Medicine

Chairman of Committee



Dr. Kinan G. Zeno, Assistant Professor
Department of Dentofacial Medicine

Advisor and Member of Committee



Dr. Samir A. Moustapha, Associate Professor
Department of Mechanical Engineering

Member of Committee



Dr. Najj Y. Abou Chebel, Clinical Associate
Department of Dentofacial Medicine

Member of Committee

Date of thesis defense: April 26, 2023

ACKNOWLEDGMENTS

I would like to express my deep appreciation to all those who have contributed to this project.

First and foremost, to Dr. Ghafari, who brought the weight of his considerable experience and knowledge to this program in general, and this project specifically. His high standards have made me better at what I do.

To Dr. Zeno's whose devotion as mentor and instructor and whose guidance were crucial in the success of this project.

I would also like to thank Dr. Mustapha for his insight on FEA.

To Dr. Abou Chebel for helping me understand the world of maxillofacial surgeries and fall in love with it.

To Dr. Karam, whose contribution in statistical analysis and reviewing this part of the manuscript was highly appreciated.

To Dr. Ammouri, whose help and advice have been invaluable.

I am also deeply grateful for my fellow residents and the people I now call family.

Lastly but most importantly, words cannot express how blessed I consider myself to be surrounded and supported by my family. Mom, Dad, Lea and my husband Maroun you are my greatest blessing.

ABSTRACT OF THE THESIS OF

Perla Jalil Riachy

for

Master of Science

Major: Orthodontics

Title: Evaluation of Different Osteotomies in Surgically Assisted Rapid Palatal Expansion: A finite element analysis study

Introduction:

Transverse maxillary deficiency (TDM) is a decrease in transverse dimension. The management of this malocclusion differs between skeletally immature patients on whom orthopedic expansion is most easily accomplished before closure of the cranial base and midfacial sutures, and skeletally mature patients to whom surgical procedures have been recommended to facilitate correction of transverse discrepancies. These procedures have conventionally been grouped into 2 categories: segmenting the maxilla during a LeFort osteotomy to reposition the individual segments in a widened transverse dimension, and surgically assisted rapid palatal expansion (SARPE) to avoid dental side effects.

Aims:

- Evaluate the success of a minimally invasive mid-palatal sagittal osteotomy in reducing stress and allowing adequate expansion
- Assess the relationship between bone thickness and the amount of stress generated on the corresponding bone structures during expansion and bone thickness' relationship with the amount of skeletal expansion in the different models/variations of osteotomies
- Evaluate the relationship of stress with the amount of expansion
- Define the model with the maximum amount of expansion
- Assess the relationship of different types and combination of osteotomies with the amount of stress and expansion

Design:

Five distinct scenarios are included in our study, each of which corresponds to a different clinical scenario but all including the same bone-borne expander. 1. The initial setup, in which no cuts were made, is referred to as our control model 2. The second setup incorporates a bone-borne expander and a mid-palatal sagittal osteotomy only, which is considered a minimally invasive SARPE cut. 3. The third setup includes setup 2 with an additional osteotomy at the level of the anterior nasal spine 4. The fourth setup consists of set-up 3 with an osteotomy at the level of the anterior nasal spine and lateral cuts extended 5 mm above the apices of the teeth from the distal of the canine to the mesial of the second molar. 5. The fifth setup includes setup 3 with a LeFort cut with a pterygomaxillary disjunction.

Methods:

In our investigation, we adapted the 3D models of the maxillary arch made by Ammoury et al. Thirteen models were created using the 13 different anatomical variables associated with bone morphology. The cortical bone thickness at the incisors, premolars, and molars, which are each separated into buccal and palatal parts, varies between these models. Each of the 13 models were subjected to the five setups, resulting in a total of 65 distinct models that were used in our study.

Results:

Stress at the mid-palatal area was highest in the control setup ($32\ 006.54 \pm 2984.55$ MPa), then in setup 2, the stress was reduced by half ($16\ 331.88 \pm 2207.93$ MPa) which marks the lowest value of stress recorded at this area. The stresses palatal to the molars and buccal to the incisors, were significantly different between the control and experimental setups and recorded the highest stress in setup 5 (3091.89 ± 991.22 MPa buccal to the incisors and 3091.89 ± 991.22 MPa palatal to the molars). However, in setup 5, the stresses measured at the maxillary extension were the lowest (14.05 ± 9.35) and at the highest at the bone buccal to the incisors (3091.89 ± 991.22 MPa). Expansion increased significantly between each setup from 1 to 5, except between setup 3 and 4 (p -value > 0.005). When performing the mid-palatal osteotomy, the thickness of the bone is not correlated to the amount of expansion. However, more thickness at the level of the palatal bone of the incisors is associated with more stress buccal and palatal to the first molars ($r = 0.681$ and $r = 0.698$ respectively). The amount of expansion obtained is mostly affected by bone thickness in setup 5.

Conclusion:

The minimally invasive mid-palatal cut performed during surgically assisted rapid palatal expansion is the most efficient at reducing stress near the mid-palatal suture which was the area of greatest observed stress. The increase in stress numbers at the farther areas from the suture is caused by a re-distribution of this stress to the whole facial skeleton. Expansion occurs as a V-shape, more anteriorly than posteriorly in all modalities, however, when more expansion is needed posteriorly, a more invasive osteotomy is necessary. The amount of expansion obtained is mostly affected by bone thickness when applying the most invasive osteotomy (LeFort), therefore for a more universal approach, incorporating a mid-palatal cut will leave less room for individual variations to affect the result. In contrast, when performing a LeFort osteotomy, bone thicknesses do not affect stress significantly

TABLE OF CONTENTS

ACKNOWLEDGMENTS	1
ABSTRACT	2
INTRODUCTION	12
1.1 Definition of transverse deficiency o the maxilla	12
1.2 Prevalence	12
LITERATURE REVIEW	13
2.1 Etiology	13
2.2 Methods of Assessment	14
2.2.1 Clinical evaluation	14
2.2.2 Evaluation of study models.....	15
2.2.3 Radiographic evaluation	18
2.2.4 Medical history	21
2.3 Suture growth and anatomy	22
2.3.1 Anatomy.....	22
2.3.2 Methods of assessment of skeletal maturity	26
2.4 Management.....	27
4.4.1 Management in skeletally immature patients	28
4.4.2 Management in skeletally mature patients.....	30
4.5 Expansion appliance during SARPE: Bone borne vs tooth borne expander.....	49
2.5.1 Design of bone-borne appliances.....	50
2.5.2 Contraindications of using bone-borne appliances.....	51
2.5.3 Appliance activation	51
2.6 Finite Element Analysis (FEA).....	52
2.6.1 Principles and applications of FEA in Orthodontics	52
2.6.2 FEA of Surgically assisted rapid palatal expansion.....	53
2.7 Significance.....	62
2.8 Specific Objectives	63
MATERIALS AND METHODS	64

3.1	Materials.....	64
3.2	Methods.....	65
3.2.1	Adaptation of the model to our study	65
3.2.2	Expansion Setups	66
3.2.3	Meshing	75
3.2.4	Finite Element Analysis.....	76
3.3	Statistical analysis.....	82
RESULTS		84
4.1	Comparison between the different setups	84
4.1.1	Stress.....	84
4.1.2	Expansion.....	88
4.1.3	Cortical bone thickness variations across the model	90
4.2	Correlations.....	90
4.2.1	Correlation between stress and expansion Error! Bookmark not defined.	
4.2.2	Correlation between bone thickness and stress..... Error! Bookmark not defined.	
4.2.3	Correlation between bone thickness and expansion Error! Bookmark not defined.	
DISCUSSION.....		94
5.1	Strengths.....	94
5.1.1	Limited osteotomy	94
5.1.2	Individual variation.....	95
5.1.3	Effect of bone characteristics on skeletal expansion	95
5.1.4	Anatomic representation from 3D model	96
5.1.5	Comparison with FEA expansion studies.....	97
5.1.6	Development of the model.....	97
5.1.7	Findings	101
5.2	Correlations.....	106
5.2.1	Correlation between stress and displacement	106
5.2.2	Correlation between bone thickness and displacement	107
5.2.3	Correlation between bone thickness and stress.....	107
5.3	Clinical implications	108
5.4	Limitations and research considerations	109

CONCLUSIONS	111
APPENDIX	112
REFERENCES.....	118

ILLUSTRATIONS

Figure

- 2.1 Diagram elaborating the technique used in the Pont analysis on study models 16
- 2.2 Clinical manifestation of transverse problems. (A) Ideal buccal occlusion; (B) Insufficient buccal overjet; (C) transverse compensation; and (D) open lingual occlusion. Adapted from (K.-J. Lee et al., 2018) 17
- 2.3 The elements of the PA cephalometric analysis. These landmarks can be used to calculate the effective maxillary width and effective mandibular width, and the fronto-lateral lines can be constructed (Adapted from Betts et al., 1995)..... 20
- 2.4 At the midsagittal plane, the bones that make up the mid-palatal suture unite (Picture from Head and Neck Cancer Guide). 23
- 2.5 Stages of mid-palatal suture maturation: (A) Diagrammatic representation of the suture of the infantile period; (B) Histologic frontal section of the infantile suture of a 1-year-old child; (C) Diagrammatic representation of the suture of the juvenile period; (D) Histologic frontal section of the juvenile suture of the 10-year-old boy; (E) Diagrammatic representation of the suture of the adolescent period; (F) Histologic frontal section through the suture of a 12.5-year-old girl. (Image adapted from Melsen, 1975). 25
- 2.7 Schematic drawing of the maturation stages observed in the mid- palatal suture (adapted from (Angelieri et al., 2017)). 27
- 2.8 Banded tooth and tissue-borne appliance; B: banded tooth-borne appliance; C: bonded tooth-borne appliance (adapted from Agarwal, 2010)..... 30
- 2.9 (A) Use of a reciprocating saw to perform the left and right lateral wall osteotomies from the pterygomaxillary junctions to the piriform rims (i). Drawing of the outline of the tooth roots adjacent to the interdental osteotomy (ii). Scoring of the interdental osteotomy only through the labial cortex by using a bur (iii). (iv) Separation of the nasal septum from the maxilla; (B) Separation of the pterygomaxillary junctions using a pterygoid osteotome (arrow); (C) Completion of the interdental osteotomy by means of a piezo surgical blade and performance of the midline palatal osteotomy using a small osteotome (Adapted from Reyneke & Conley, 2020). 37
- 2.10 (A) A bone-borne distractor; (B) Observation of the diastema developing 3 days after activation and (C) 7 days after activation; (C) Consolidation phase after an 8 mm expansion. The expander was locked and acted as a retainer for 4 to 8 weeks; (D) Following the consolidation phase, the orthodontist used the additional space to close the space and align the teeth (Adapted from (Reyneke & Conley, 2020))..... 38
- 2.11 Schematic representation of the facial skeleton. The Piriform aperture is highlighted in yellow, and its dimension is defined by the vertical red line. 40
- 2.12 Schematic representation of the facial skeleton showing the zygomatic – maxillary buttress between the zygomatic and maxillary bones..... 41
- 2.13 Picture of a dry skull (axial view) with an osteotome pointing at the pterygo-maxillary junction. 41

2.14	Surgical field when the osteotomies have been completed (Adapted from (Hernandez-Alfaro et al., 2010)).....	47
2.15	MISMARPE technique. (A) Expander in place; (B) Sub spinal osteotomy and vertical osteotomy; (C) Horizontal osteotomy and intranasal osteotomy; (D) Expander activation and suture.....	48
2.16	Skull base model. The osteotome progresses along the horizontal osteotomy from the pyriform buttress back to the pterygomaxillary junction (Hernández-Alfaro & Guijarro-Martínez, 2013).....	49
2.17	Illustration of the different types of bone – borne expanders: (A) The trans palatal distractor; (B) The Magdenburg palatal distractor; (C) The Rotterdam palatal distractor.	51
2.18	Clinical photographs of the two different types of bone expander: (A) palatal bone-borne device; (B) alveolar ridge bone-borne device (adapted from (Möhlhenrich et al., 2017)).....	53
2.19	The three different types of osteotomies for the SARPE procedure, visualized as blue lines with a thickness of 1 mm, as modelled in the simulations: (A) median osteotomy; (B) additional lateral osteotomy; (C) additional lateral osteotomy with pterygomaxillary separation (adapted from (Möhlhenrich et al., 2017)).....	54
2.20	Stress distributions in the midface with rapid maxillary expansion (5 mm) depending on the surgical procedure (adapted from Holberg et al., 2007).	55
2.21	Von Mises stresses at 3 anatomic structures of the midface with different surgical procedures. (Adapted from (Holberg et al., 2007)).....	56
2.22	(A) Test 1: Le-fort I Osteotomy (B) Test 2: Le-fort I Osteotomy + Para-median Osteotomy (C) Test 3: Le-fort I Osteotomy + Pterygomaxillary separation and (D) Test 4: Le-fort I Osteotomy + para-median Osteotomy and Pterygomaxillary separation (adapted from Zai et al., 2015).....	57
2.23	Displacement of maxilla in the y-axis with SARME by different surgical procedures (top view). (A) Group I (no surgery); (B) Group II (Le Fort I osteotomy); (C) Group III (Le Fort I osteotomy + paramedian osteotomy); (D) Group VI (Le Fort I osteotomy + pterygomaxillary separation); (E) Group V (Le Fort I + paramedian osteotomy + pterygomaxillary separation (adapted Han et al., 2009)).....	60
2.24	Displacement of the landmarks due to SARPE after 5 mm activation of the expander apparatus for the model simulated with median and lateral osteotomies without PMS disjunction: frontal view simulation. (A) and occlusal view simulation; (B) V – shaped opening of the mid-palatal suture can be observed (wider anteriorly than posteriorly) (Adapted from Koç & Jacob, 2022).....	61
2.25	Displacement of the landmarks due to SARPE after 5 mm activation of the expander apparatus for the model simulated with median and lateral osteotomies with PMS disjunction: frontal view simulation (A) and occlusal view simulation (B). More parallel opening of the mid-palatal suture is noted (adapted from (Koç & Jacob, 2022)).	61
3.1	(A) Lateral view of the maxillary arch with 1- Buccal incisors region; 2- Buccal premolars region and 3- Buccal molars region; 4- Tuberosity region; 5- Maxilla. (B) Occlusal view of the maxillary arch with 6- Palatal incisors region; 7- Palatal premolars region and 8- Palatal molars region. A mini – screw is simulated between	

the roots of second premolar and first molar, and a bonded bracket is simulated on the buccal surface of the canine (Ammoury et al., 2019).....	65
3.2 (A) Frontal view and (B) Lateral view of the model showing the “Maxillary Extension mask” in opaque color.	66
3.3 Maxillary model of setup 1 (control model): (A) Occlusal view (B) Posterior view (C) Anterior view (D) Right side lateral view	67
3.4 Maxillary model of setup 2: Palatal view showing the mid-palatal sagittal osteotomy	68
3.5 Maxillary model of setup 3: (A) Occlusal view of the maxillary model showing the mid-palatal sagittal cut; and (B) Frontal view showing the anterior maxillary cut below ANS.....	68
3.6 Maxillary model of setup 4: (A) Lateral view that shows the lateral and ANS osteotomy; (B) Frontal view; (C) Occlusal view that shows the mid-palatal sagittal osteotomy.....	69
3.7 Maxillary model of setup 5: (A) Right lateral posterior view that shows the pterygomaxillary disjunction; (B) Right lateral view; (C) Frontal view	69
3.8 Computed Tomography of the head with multiple views of the mid-palatal sagittal osteotomy in dark brown captured from ScanIP software. (A) Sagittal view; (B) Sagittal view including the other bone masks; (C) Coronal view including other bone masks and (D) Axial view including other bone masks	71
3.9 Computed Tomography of the head with multiple views of the osteotomy at the anterior nasal spine captured from ScanIP. (A) Sagittal view showing the ANS osteotomy only (in blue); (B) Sagittal view including the mid-palatal sagittal osteotomy (in purple), the osteotomy at ANS (in blue) and the other masks; (C) Sagittal view highlighting the two mid-palatal sagittal and ANS osteotomy; (D) Axial view showing the osteotomy at ANS; (E) Coronal view showing the osteotomy at ANS alone; (F) Coronal view showing the osteotomies at ANS and the midsagittal area.....	72
3.10 Computed Tomography of the head with multiple views of the lateral osteotomies along with the mid-palatal sagittal osteotomy. (A) Sagittal view showing the right lateral osteotomy (in red); (B) Axial view showing both the lateral and mid-palatal sagittal osteotomies; (C) Coronal view showing both the right (red) and left (green) lateral and mid-palatal sagittal osteotomies.....	73
3.11 Computed Tomography of the head with multiple views displaying the LeFort osteotomy in addition to the mid-palatal sagittal and ANS osteotomies. (A) Sagittal view showing the LeFort, mid-palatal sagittal and ANS osteotomies; (B) Axial view showing the Lefort and mid-palatal sagittal osteotomies; (C) Coronal view showing the Lefort, mid-palatal sagittal and ANS osteotomies.....	74
3.12 To simulate the MARPE, four rectangular spaces (pointed with red arrows) were constructed in the palatal region, where the force of expansion will be applied.....	75
3.13 Frontal view of the meshed model of the maxilla.	76
3.14 Meshed maxillary model with the boundary conditions applied (selected elements highlighted in pink and blue): models constrained from translation and rotation representing the areas of attachments of the maxilla to adjacent bones: zygomatic, palatal and sphenoid. A superior view; B, posterior view, and C, lateral view.....	78

3.15 Load application: 10 nodes are selected on each mini screw and an expansion of 4 mm referred to as U1 in the x axis, is applied on each mini screw, (- 4) mm on the left and (+ 4) mm on the right.....	79
3.16 Different views of the meshed maxillary model showing the elements selection (red) in various regions. (A) Elements selected along the mid-palatal suture mesial to the force application points; (B) Elements selected on the buccal bone of the incisors mask; (C) Elements selected on the palatal bone of the incisors; (D) Elements selected on the buccal bone of the molars; (E) Element selected on the palatal bone of the molars; (F) Elements selected on the maxillary extension; (G) Element selected on the maxilla	80
3.17 Lateral view of the right side of the model with nodes selected in the cervical part of the buccal bone of the right central incisor, canine and first molar, to measure the amount of expansion (displacement).....	81
4.1 Visualization of stress distribution in the mid-palatal area. (A) Palatal view of the control setup model; (B) Palatal view of setup 2 model; (C) Palatal view of setup 3 model; (D) Palatal view of setup 4 model; (E) Palatal view of setup 5 model.....	84
4.2 Visualization of stress distribution on the buccal bone of the incisors and the maxillary extension. (A) Frontal view of the control setup model; (B) Frontal view of the setup 2 model; (C) Frontal view of the setup 3 model; (D) Frontal view of the setup 4 model; (E) Frontal view of the setup 5 model.	86
4.3 Visualization of stress distribution on the buccal bone of the molars. (A) Right side view of the model of control setup; (B) Right side view of setup 2 model; (C) Right side view of setup 3 model; (D) Right side view of setup 4 model; (E) Right side view of setup 5 model.....	87
4.4 Visualization of stress distribution on the palatal bone of incisors and molars. (A) palatal view of the right side of control setup model; (B) Palatal view of the right side of setup 1 model; (C) Palatal view of the right side of setup 2 model; (D) Palatal view of the right side of setup 3 model; (E) Palatal view of the right side of setup 4 model.	87

TABLES

Table

3.1 The different included setups.....	70
3.2 Material properties of anatomical components used in orthodontic FEA study (Field et al., 2009; Kojima et al., 2012; Lim et al., 2003).....	77
4.1 Descriptive statistics for the stresses at the level of the different bone parts	85
4.2 Pairwise comparison (Wilcoxon test) of stress at the different bone parts.....	88
4.3 Descriptive statistics of the expansion at three different locations.....	89
4.4 Pairwise comparison (Wilcoxon test) of expansion at various locations	89
4.5 Mean of cortical bone thickness at the first molars and incisors level	90
4.6 Correlations between stress, expansion, and cortical bone thickness of setup 1	93

CHAPTER 1

INTRODUCTION

1.1 Definition of transverse deficiency of the maxilla

Skeletal malocclusions that affect the maxilla can be categorized into vertical, horizontal, or transverse discrepancies. They are most common in the transverse dimension (Betts et al., 1995).

A decrease in transverse dimension is the most frequent type of transverse malocclusion (Pogrel et al., 1992). This is also frequently referred to as a transverse deficiency of the maxilla (TDM). Dentally, TDM is often characterized by the presence of posterior crossbite involving one or several teeth on one or both sides of the jaws. In rare circumstances, TDM can be accompanied by normal transverse occlusion, when mandibular posterior teeth exhibit dental compensation with lingual crown inclination (buccal root torque) of these teeth.

1.2 Prevalence

The occurrence of the TDM in the entire population is estimated at 9.4%. Almost 30% of orthodontically treated adult patients are affected by this abnormality in which half of the lower dental arch overlaps the upper arch (Proffit & White, 1990). Complete crossbite occurs in 13–24% of the European children population, 7% in American and less than 1–2% in African children (Chamberland & Proffit, 2011).

CHAPTER 2

LITERATURE REVIEW

2.1 Etiology

The development of transverse maxillary deficiency has been shown in the literature, to be affected by several factors, such as:

- Habits, for example, thumb sucking (Zhu et al., 1996) (Oulis et al., 1994)
- Obstructive sleep apnea (Oulis et al., 1994)
- Iatrogenic reasons (cleft repair) (Capelozza Filho et al., 1996) ,(Kim et al., 2002) (Ishikawa et al., 1998)
- Palatal dimensions and inheritance (King et al., 1993) (Westling & Mohlin, 1996)
- Muscular (Oulis et al., 1994), (Symons et al., 2002)
- Syndromes : Klippel-Feil syndrome (Barbosa et al., 2005), Cleft lip and palate (Susami et al., 1996), Congenital nasal pyriform aperture stenosis, Marfan syndrome, Craniosynostosis (Apert's, Crouzon's disease, Carpenter's), Osteopatia striata (Koudstaal et al., 2006), Treacher Collins (Koudstaal et al., 2006)
- Duchenne muscular dystrophy (Symons et al., 2002)
- Nonsyndromic palatal synostosis (Rice et al., 2003)
- Multifactorial

2.2 Methods of Assessment

To effectively correct any dentofacial deformations that involve transverse deficiency, early and accurate diagnosis, and treatment are imperative to stability (Betts, 2016). Determining whether or what type of deficiency is present in the maxilla is the first step. Transverse maxillary deficiency is more difficult to assess than vertical or sagittal discrepancy, as there are few changes in soft tissue that result from hypoplasia of the maxilla in the transverse direction (Betts, 2016; Reyneke & Conley, 2020). Such soft tissue changes are much more prevalent when deformations are isolated to the anteroposterior or vertical (Betts, 2016). Accurate diagnosis relies on multiple examinations such as clinical evaluation, evaluation of study models, and radiographic evaluation.

2.2.1 Clinical evaluation

1. Extra-oral examination: soft tissue changes associated with TDM are minimal, which may complicate the diagnosis. These few manifestations include hollowing of the paranasal region, excessive width of the buccal corridors, nasolabial fold deepening, or narrowing of the alar bases (Bin Dakhil & Bin Salamah, n.d.).
Associated skeletal deformities include maxillary vertical and anteroposterior hypoplasia and zygomatic hypoplasia (as a result of growth issues). Other associated dentofacial deformities include vertical maxillary excess, mandibular prognathism or mandibular sagittal deficiency, apertognathia, and repaired cleft palate (Betts, 2016).
2. Intra-oral examination: manifestations include severe crowding, rotation, or buccal/palatal displacement of the teeth, crossbite (uni- or bilateral), high palatal vault, and hourglass- or V-shaped arch forms (Bin Dakhil & Bin Salamah, n.d.).

3. Assessment of function: Mouth breathing is one of the etiologies of TDM.

Therefore, patients with TDM should be evaluated for the possibility of mouth breathing and must be referred to the appropriate specialist as indicated.

Also, mandibular shift upon closure should be examined posterior crossbite resulting from TDM may result in premature contacts during occlusion leading to mandibular deviation. This “functional shift” from the centric relation may develop into skeletal asymmetry if not treated at a young age. Lateral chin deviation may be noted in a frontal facial examination, and if so, its root cause needs to be identified. This could be due to a functional shift from centric relation, or actual skeletal asymmetry.

2.2.2 Evaluation of study models

The form and shape of the arch should be evaluated using study models. This will allow for specific measurements to be made that evaluate the transverse deficiency of the maxilla. Pont provides the most common index for such lateral measurements (Rakosi et al., 1993) (Fig.2.1). Linder-Harth’s analysis is similar to Pont’s analysis, but with a variation in the equation that determines the calculated molar and premolar value (calculated premolar value = $(SI \times 100) / 85$ and calculated molar value = $(SI \times 100) / 64$). The Korkhaus analysis uses the Linder-Harth’s formulas but with an additional measurement: for a given width of the upper incisors, a specific value of the distance between the mid-point of the inter-premolar line to the point between the two central incisors should exist.

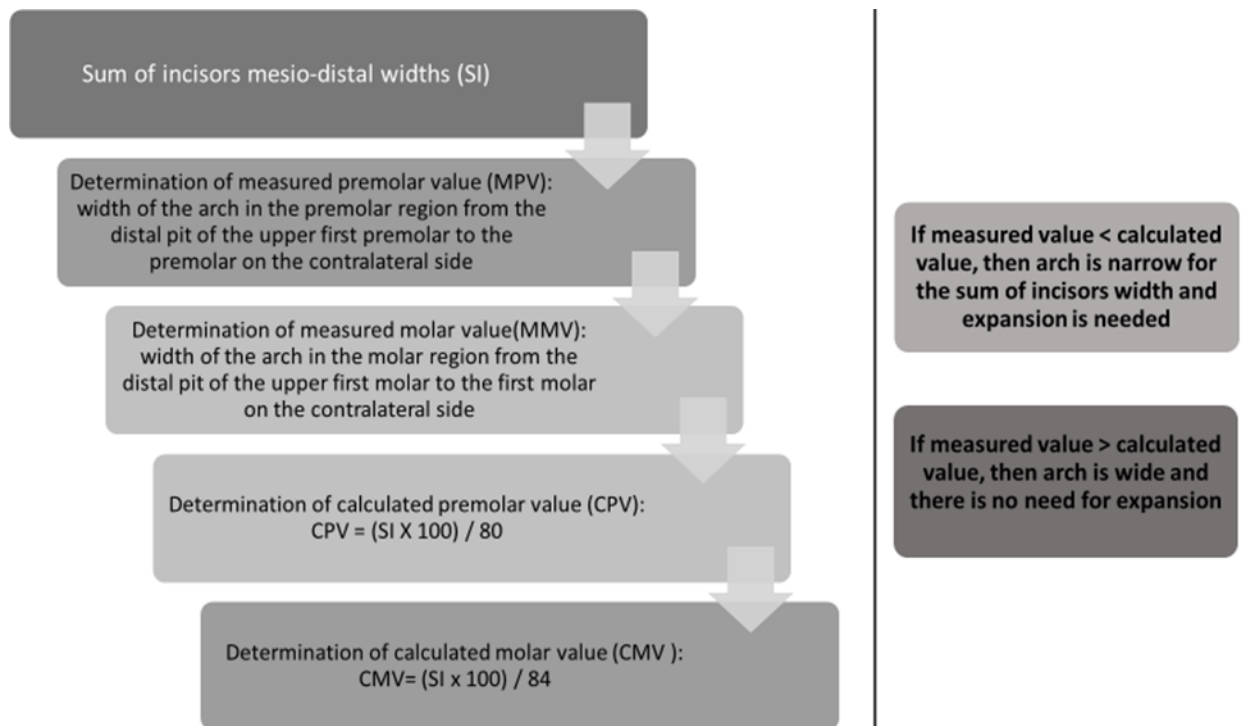


Figure 2.1 Diagram elaborating the technique used in the Pont analysis on study models

In fact, narrow maxillary arch may be expressed in various ways. Even in the absence of obvious buccal ‘crossbite’, TDM may be expressed by insufficient buccal overjet, transverse dental compensation in the posterior segment or open lingual occlusion (K.-J. Lee et al., 2018) (Fig. 2.2).

Study models are used to differentiate between absolute or relative transverse deficiencies (Marshall et al., 2005). A relative transverse discrepancy is present when the posterior teeth can be brought into correct transverse occlusion when manipulating the study models into class I canines if tooth alignment was acceptable. In contrast, absolute transverse discrepancy does not allow correct occlusion when manipulating the models.

In the case of an absolute transverse discrepancy being present, the origin (skeletal or dental) and magnitude of the discrepancy may be determined via study

casts. Posterior dental compensations in the cast should be investigated first. These will present in the form of variations of the permanent first molars' transverse axial inclination - most frequently, excessive buccal crown torque of the maxillary molars and/or the lingual crown torque of the mandibular molars relative to the frontal plane (Marshall et al., 2005).

If improvement of the posterior transverse inter-arch relationship results from up righting of the molars in the cast (i.e., removal of the transverse compensations), then a dental origin is likely for the transverse discrepancy. Dental movement alone could then be applied as treatment. However, if removal of the transverse compensation leads to worsening of the posterior transverse inter-arch relationship, then a skeletal origin for the discrepancy is much more likely (Marshall et al., 2005).

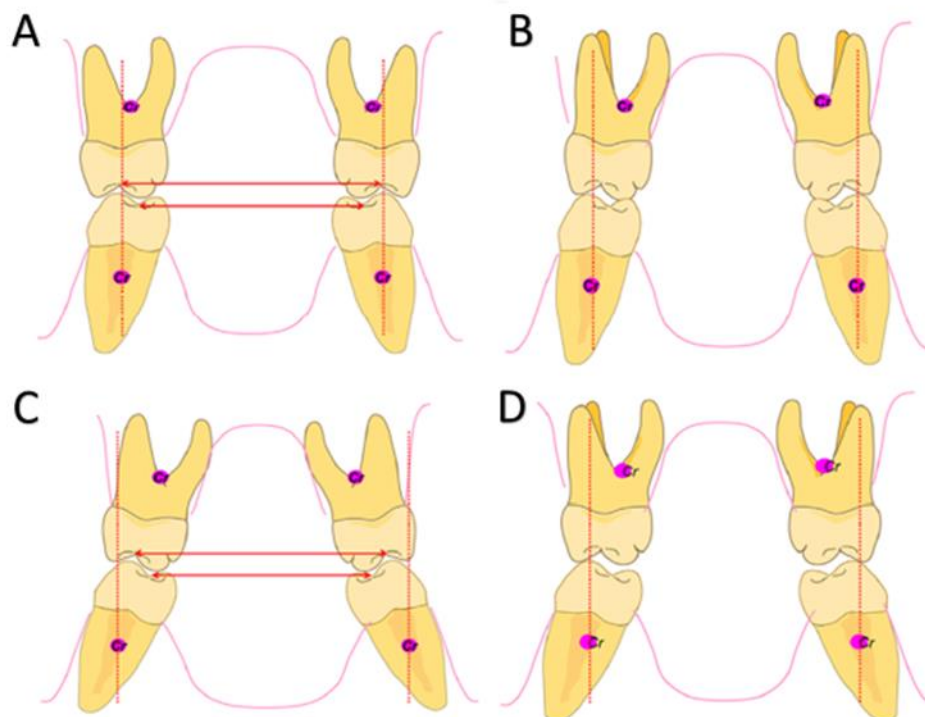


Figure 2.2 Clinical manifestation of transverse problems. (A) Ideal buccal occlusion; (B) Insufficient buccal overjet; (C) transverse compensation; and (D) open lingual occlusion. Adapted from (K.-J. Lee et al., 2018)

2.2.3 Radiographic evaluation

2.2.3.1 Postero-anterior cephalogram

A standard posteroanterior (PA) cephalogram is the radiograph of choice for identification and evaluation of a transverse discrepancy (Betts et al., 1995). Several analyses were proposed to diagnose TDM. Among these analyses, - the “Rocky Mountain analysis” developed by Ricketts’ seems to be the most widely used, perhaps because it provides normative values for different ages. In this analysis, relative norms were established using specific radiographic landmarks and measurements to analyze transverse discrepancy between the maxilla and mandible (Ricketts, 1981).

The skeletal landmarks used in the evaluation of maxillo-mandibular transverse discrepancy are (Fig 2.3):

- a. JR (jugale right) and JL (jugale left): The intersection of the maxillary tuberosity and the zygomatic buttress.
- b. AG (antegonion right) and GA (antegonion left): The inferior margin of the antegonial protuberance, below the antegonial trihedral area.
- c. OR (orbitale right) and OL (orbitale left): The intersection of the orbits with the middle cranial fossa. (Betts, 2016).

These landmarks are used to determine the effective maxillary width, effective mandibular width, and frontolateral facial lines (Fig. 2.3):

- a. The effective maxillary width is the width of the maxilla between the points JL (jugale left) and JR (jugale right).
- b. The effective mandibular width is the width of the mandible between AG and GA

- c. The frontolateral facial lines are the lateral lines constructed from OR (orbitale right) and OL (orbitale left) to the points AG and GA, respectively.

Using these cephalometric landmarks, it is possible to determine:

- a. The maxillo-mandibular width differential: the distance (in millimeters) measured from the frontolateral facial line to Jugale L and Jugale R, respectively, along a line from the frontolateral facial lines through Jugale R and Jugale L. This measurement is calculated independently for each side and compared with a normal value of 10 ± 1.5 mm. If this value is greater than 10 mm, a transverse discrepancy between the maxilla and mandible exists. The values greater than 10 mm on each side are summed to quantify the total transverse deficiency. This technique is useful in determining the total discrepancy and show whether there is a greater deficiency or excess on 1 side or the other. However, this differential does not elucidate in which jaw the discrepancy exists and may be misinterpreted when mandibular asymmetry is present.
- b. The maxillomandibular transverse differential index for quantification of the transverse maxillary discrepancy: the age-specific expected maxillo-mandibular difference minus the actual measured maxillo-mandibular difference. The expected maxillo-mandibular difference is the age-appropriate expected AG-GA distance minus the age-appropriate expected JR-JL distance. The actual maxillomandibular difference is the actual AG-GA measurement minus the actual JR-JL measurement. In an adult patient, a maxillomandibular transverse differential index greater than 5 mm suggests a need for surgical expansion.

As well as quantifying the total discrepancy, this method allows for the identification of which jaw is deficient or excessive, because actual values can be compared with normal values. Normal values have been suggested only for Caucasian, and these values should not be considered normal values for other races.

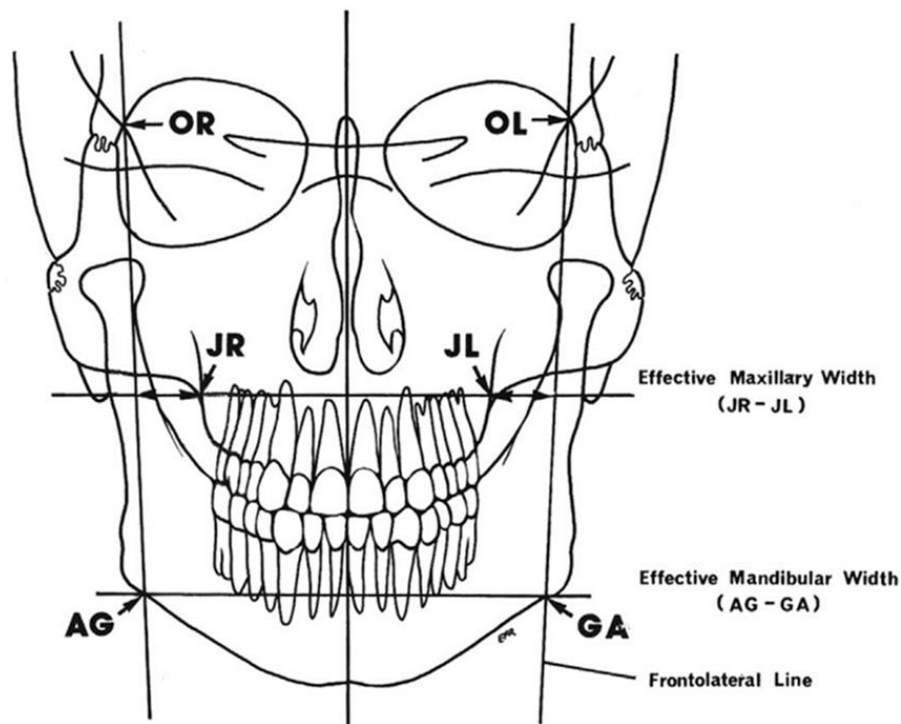


Figure 2.3 The elements of the PA cephalometric analysis. These landmarks can be used to calculate the effective maxillary width and effective mandibular width, and the fronto-lateral lines can be constructed (Adapted from Betts et al., 1995)

Differences exist, however, between the norms given by the various studies, and warrant the establishment of standards based on longitudinal records collected with methodical rigor. Cortella et al. collected the norms for the Bolton-Brush material, recognized as a controlled longitudinal record of growing children, and offered the basis for generating normative data. A major advantage of this study is the availability of

norms that are adjusted for radiographic enlargement, a critical factor in cephalometrics. Therefore they may be used as the basic guideline for diagnosis (Cortella et al., 1997).

2.2.3.2 Occlusal or palatal radiographs

These radiographs are an essential tool for evaluating mid-palatal suture ossification (Lehman et al., 1984). However, the superposition onto the mid-palatal suture or other bony structures and the inability to effectively visualize the posterior intermaxillary suture, make this an unreliable method overall (Bin Dakhil & Bin Salamah, 2023).

2.2.3.3 Cone-Beam Computed Tomography for evaluation of suture maturation

Maxillary occlusal radiographs were used in the past to assess the mid-palatal suture, but this technique had some drawbacks. Because the nasal structures and the vomer bone are superimposed on the mid-palatal region of the occlusal radiographs, which are a 2D representation of a 3D structure, there is a chance that the radiograph may be misinterpreted. The CBCT, the most recent advancement in dental imaging, bridges this shortcoming by addressing the issues with 2D imaging methods. The craniofacial structures can be visualized in high-resolution 3D via CBCT. Additional benefits include the absence of any anatomic superimpositions, high dimensional precision, noninvasive nature, timesaving, ease of access, and high degree of accuracy. (add ref)

2.2.4 *Medical history*

The medical history must be carefully evaluated since developmental dynamics and environmental influences can affect the ability of a suture to respond to external force application. In fact, OME (Orthopedic Maxillary Expansion) depends on the

sutural patency and the flexibility of the craniofacial skeleton to adapt to controlled mechanical forces. Therefore, it is essential to recognize medical conditions that can influence the results of OME (Suri & Taneja, 2008).

Several metabolic conditions have been linked to sutural synostoses. These include hyperthyroidism (Alden et al., 1999) (Hirano et al., 1995), hypophosphatemic vitamin D-resistant rickets (Carlsen et al., 1984) and mucopolysaccharidoses and mucopolipidoses (Alden et al., 1999) (Cohen, 1993). A common link in all these conditions is an underlying abnormality in bone metabolism.

2.3 Suture growth and anatomy

2.3.1 Anatomy

The maxillary and palatine bones' opposing midline portions are connected by the mid-palatal suture. The palatine processes of the two maxillary bones that intersect in the midsagittal plane make up the anterior part of the hard palate. The horizontal plates of the palatine bones connect at the midline immediately posterior to the maxillary region of the palate to create the posterior aspect of the mid-palatal suture (Fig. 2.4). The interpalatine suture, which connects the maxillary and palatine bones, is parallel to the mid-palatal suture.

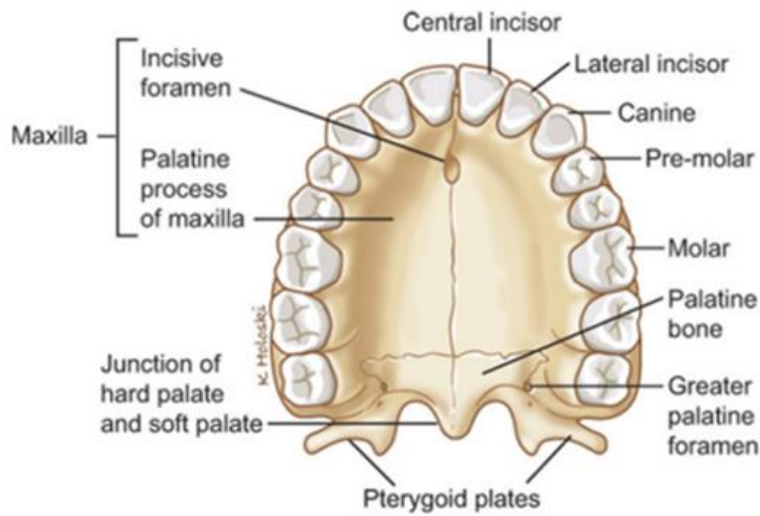


Figure 2.4 At the midsagittal plane, the bones that make up the mid-palatal suture unite (Picture from Head and Neck Cancer Guide).

The morphology of the mid-palatal suture changes during growth (Fig. 2.5). The postnatal development could be divided into three stages which corresponded to the stages of development used by Björk and Helm (Björk & Helm, 1967):

1. During the first stage, covering the infantile period, the suture was very broad and Y shaped, with the vomerine bone placed in a V-shaped groove between the two halves of the maxilla
2. During the second stage, which corresponds to the juvenile period, the suture was found to be wavier.
3. In the third stage, the adolescent period, the suture was characterized by a more tortuous course with increasing interdigitation

Even at the age when the suture was characterized by heavy interdigitation, a distinct stratification of the connective tissue into three layers was seen. In the lower part of the suture, the fibers from the periosteum were found to extend into the central layer of the suture parallel with the two bone surfaces. In the inactive suture of the oldest persons, Sharpey's fibers could be followed uninterruptedly across the suture. The transverse growth of the mid-palatal suture continued up to the age of 16 in girls and 18 in boys (Melsen, 1975).

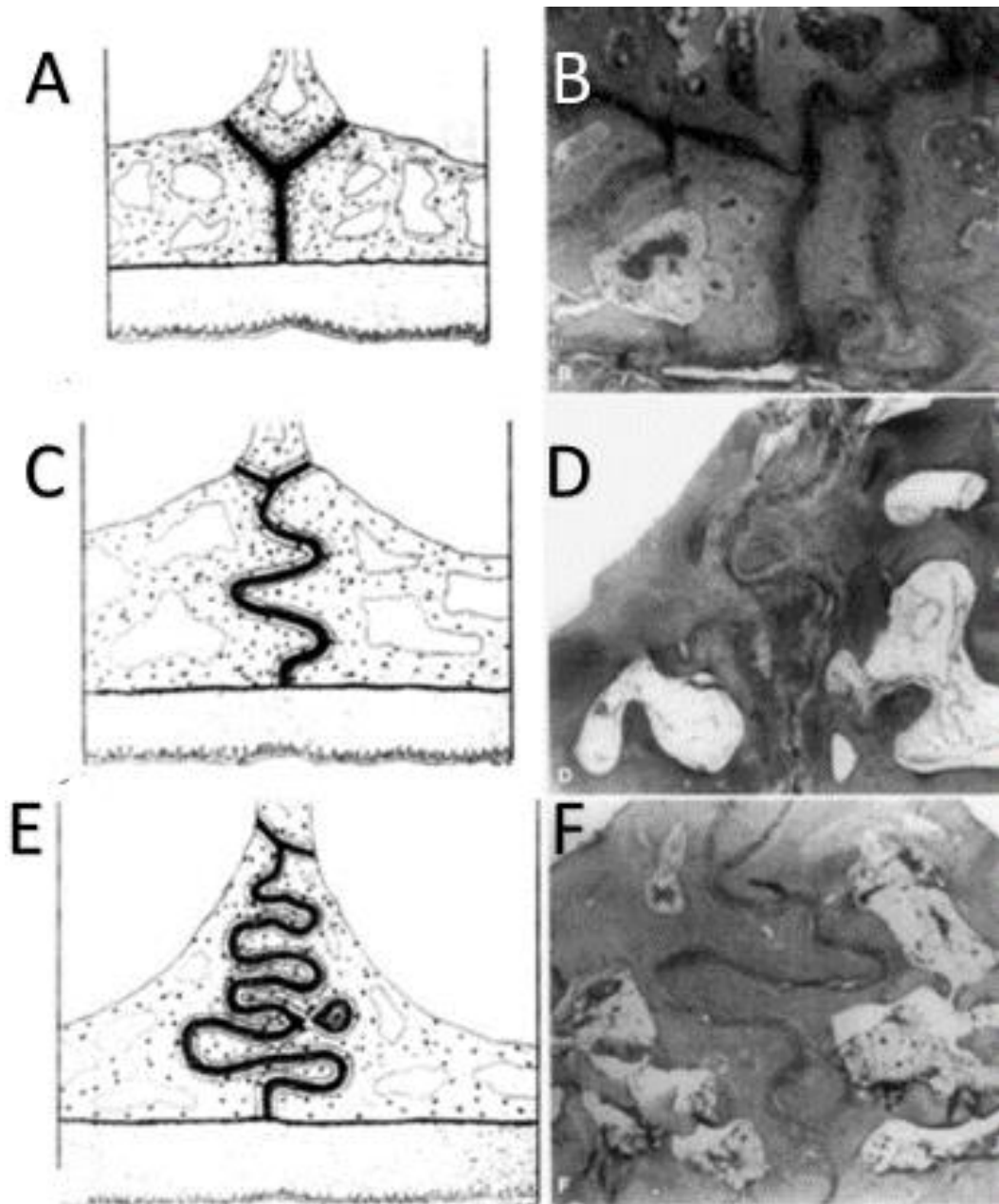


Figure 2.5 Stages of mid-palatal suture maturation: (A) Diagrammatic representation of the suture of the infantile period; (B) Histologic frontal section of the infantile suture of a 1-year-old child; (C) Diagrammatic representation of the suture of the juvenile period; (D) Histologic frontal section of the juvenile suture of the 10-year-old boy; (E) Diagrammatic representation of the suture of the adolescent period; (F) Histologic frontal section through the suture of a 12.5-year-old girl. (Image adapted from Melsen, 1975).

2.3.2 Methods of assessment of skeletal maturity

Assessments of skeletal maturity have been proposed, among them cervical vertebral maturation, hand wrist radiographs, and more recently using CBCT to assess maxillary sutural maturity. (Angelieri et al., 2017).

The gold standard for assessing skeletal maturation is the hand wrist maturation (HWM), a method that needs an extra hand and wrist X-ray. In this context, Lamparski et al. introduced a method for assessing cervical vertebral maturation on the cephalometric radiographs. As a result, additional patient radiation was eliminated. Currently, this type of radiograph is routinely applied in orthodontic treatment (Shayani et al., 2022).

Cone-beam computed tomography (CBCT) provides 3-dimensional visualization of the mid palatal suture in vivo, without any overlapping of anatomic structures, at relatively low cost. This recent method identifies five stages of maturation of the mid-palatal suture (Angelieri et al., 2013) (Fig. 2.6) :

- a. **Stage A:** straight high-density sutural line, with no or little interdigitation
- b. **Stage B:** scalloped appearance of the high-density sutural line
- c. **Stage C:** two parallel, scalloped, high-density lines that were close to each other, separated in some areas by small low-density spaces
- d. **Stage D:** fusion completed in the palatine bone, with no evidence of a suture
- e. **Stage E:** fusion anteriorly in the maxilla

Stages A and B were frequently seen up to the age of 13, and stage C was mostly seen between the ages of 11 and 17, with sporadic occurrences in lower and older age groups. Only in girls did the mid-palatal suture's fusion of the palatine (stage D) and maxillary (stage E) regions take place after 11 years. Three out of thirteen (23%) males

between the ages of 14 and 17 only had palatine bone fusion (stage D). Although the mid-palatal suture maturation approach has the potential to be employed for diagnostic purposes, clinicians are advised to use caution before regularly employing it because a comprehensive training and calibration program need be completed before (Shayani et al., 2022).

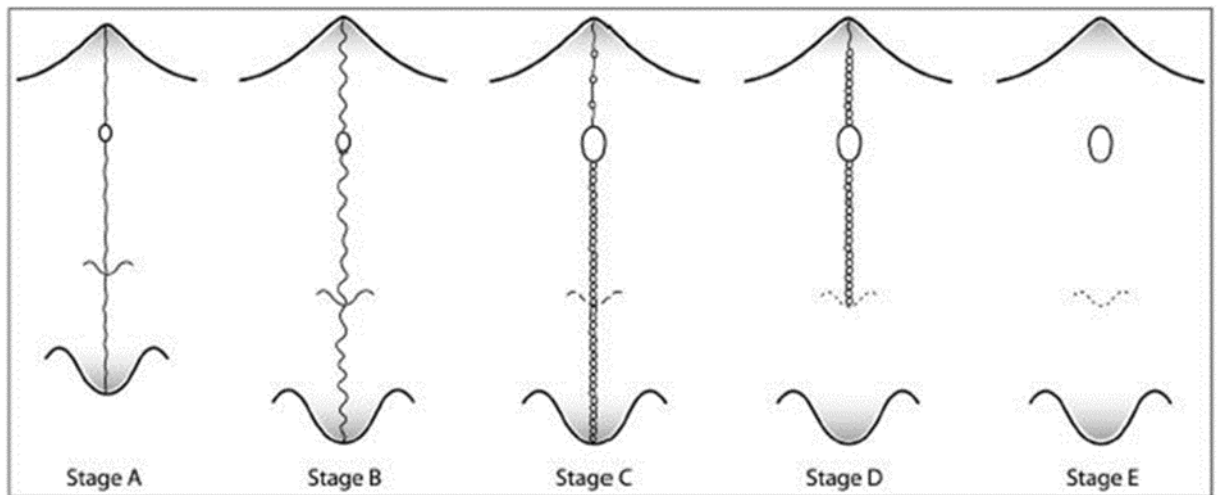


Figure 2.6 Schematic drawing of the maturation stages observed in the mid- palatal suture (adapted from (Angelier et al., 2017)).

2.4 Management

Treatment for TDM aims to reduce the potential for periodontal disease, enhance skeletal and dental stability, and improve the aesthetics of the smile (Bin Dakhil & Bin Salamah, 2023). The choice of a treatment alternative depends on certain factors, such as age, sex, degree of maxillary hypoplasia and maturation of the mid-palatal suture.

2.4.1 Management in skeletally immature patients

Maxillary expansion on skeletally immature patients has been discussed for more than a century. Modern approaches to expansion in the United States began in the late 1950s when Korkhaus introduced the technique which was then mainly popularized by Haas (Haas, 1970).

It is important to differentiate between dental and orthopedic expansion. In fact, expansion of the dental arch can be achieved with several dental expansion devices:

orthodontic brackets with a wide arch wire can be among the simplest approaches.

Other approaches include trans-palatal arches (TPA), quad helix, and cross-arch elastics (Reyneke & Conley, 2020).

Orthopedic expansion allows widening of the basal bones. Benefits include:

1. Preventing asymmetric growth in the case of bilateral crossbite with functional shift.
2. Achieving orthopedic expansion can also reduce or eliminate the need for later surgical correction.
3. Additional arch perimeter for future alignment of the teeth, mild improvement in the sagittal malocclusion (McNamara et al., 2010)
4. Possible improvement in airways: maxillary bones form half of the nasal cavity's anatomic structure, it has been hypothesized that mid-palatal disjunction would affect the anatomy and the physiology of the nasal cavity. The nasal valves are the minimal cross-sectional areas of the nose and, therefore, the site of greatest resistance to nasal airflow. Rapid maxillary expansion promotes the separation of the maxillary bones in a pyramidal shape in which maximum expansion is at the level of the incisors, just below the nasal valves. Palatal disjunction can also cause a total increase in the nasal cavity's volume since its lateral walls are displaced apart.

Ultimately, a combination of these phenomena could result in improvement in the patient's ability to breathe through the nose (Oliveira De Felipe et al., 2008).

Orthopedic expansion is most easily accomplished before closure of the cranial base and midfacial sutures. Previous research indicates that the transverse dimension is the first plane of space to cease growth, most notably at the inter-ethmoidal and intersphenoidal sutures. After their closure, increasing amounts of dental expansion and decreasing amounts of skeletal expansion are achieved until finally in late adolescence minimal to no skeletal expansion can be obtained (Baccetti et al., 2001). The circummaxillary sutures follow a similar pattern of increasing complexity and decreasing patency with increasing age (Reyneke & Conley, 2020a).

Orthopedic expansion appliances generally fall into 2 types (Fig. 2.7) : tooth-borne hygienic rapid palatal expanders (Hyrax) or tooth plus tissue-borne expanders (Haas, 1961). Both types can be banded and bonded to the teeth. Activation protocols range from slow (1 turn every 2–3 days) to rapid (1–2 turns each day) (Proffit et al., 2006).

Indications for orthopedic skeletal expansion:

1. Presence of cross bite
2. Class II patients with narrow maxillae, particularly when the patient protrudes and a crossbite exists in Class I (McNamara et al., 2010).
3. Class III patients for whom simultaneous expansion and protraction is considered:
Rapid maxillary expansion (RME) has been recommended for use in conjunction with facemask because it disrupts circummaxillary and intermaxillary sutures and facilitates the orthopedic effect of facemask. However, it has been reported that circummaxillary sutures may not be well disarticulated by use of RME alone and

might be better managed by the use of alternate RME and constriction (D. Kaya et al., 2011).

4. Growing (i.e., not skeletally mature) patient
5. Crowding, ectopic, and impacted canines
6. Smile esthetics: dark buccal corridors

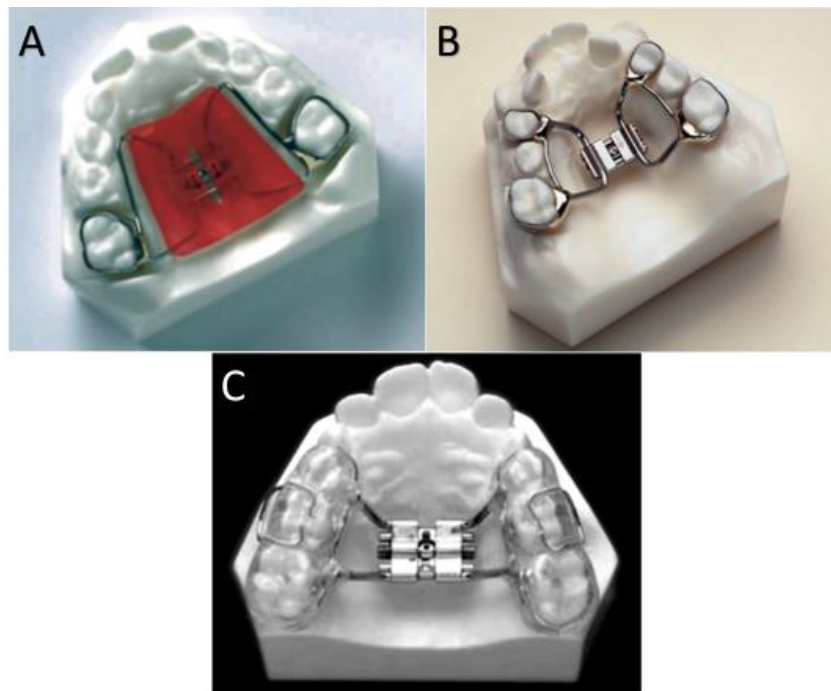


Figure 2.7 Banded tooth and tissue-borne appliance; B: banded tooth-borne appliance; C: bonded tooth-borne appliance (adapted from Agarwal, 2010).

2.4.2 Management in skeletally mature patients

In skeletally mature patients (i.e., non-growing), maxillary dental arch expansion can only be achieved through dental movement. Adult patients who exhibit skeletal transverse deficiency may need tooth movement that extends further than the alveolar bony base of the maxilla.

2.4.2.1 Rationale of transverse correction

Inadequate transverse occlusion has been claimed to co-exist with non-carious cervical wear, i.e., abfraction, possibly by increase of non-axial loading causing cusp flexure and stress concentration in the cervical region. (Bartlett & Shah, 2006) (Michael et al., 2009). Recessions were also described in cases of abnormal transverse occlusion (Betts et al., 1995). In terms of the masticatory function, subjects with non-sagittal transverse malocclusion, such as buccal edge bite or crossbite, exhibited remarkably low masticatory ability index (MAI) and food intake ability (FIA), indicating a strong rationale for the treatment of transverse malocclusion (Choi et al., 2015).

After sutural closure or completion of transverse growth, orthopedic expansion alone is often unsuccessful and possible problems include:

1. Inability to activate appliance
2. Severe pain with activation
3. Pressure necrosis under the appliance
4. Bending of alveolar bone
5. Unstable results with relapse
6. The posterior teeth tip leading to poor occlusion and instability.
7. This further leads to clockwise mandibular rotation, opening the bite and increasing facial height.
8. The maxillary posterior teeth are displaced buccally through the alveolus leading to gingival recession, bone loss and root resorption (Menon et al., 2010).
9. Periodontal ligament compression
10. Fenestration of the buccal cortical plate (Verstraaten et al., 2010)

Because of these complications following the attempts to orthopedically alter the transverse dimension of the maxilla with advancing age, surgical procedures have been recommended to facilitate correction of transverse discrepancies. These procedures have conventionally been grouped into 2 categories: segmenting the maxilla during a LeFort osteotomy to reposition the individual segments in a widened transverse dimension, and surgically assisted rapid palatal expansion (SARPE).

2.4.2.2 Segmental Le Fort I osteotomy

2.4.2.2.1 Definition

Le Fort I type osteotomy which requires a down-fracture allowing the entire maxilla to be adjusted and repositioned in all three dimensions.

2.4.2.2.2 Indications

1. Expansions for modest defects (up to 6–7 mm)
2. When the transverse deficit is one of numerous maxillary skeletal deficits, including sagittal and vertical defects that would require surgical attention as well.
3. When more stability is required, segmental LeFort I osteotomy is a better option.

Compared to segmental Le Fort I osteotomy, relapse appear to be considerably greater with tooth-borne surgically assisted rapid maxillary expansion (Starch-Jensen & Blæhr, 2016).

2.4.2.3 Surgically assisted rapid palatal expansion (SARPE)

2.4.2.3.1 Definition

Due to the increased skeletal resistance and the previously mentioned side effects caused by orthopedic rapid maxillary expansion: The alternative of surgically assisted rapid maxillary expansion in adults, with maxillary expander appliances and

corticotomies of the areas of skeletal resistance (piriform aperture, zygomatic buttress, pterygoid junction, and mid-palatal suture), is nowadays an accepted treatment option for transverse maxillary hypoplasia. This surgical procedure employs a maxillary expander device that can be attached to the bone (bone-anchored) or existing teeth (tooth-borne). These devices are equipped with activating screws that allow the patients or care provider to incrementally expand the maxilla, following the principles of osteogenic distraction. Daily activations are typically performed until efficient expansion is achieved (Barone et al., 2020).

2.4.2.3.2 Indications

The following conditions—all of which pertain to skeletally mature patients with a constricted maxillary arch—have been listed in the literature as indications for SARPE:

1. Cases with a severe transverse deficit or when the transverse problem of the maxillary bone is an isolated skeletal anomaly (Marchetti et al., 2009).
2. To increase maxillary arch perimeter, to correct posterior crossbite, and when no additional surgical jaw movements are planned.
3. To widen the maxillary arch as a preliminary procedure, even if further orthognathic surgery is planned. This is to avoid increased risks, inaccuracy, and instability associated with segmental maxillary osteotomy.
4. To provide space for a crowded maxillary dentition when extractions are not indicated.
5. To widen maxillary hypoplasia associated with clefts of the palate.

6. To reduce wide black buccal corridors when smiling.
7. To overcome the resistance of the sutures when orthopedic maxillary expansion has failed (Suri & Taneja, 2008).

2.4.2.3.3 Advantages

1. This procedure minimizes relapse after maxillary expansion in patients with complete skeletal maturation (Jensen et al., 2015).
2. Perinasal soft tissue sustain changes: After SARPE, the nose tends to widen, move forward, and downwards, resulting in greater nasal volume. Alar width may also increase. Alar base widening should be manageable, nonetheless, by perinasal soft tissue repair using an alar cinch and minimally invasive techniques (Hernández-Alfaro & Valls-Ontañón, 2021).
3. Less morbidity than full orthognathic surgery (Bays & Greco, 1992).

2.4.2.3.4 Orthodontic preparation before the surgery

Some orthodontic preparations should be performed before the patient has the surgery done:

1. Enough space must be present between the roots of the central incisors for a midline split: A periapical or occlusal radiograph should be taken, and the interradicular bone evaluated. If space is inadequate, pre-operative root divergence should be created (Suri & Taneja, 2008).
2. The mandibular dentition should be decompensated before surgery to establish arch coordination, to determine the amount of transverse expansion required, and help prevent post-expansion relapse with proper dental interdigitation.

The tooth-borne appliance should be inserted before surgery, and the appliance key has to be present in the operating room to enable intraoperative activation. But if a bone-borne palatal distractor is required, it is inserted during surgery after the maxillary articulations are severed (Betts et al., 1995).

2.4.2.3.5 SARPE: Detailed surgical technique and appliance management

There are many surgical procedures available depending on where the treatment team anticipates the main points of resistance will be and where the greatest amount of palate expansion is needed (Reyneke & Conley, 2020). However, in this manuscript, only the 2-piece Le Fort I osteotomy will be detailed. It is performed without down-fracture, under general anesthesia through endotracheal intubation in an operating room setting.

1. An upper buccal mucosal and periosteal incision is performed from the second premolar on one side to the second premolar on the contralateral side
2. The submucosal dissection at the piriform aperture is started on one side and carried backward to the pterygomaxillary junction. The dissection is completed on the opposite side.
3. The left and right linear osteotomies are applied from the pterygomaxillary junction to the piriform aperture using a reciprocating saw. Osteotomies should be straight, horizontal, and perpendicular the palatal plane. Resistance to movement may be present if an osteotomy is performed at an angle (Fig. 2.8 A [iv]).
4. The nasal mucosa is dissected off the nasal floor
5. The nasal septum is separated using a nasal septal osteotome. Maintaining the septum attached to one of the two maxillary segments will prevent postoperative nasal deviation.

6. A line is marked on the labial cortex between the upper central incisor teeth with a burr, then the osteotomy is completed using piezo surgery or a spatula osteotome (Fig. 2.8 A [iii]).
7. The pterygomaxillary junctures are separated on both sides using the pterygomaxillary osteotome (Fig. 2.8 B).
8. A thin 5-mm osteotome is placed between the incisors in the osteotomy line while the surgeon's index finger palpates the palatal mucosa feeling the osteotome as it is tapped by the assistant, posteriorly to complete the palatal osteotomy (Fig. 2.8 C).
9. The planned positions of the footplates are marked on the mucosa.
10. An incision ± 6 mm long is now made bilaterally, and the muco-periosteum reflected to accommodate the footplates of the device.
11. The footplates are inserted by using an appropriate length of screws.
12. Once the distractor is secured in place (Fig. 2.9 A) it should be activated with a few turns to ensure the mobility of the maxillary segments.
13. After a latent period of 5 days, the distractor is activated and turned twice daily. For most distractors, each turn would represent 0.25 mm (Fig. 2.9 B and C).
14. Once the planned expansion has been achieved, the distractor can be locked and left in position for 4 to 8 weeks to act as a retainer (Fig. 2.9 C).

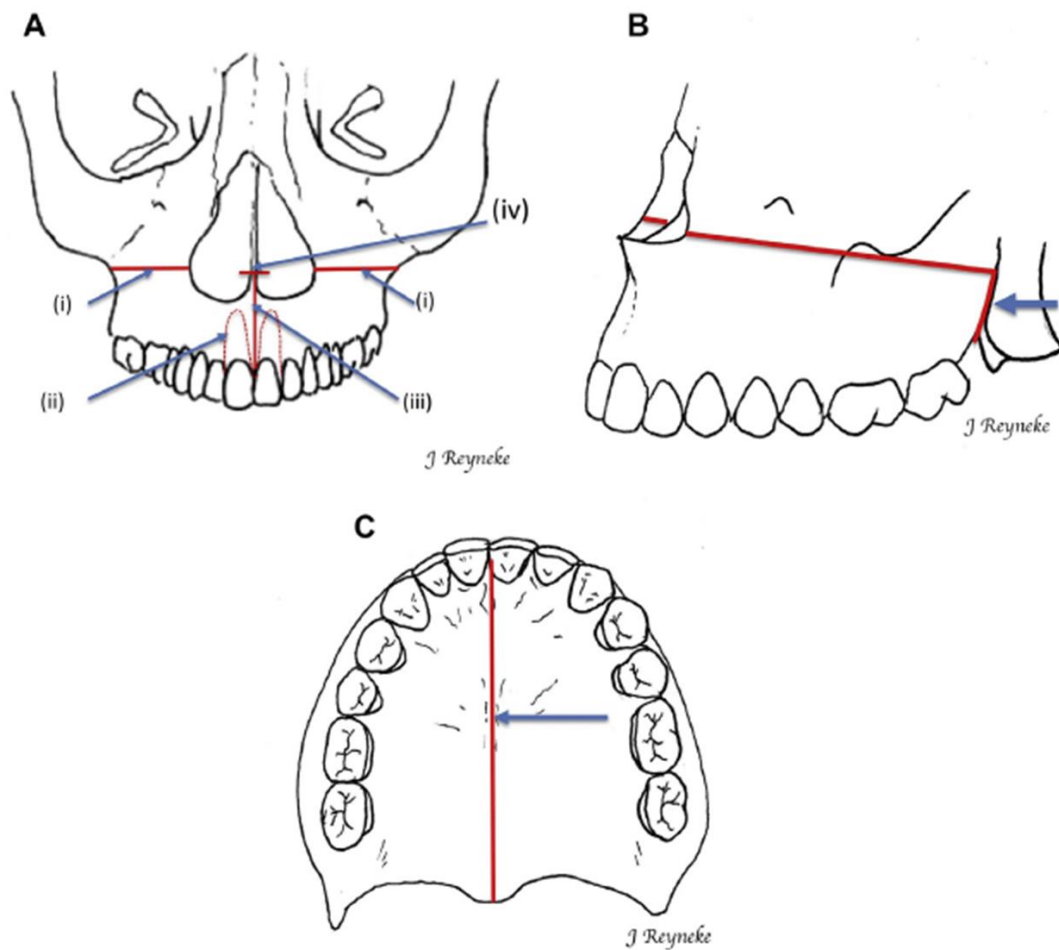


Figure 2.8 (A) Use of a reciprocating saw to perform the left and right lateral wall osteotomies from the pterygomaxillary junctions to the piriform rims (i). Drawing of the outline of the tooth roots adjacent to the interdental osteotomy (ii). Scoring of the interdental osteotomy only through the labial cortex by using a bur (iii). (iv) Separation of the nasal septum from the maxilla; (B) Separation of the pterygomaxillary junctions using a pterygoid osteotome (arrow); (C) Completion of the interdental osteotomy by means of a piezo surgical blade and performance of the midline palatal osteotomy using a small osteotome (Adapted from Reyneke & Conley, 2020).

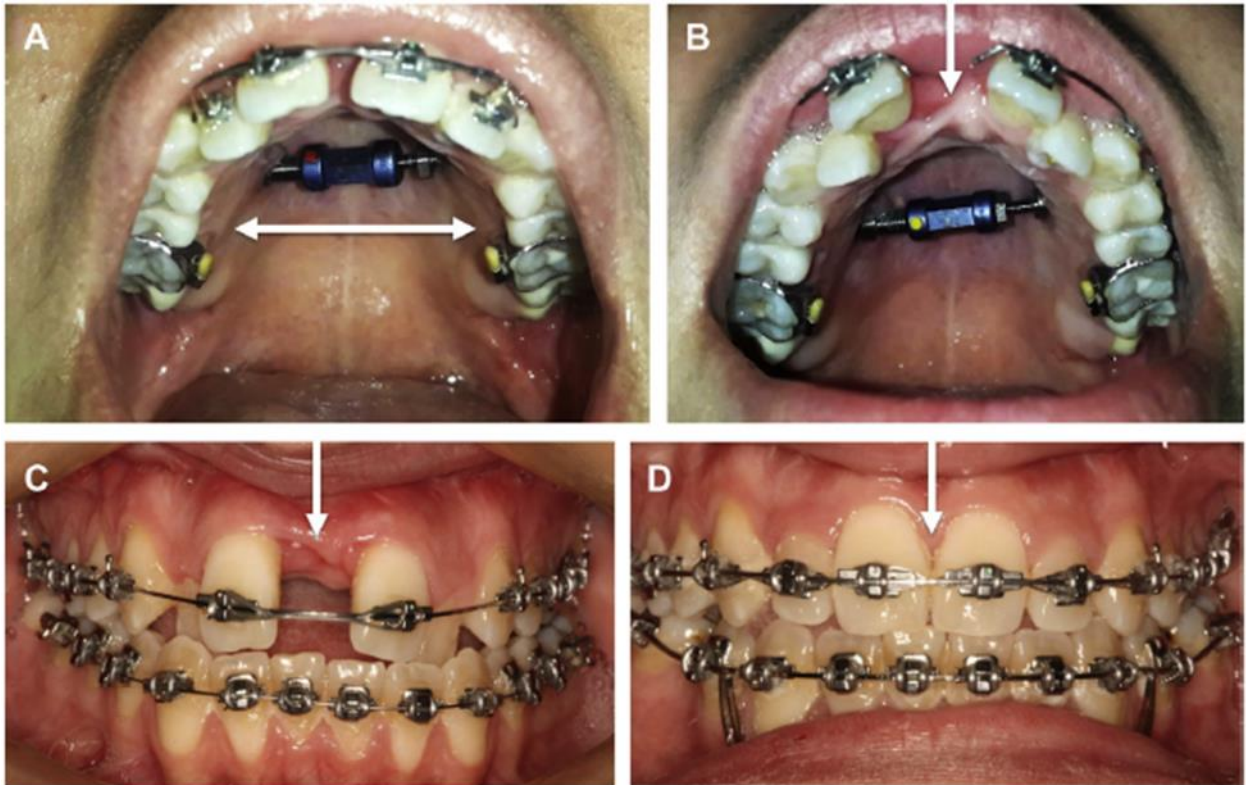


Figure 2.9 (A) A bone-borne distractor; (B) Observation of the diastema developing 3 days after activation and (C) 7 days after activation; (C) Consolidation phase after an 8 mm expansion. The expander was locked and acted as a retainer for 4 to 8 weeks; (D) Following the consolidation phase, the orthodontist used the additional space to close the space and align the teeth (Adapted from (Reyneke & Conley, 2020)).

2.4.2.3.6 SARPE: Different surgical approaches

Various SARPE techniques, combined with various osteotomies, have been developed to reduce areas of expansion resistance and to aid in the disjunction of the median palatine suture in adult patients. For example, different osteotomy combinations include the following: anterior wall of the maxillary sinus, lateral of the nose, nasal septum, intermaxillary suture, zygomaticomaxillary suture, and pterygomaxillary suture, with each type of osteotomy being based on different theories on zones of expansion resistance.

Below is a chronological listing of studies and groups reporting different surgical procedures and treatment protocols:

The initial surgical technique for SARPE involving a mid-palatal split was described in 1938 by Brown. The use of selective dentoalveolar osteotomies to section the cortical bone and reduce the resistance to orthodontic movement was advocated in the second half of the century (Kole, 1959).

In 1969, both labial and palatal cortical osteotomies were recommended during expansion (Converse & Horowitz, 1969).

The areas of resistance have been classified as:

1. Anterior support (piriform aperture pillars) (Fig. 2.10)
2. Lateral support (zygomatic buttresses) (Fig. 2.11)
3. Posterior support (pterygoid junctions) (Fig. 2.12)
4. Median support (mid-palatal suture) (Fig 2.4).

These areas of resistance to lateral expansion in the midface have been addressed with numerous surgical methods (Suri & Taneja, 2008).

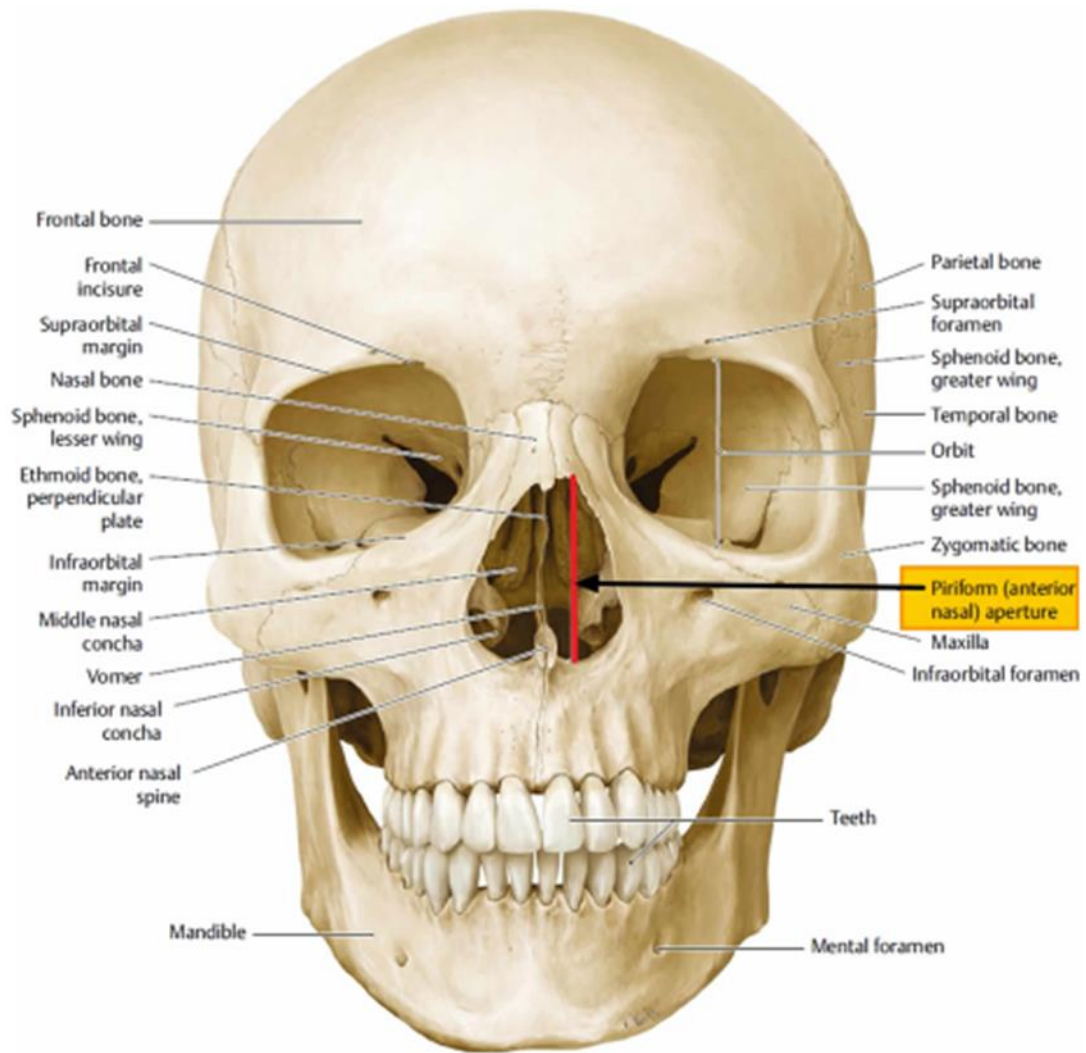


Figure 2.10 Schematic representation of the facial skeleton. The Piriform aperture is highlighted in yellow, and its dimension is defined by the vertical red line.

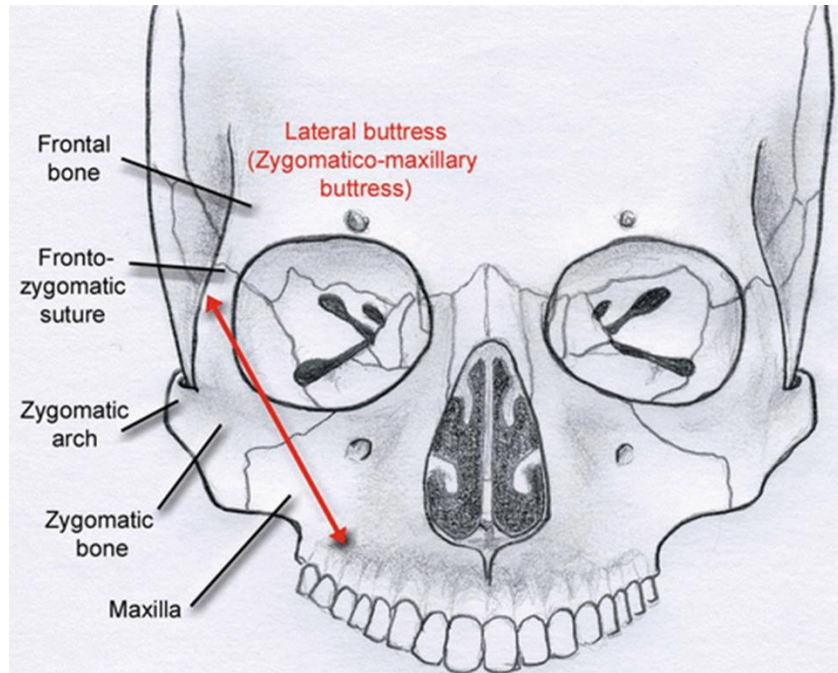


Figure 2.11 Schematic representation of the facial skeleton showing the zygomatic – maxillary buttress between the zygomatic and maxillary bones

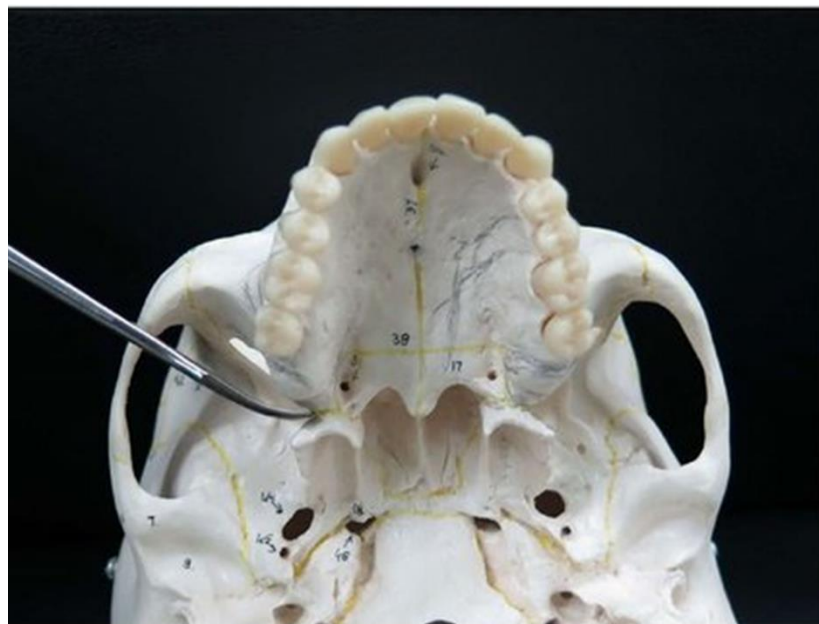


Figure 2.12 Picture of a dry skull (axial view) with an osteotome pointing at the pterygo-maxillary junction.

Initial reports described the mid-palatal suture as the area of greatest resistance to maxillary expansion (Melsen, 1975; Persson & Thilander, 1977; Timms & Vero, 1981).

However, later reports highlighted the zygomatic buttress and the pterygomaxillary junction as critical areas of resistance (Bell & Jacobs, 1979; Kennedy et al., 1976; Lines, 1975). In fact, a study done on rhesus monkeys concluded that reducing or eliminating the resistance to lateral movement by osteotomy allows for movement of the basal bone of the maxilla (Kennedy et al., 1976).

A more invasive approach described by Betts et al in 2016 included a total bilateral maxillary osteotomy from the pyriform aperture to the pterygomaxillary fissure along with a mid-palatal split from the anterior to the posterior nasal spines. The authors recommended sectioning all articulations and areas of resistance— anterior, lateral, posterior—and median support of the maxillary arch. The osteotomy should be placed approximately 4 to 5 mm above the apices of the maxillary teeth. They also recommended releases from the nasal septum and the pterygoid plates (Betts, 2016).

Another more conservative technique would be to avoid performing a palatal split and remove the resistance from the zygomatic buttress only (Glassman et al., 1984; Lehman et al., 1984; Schimming et al., 2000).

Also, opinions differ around the need for a pterygomaxillary disjunction: some advocate that no attempt should be made to separate the maxilla from the pterygoid plates to avoid invasion into the pterygomaxillary junction, as such a separation requires extreme force and usually causes the plates to fracture (Bays & Greco, 1992; Northway & Meade, 1997). Others advise pterygomaxillary disjunction in periodontally

compromised patients, since more pronounced buccal alveolar bending and buccal tipping of the posterior teeth were found when the pterygomaxillary disjunction was not performed (Sygouros et al., 2014).

Some authors recommended only a mid-palatal cut in addition to the transection of the lateral support (Pogrel et al., 1992). Other authors, described 2 paramedian palatal osteotomies from the posterior nasal spine to a point just posterior to the incisive canal instead of the single midline split of the maxilla (Bierenbroodspot et al., 2002; Koudstaal et al., 2006).

Variations in surgical technique have also been recommended based on the patient's age, presence of palatal torus, missing teeth, presence of or tendency toward an anterior open bite, need for a secondary Lefort osteotomy, extremely tapered arch form, and the requirement for only unilateral maxillary expansion (Suri & Taneja, 2008).

It is notable from the analysis of the literature that there is disagreement over the scope and treatment of SARPE. However, there are no conclusive ways to identify the regions that impede lateral maxillary extension or determine the individualization of the surgical incisions. In ideal circumstances, the degree of surgery should be determined by the areas of resistance according to each individual.

2.4.2.3.7 Post-surgical orthodontics

To ensure the postoperative and posttreatment health of the teeth and the gingiva between the central incisors, the patient should be seen regularly by a periodontist.

A significant midline diastema results from expansion, and the central incisors should be moved reciprocally at a controlled pace.

Sometimes clinicians will position a pontic tooth in the midline and gradually grind down its proximal surfaces to allow the central incisors to drift toward one another (Suri & Taneja, 2008).

2.4.2.3.8 Stability

Most studies indicate that surgical expansion is generally more stable than orthopedic maxillary expansion (Bays & Greco, 1992; Kennedy et al., 1976; Kraut, 1984; Lehman et al., 1984). The relapse rates for SARPE vary from 5% to about 25%. These rates are significantly lower than the relapse rate of orthopedic maxillary expansion, which can be as high as 63% (Suri & Taneja, 2008).

According to certain authors, orthodontic treatment can begin without a waiting phase and retention is not necessary for SARPE (Bays & Greco, 1992). Some publications suggested a retention period following expansion ranging from 2 to 12 months (Byloff & Mossaz, 2004; Glassman et al., 1984; Koudstaal et al., 2006; Kraut, 1984; Northway & Meade, 1997).

According to the literature, skeletal relapse varied from 0 to 1.8 mm. The reported relapse generally is around 22% in the inter-canine region, around 18% in the inter-molar region, and 19% at the skeletal level, showing a favorable outcome (Gogna et al., 2020). Furthermore, the benefit in using a retention device post SARPE to prevent relapse is unclear based on the qualitative evaluation of two randomized clinical trials that researched this particular question (Aloise et al., 2007; Prado et al., 2014).

Most studies on SARPE mentioned relapse as a problem that the clinician should be aware of, yet they also stated that recurrence rates were minimal.

Few studies mention the need to overexpand when performing SARPE (Kraut, 1984; Lehman et al., 1984; Pogrel et al., 1992).

2.4.2.3.9 Risks, limitations and complications of SARPE

Generally, SARPE operations have been reported to have low morbidity, especially when compared to other orthognathic surgical procedures (Bays & Greco, 1992).

However, when recommending SARPE to a patient, the surgeon and the orthodontist must be aware of the numerous side effects that have been reported. SARPE complications that have been documented in the literature include (Suri & Taneja, 2008):

1. Significant hemorrhage
2. Gingival recession
3. Root resorption
4. Injury to the branches of the maxillary nerve
5. Infection
6. Pain
7. Devitalization of teeth and altered pulpal blood flow
8. Periodontal breakdown
9. Sinus infection
10. Alar base flaring
11. Extrusion of teeth attached to the appliance
12. Relapse
13. Unilateral expansion

14. Hemorrhage which can be life threatening or require blood transfusions and an additional hospital stay.

15. The maxillary articulation can have abnormal fractures occasionally. They are particularly frequent when areas of resistance persist.

Signs of aberrant fractures include: increased mobility, gingival recession, dehiscence, and periodontal defects on the incisors (Suri & Taneja, 2008).

Minor complications were more common when the pterygomaxillary disjunction was not performed, and asymmetric expansion was more common when the expansion rate was less than 0.5 mm per day (Carvalho et al., 2020).

Additional complications that are related to the expansion appliance include:

1. Impingement on palatal soft tissue (palatal tissue irritation): About 1.8% of patients have frank aseptic tissue necrosis, and at least 5% of them have some palatal mucosal ulcers (Lehman et al., 1984).
2. Loosening (more common with bone-borne distractors)
3. Breakage and stripping or locking of the appliance screw

2.4.2.4 Minimally invasive SARPE

A case report of 283 patients (Hernandez-Alfaro et al., 2010) studied a technique with incision performed horizontally to reach the level of the laterals. Osteotomies of lateral walls and pterygoid disjunction were applied in all cases (Fig. 2.13). Patients were discharged after recovery from sedation. This method sought to combine two aspects: it allowed rapid intervention under local anesthesia plus sedation, and a minimal approach with a total liberation of the maxillary resistances (piriform aperture pillars, zygomatic buttresses, mid-palatal suture, and pterygoid junctions). The minimal

approach and incision associated with this technique ensured vascular support to the maxilla via the vestibular corridors.

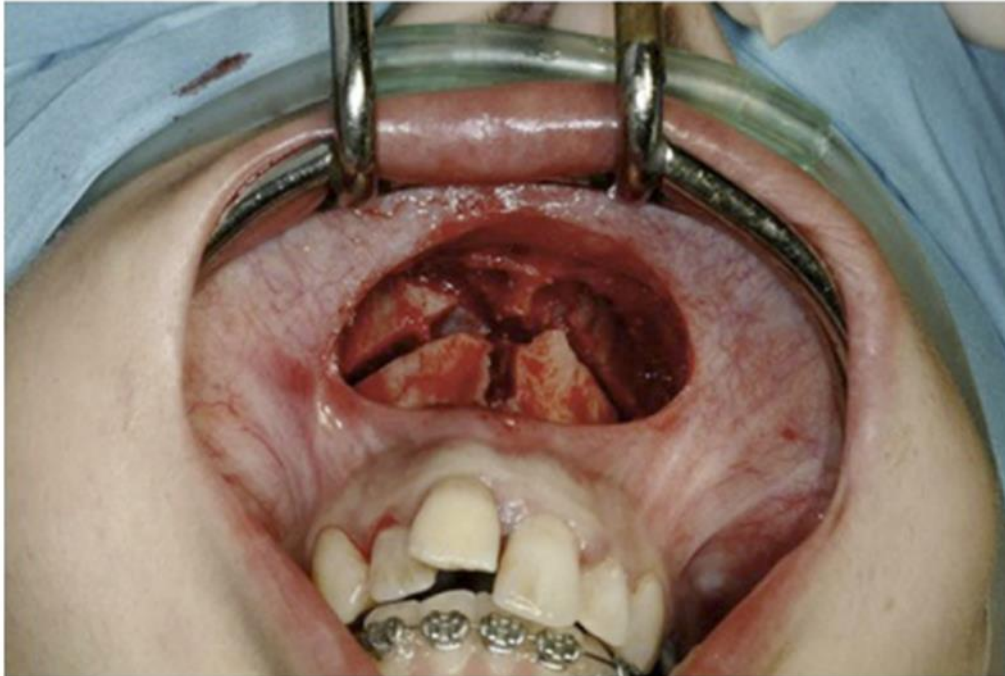


Figure 2.13 Surgical field when the osteotomies have been completed (Adapted from (Hernandez-Alfaro et al., 2010))

Also, Betts et al. described SARPE with a piezoelectric device in 6 patients, with local anesthesia plus oral sedation (Betts et al., 1995).

In a more recent study, patients underwent MISMARPE (minimally invasive surgical mini screw assisted rapid palatal expansion) with minimally invasive osteotomies under local anesthesia. Four osteotomies were made: one sub spinal osteotomy to separate the anterior nasal spine, one vertical midline osteotomy extended into the nasal floor to the level of the medium thirds of the central incisors' roots (Fig. 2.14 B), and two horizontal lateral osteotomies extending from the piriform aperture to

the posterior maxilla (one per side) (Fig 2.14 C). This technique does not involve pterygomaxillary disjunction (Camps-Perepérez et al., 2023).

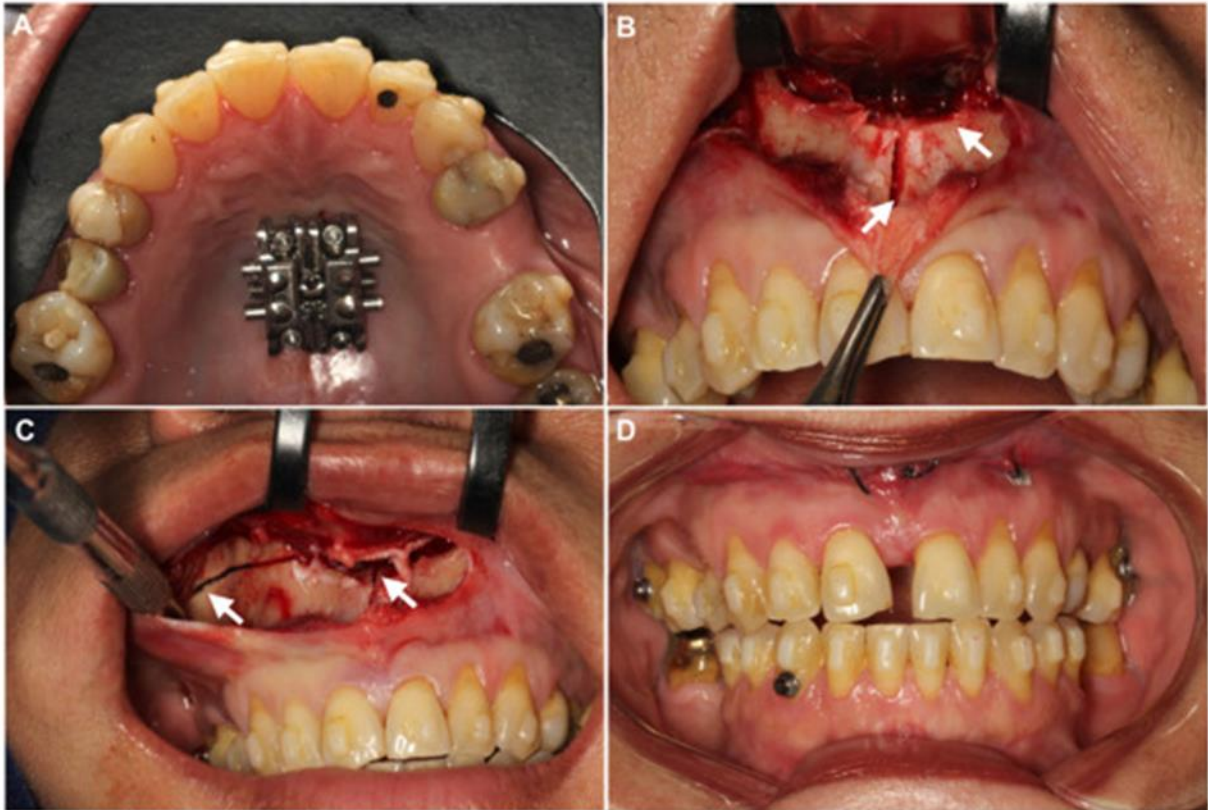


Figure 2.14 MISMARPE technique. (A) Expander in place; (B) Sub spinal osteotomy and vertical osteotomy; (C) Horizontal osteotomy and intranasal osteotomy; (D) Expander activation and suture.

A different study applied the “Twist technique” for pterygomaxillary disjunction in minimally invasive Le Fort I osteotomy (Hernández-Alfaro & Guijarro-Martínez, 2013). The pterygomaxillary osteotomies of the classic lateral approach were not performed. Instead, the osteotome was driven through the horizontal osteotomy, back to the posterior wall of the maxillary sinus and then, at the level of the zygomatic buttress, it was twisted, resulting in a non-total down- fracturing of the maxilla and achieving the pterygomaxillary suture disjunction (Fig. 2.15). The surgical protocol analyzed in this

study was performed with total release of the anterior, lateral, posterior, and medial buttresses, proving to be an effective method to correct maxillary transverse discrepancies greater than 5 mm in patients without growth. With a standardized minimally invasive technique, it was possible to reduce surgical morbidity when performed in an outpatient setting under sedation, resulting in less oedema and impairment of nerve function in the nasolabial region and preserving muscle function. Moreover, this improves the patient quality of life, with a postoperative period with a lower chance of complications and a faster recovery.



Figure 2.15 Skull base model. The osteotome progresses along the horizontal osteotomy from the pyriform buttress back to the pterygomaxillary junction (Hernández-Alfaro & Guijarro-Martínez, 2013).

2.5 Expansion appliance during SARPE: Bone borne vs tooth borne expander

Tooth-borne appliances deliver stresses to the roots and periodontal ligaments of the supporting teeth as well as the alveolar bone during expansion. The side effects are presumably due to the tooth-borne anchorage of conventional appliances. Also, the bony movement is not retained during the consolidation period. They produce greater

loss of anchorage and more skeletal relapse both during and after expansion (Mommaerts, 1999). This led to the introduction of the first bone-borne appliance (distractor) in 1999, which delivers the expansion force directly to the maxillary bone and would avoid the negative orthodontic and periodontal effects (Mommaerts, 1999).

The use of a bone-borne titanium device with interchangeable expansion modules was suggested rather than a conventional tooth-borne appliance, for two other reasons:

1. Higher incidences of cortical fenestration and buccal root resorption are observed with tooth-borne appliances compared with absolute bone-borne appliances.
2. Bone borne distractor can be used in patients with missing teeth even edentulous patients (Hernández-Alfaro & Valls-Ontañón, 2021; Mommaerts, 1999; Suri & Taneja, 2008).

Some studies results suggest that the selection of the type of expander depends on the location of the greater maxillary constriction area in each patient. Moreover, tooth-borne expanders are preferable for patients with expansion requirements in the posterior region while bone-anchored expanders are more suitable for individuals with maxillary atresia in the anterior region. Furthermore, the choice of expander type should not be influenced by dental inclination, as both bone-borne and tooth-borne expanders showed similar variations in the inter-dental and inter-gingival distances (Barone et al., 2020; Koudstaal et al., 2006).

2.5.1 Design of bone-borne appliances

There are now a variety of commercially available bone-borne distractors, these include:

1. The transpalatal distractor (Fig. 2.16 A)
2. The Magdenburg palatal distractor (Fig. 2.16 B)
3. The Rotterdam palatal distractor (Fig. 2.16 C)

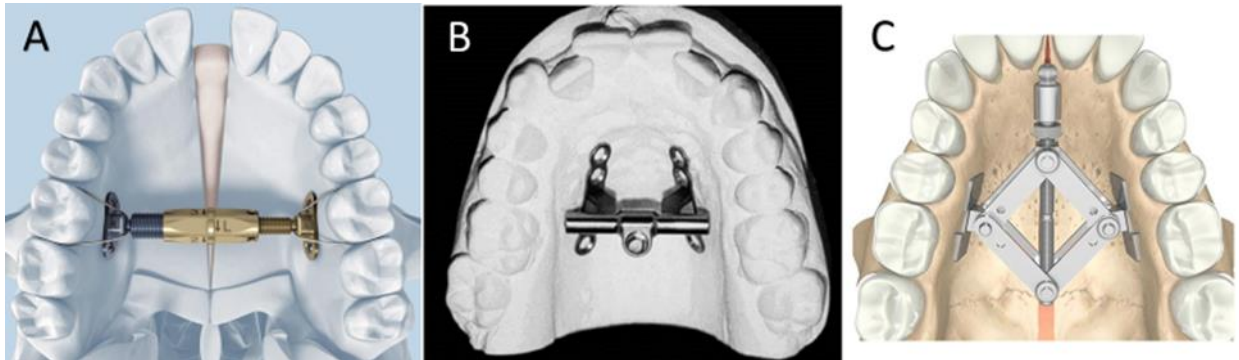


Figure 2.16 Illustration of the different types of bone – borne expanders: (A) The trans palatal distractor; (B) The Magdenburg palatal distractor; (C) The Rotterdam palatal distractor.

2.5.2 Contraindications of using bone-borne appliances

1. Patients with extremely low palates, because the nails of the abutment plates loosen more easily which causes the distractor to be unstable.
2. Patients with immunodeficiency conditions and prior radiation therapy

2.5.3 Appliance activation

Most authors recommend that appliance activation should be started intraoperatively. This is done to ensure that the appliance is stable and that the areas of resistance of the 2 halves of the maxilla have been removed. Postoperative protocols vary between authors, and the activation rates are from 0.25 to 1 mm per day (Suri & Taneja, 2008).

The surgical corticotomy and the initial appliance activation intraoperatively are followed by a period of rest before starting expansion of the appliance. This rest period is called the latency period. This gives the tissues time to form a callus but is too short to allow for consolidation (Koudstaal et al., 2006). Callus distraction has been reported to create a tissue that readily ossifies and stabilizes and thus provides increased stability (Karp et al., 1992). Latency period varies from 2 to 7 days according to different authors (Suri & Taneja, 2008).

2.6 Finite Element Analysis (FEA)

2.6.1 Principles and applications of FEA in Orthodontics

The finite element method (FEM) is an engineering tool used to calculate the stress and deformation of complex structures and has been widely used in orthodontic research. It has demonstrated its value as a tool in orthodontic research by highlighting several points, including stress distribution areas in the periodontal ligament and alveolar bone during tooth movements; direction of tooth displacement; the ideal position of orthodontic appliances during specific mechanics; areas most likely to present root resorption, the stress distribution on the archwires. Because this method is precise, noninvasive, regulates the study variables, and offers quantitative data regarding internal nasomaxillary complex structures like the periodontal ligament, it is able to address the drawbacks of other experimental approaches. The solution, however, necessitates computer engineering expertise because it runs on very specialized software.

2.6.2 FEA of Surgically assisted rapid palatal expansion

The surgical stage of SARPE can be performed using several techniques. Those with a larger number of osteotomies have been considered essential in the treatment of older patients, because they weaken the pillars that strengthen the face and decrease the resistance to expansion found in adults. Osteotomy variations change the expected pattern of stress dissipation. For this reason, finite element studies evaluated the results on bony and dental structures when using different types of expanders and performing various configurations of osteotomies.

Some only included bone-borne expanders in their variations but with different areas of support: alveolar ridge or palatal bone-borne appliances (Möhlhenrich et al., 2017) (Fig. 2.17).

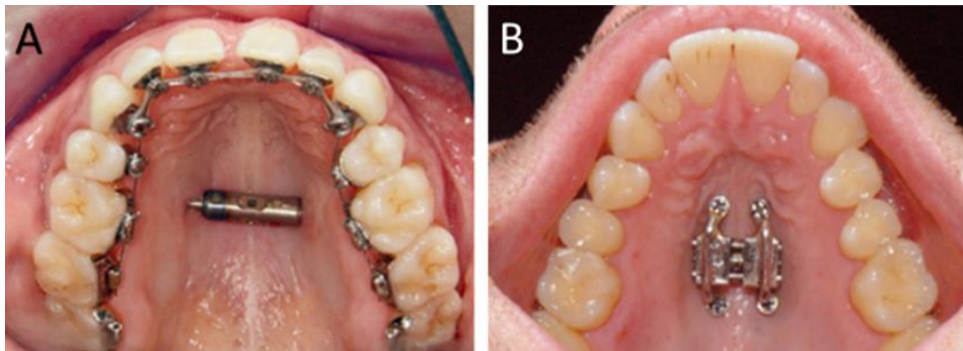


Figure 2.17 Clinical photographs of the two different types of bone expander: (A) palatal bone-borne device; (B) alveolar ridge bone-borne device (adapted from (Möhlhenrich et al., 2017)).

Möhlhenrich et al. evaluated different combinations of osteotomies: exclusive median osteotomy, median osteotomy with additional lateral osteotomy then finally, medial and lateral osteotomy with additional pterygomaxillary disjunction (Holberg et al., 2007; Möhlhenrich et al., 2017) (Fig. 2.18).

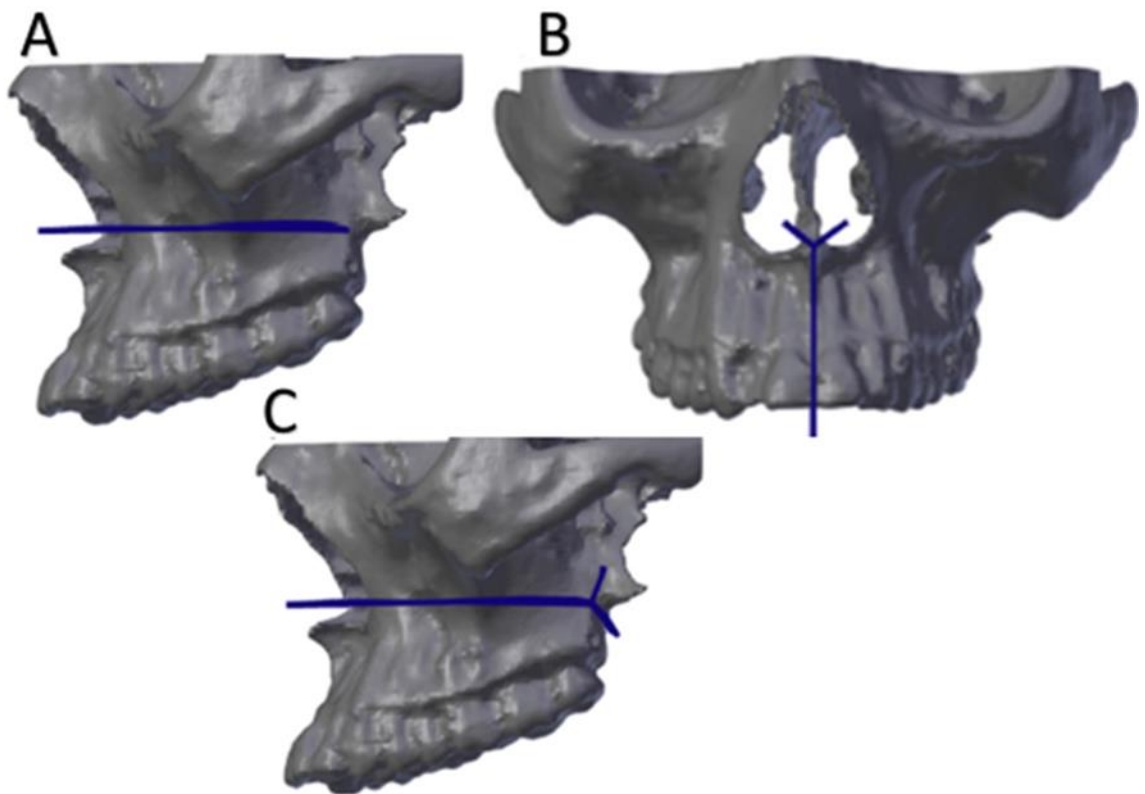


Figure 2.18 The three different types of osteotomies for the SARPE procedure, visualized as blue lines with a thickness of 1 mm, as modelled in the simulations: (A) median osteotomy; (B) additional lateral osteotomy; (C) additional lateral osteotomy with pterygomaxillary separation (adapted from (Möhlhenrich et al., 2017))

Möhlhenrich et al. noted a gradual decrease in stress in the midface and maxilla with each additional osteotomy. Especially when adding the pterygomaxillary disjunction, which was the most effective. Also, when all osteotomies are performed in one model, the area of maximum displacement is at the level of first and second molars and this may suggest that the combination of all three of the osteotomies used here are helpful when try to increase the amount of expansion in the posterior area. However, Holberg et al. reported an increase in von Mises stresses from 20.1 MPa (without surgery) to 180.8 MPa (with conventional surgery) after surgical weakening of the lateral maxillary sinus walls, specifically at the anterior wall of the maxillary sinus.

However, a decrease in stress in other structures (zygoma and nasofrontal areas) was observed. (Holberg et al., 2007) (Fig. 2.19 and Fig. 2. 20).

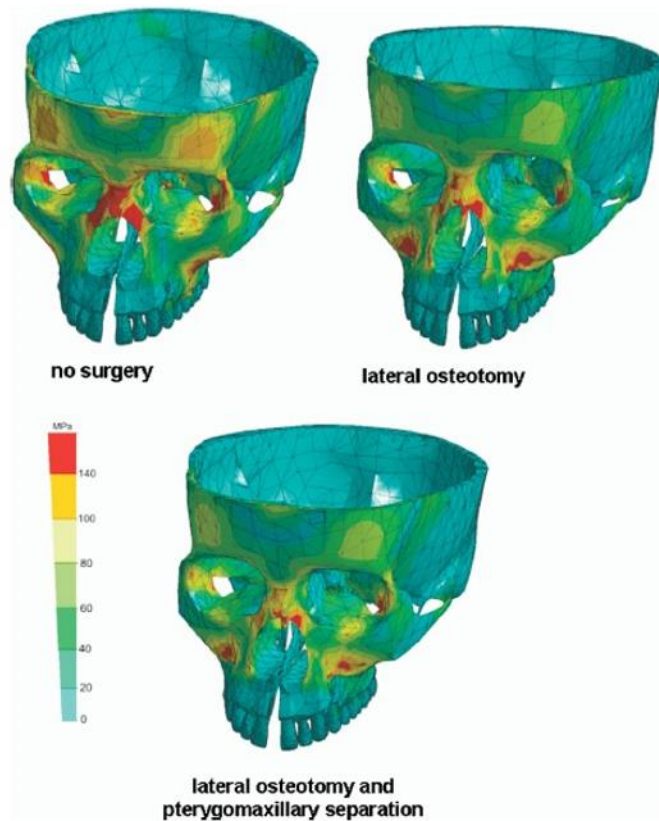


Figure 2.19 Stress distributions in the midface with rapid maxillary expansion (5 mm) depending on the surgical procedure (adapted from Holberg et al., 2007).

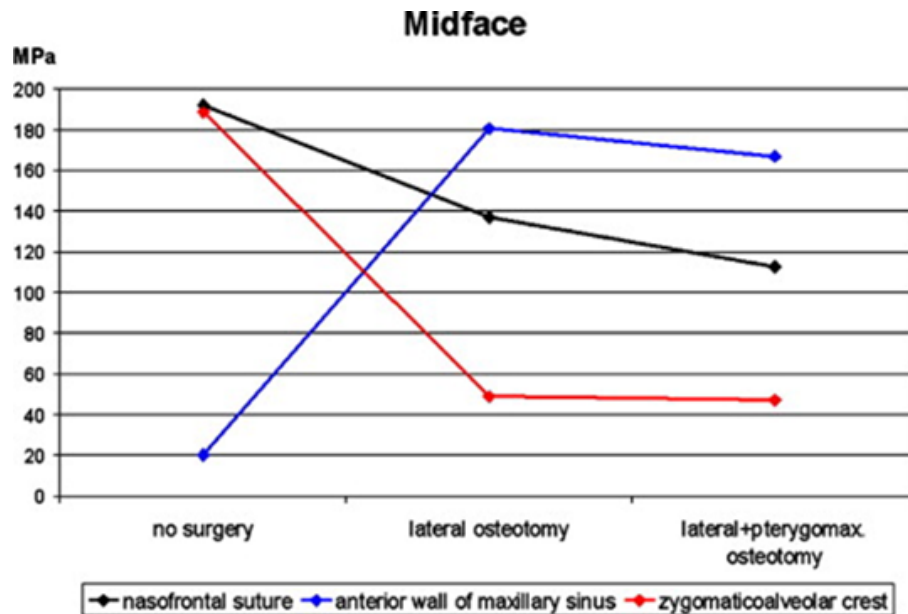


Figure 2.20 Von Mises stresses at 3 anatomic structures of the midface with different surgical procedures. (Adapted from (Holberg et al., 2007).

Zai et al. (Zai et al., 2015), evaluated the application of a LeFort 1 osteotomy on different models, including a variation of additional osteotomies:

Control group: No surgery

Test group: With surgery

1. Test 1: Le-fort I Osteotomy

2. Test 2: Le-fort I Osteotomy + Para-median Osteotomy

3. Test 3: Le-fort I Osteotomy + Pterygomaxillary separation

4. Test 4: Le-fort I Osteotomy + Para-median Osteotomy + Pterygomaxillary separation

(Fig. 2.21).

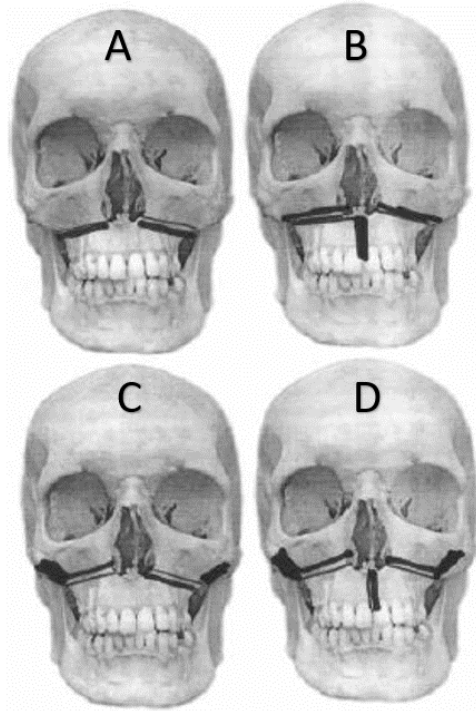


Figure 2.21 (A) Test 1: Le-fort I Osteotomy (B) Test 2: Le-fort I Osteotomy + Para-median Osteotomy (C) Test 3: Le-fort I Osteotomy + Pterygomaxillary separation and (D) Test 4: Le-fort I Osteotomy + para-median Osteotomy and Pterygomaxillary separation (adapted from Zai et al., 2015).

The results indicated that a stress concentration of $900 \times 10^{-3} \text{ kgf/mm}^2$ at the area of the pterygomaxillary junction. Le-fort I osteotomy and pterygomaxillary separation greatly relieved the level of stress to $153.03 \times 10^{-3} \text{ kgf/mm}^2$ at first molar, premolar and hard palate. They observed that stress concentration was reduced to the level of $0.0014 \times 10^{-3} \text{ kgf/mm}^2$ at the area where pterygomaxillary separation was applied (Zai et al., 2015).

Similarly, different groups who included similar variations in their protocol found that when applying Lefort I osteotomy and pterygomaxillary separation in the same model, the mean stress in the maxilla was the greatest. This increase of maxillary stress may be correlated with the decreased stress of suture and thus re-distribution of stress inside the palatal vault (Han et al., 2009; Zawisłak et al., 2020). Dalband et al.

highlighted a gradual decrease in stress values around the palatal area of the maxillary bone with each additional osteotomy to the LeFort osteotomy (Dalband et al., 2015).

An opposing outcome was noted in another research: the model with median and lateral osteotomies **without** pterygomaxillary disjunction presented the highest stress values at the medial pterygoid plate, mini-screw area, and lateral pterygoid plate (350.8 MPa, 306.7 MPa and 67.99 MPa, respectively). A decrease in stress to nearly zero at medial pterygoid plate, mini-screw region, lateral pterygoid plate, first molar tooth and frontozygomatic suture was noted after adding the pterygomaxillary disjunction (Koç & Jacob, 2022).

Different LeFort osteotomies anatomies were compared as well: with or without the presence of a step in the zygomaticomaxillary buttress. Results show that the steps in the zygomaticomaxillary buttress and the pterygomaxillary disjunction seem to be important to decrease the harmful dissipation of tensions during SARPE (de Assis et al., 2014).

Furthermore, another study compared the application of a mid-palatal cortico-puncture and cortico-puncture on the LeFort I osteotomy line with a traditional LeFort osteotomy (with and without a pterygomaxillary disjunction), the findings indicated that traditional LeFort cuts were effective in reducing stress on the teeth, but the cortico-puncture application affected neither the stress values on the teeth nor the transverse displacement in the tooth-borne expanders (N. Kaya et al., 2023).

Different research compared five designs of rapid maxillary expanders: a tooth-borne hyrax expander; a bone-borne expander; and 3 bone-borne surgically assisted modalities: separation of the mid-palatal suture, added separation of the pterygomaxillary sutures, and added LeFort I corticotomy. They asserted that a less

invasive technique that involves an osteotomy at the mid-palatal suture coupled with a bone-borne device is just as effective when used alone as it is when combined with additional LeFort I corticotomy or additional pterygomaxillary suture separation (S. C. Lee et al., 2014a).

Han et al. measured displacement in 5 groups with different osteotomy configurations: including control group (Group I) and four experimental groups (Group II to V). The experimental groups were as follows; Group II (Le Fort I osteotomy), Group III (Le Fort I osteotomy and paramedian osteotomy), Group IV (Le Fort I osteotomy and bilateral pterygomaxillary separation), and Group V (Le Fort I osteotomy, paramedian osteotomy and bilateral pterygomaxillary separation). They showed that from Group I to Group V, the displacement increased posteriorly on the x-axis (transverse axis). In the Group V, the area of maximum displacement moved from first premolars and first molars to first and second molars (Fig. 2.22) and this may suggest that the combination of all three of the osteotomies used here are helpful when trying to increase the amount of expansion in the posterior area (Han et al., 2009).

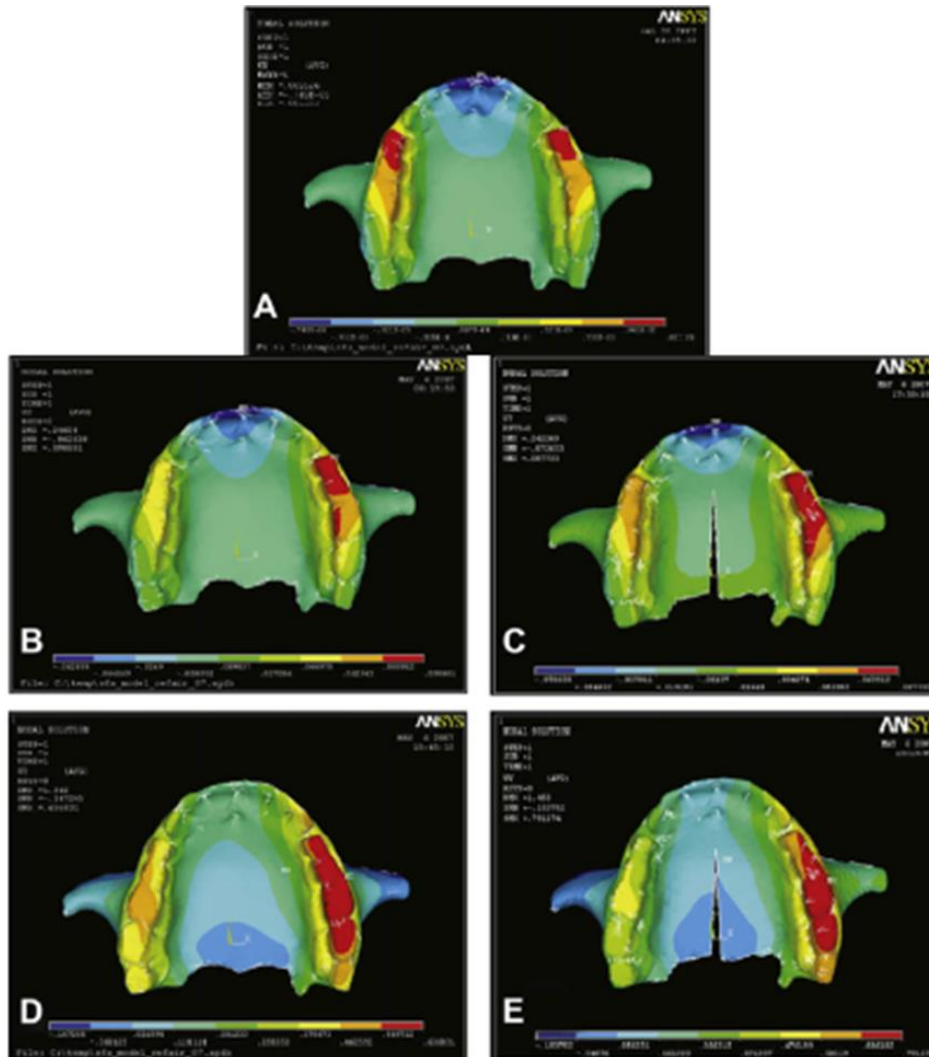


Figure 2.22 Displacement of maxilla in the y-axis with SARME by different surgical procedures (top view). (A) Group I (no surgery); (B) Group II (Le Fort I osteotomy); (C) Group III (Le Fort I osteotomy + paramedian osteotomy); (D) Group VI (Le Fort I osteotomy + pterygomaxillary separation); (E) Group V (Le Fort I + paramedian osteotomy + pterygomaxillary separation (adapted Han et al., 2009).

Another study highlights a more parallel transverse displacement after median and lateral osteotomies with PMS disjunction while the models without PMS disjunction showed a dental transverse displacement decreasing gradually from the central incisor to the second molar. This explains that when transverse maxillary expansion is needed more anteriorly than posteriorly, only lateral and median osteotomy should be performed without PMS osteotomy (Fig. 2.23), while additional PMS separation should

be sufficient for a parallel transverse maxillary expansion (Fig. 2.24) (Koç & Jacob, 2022).

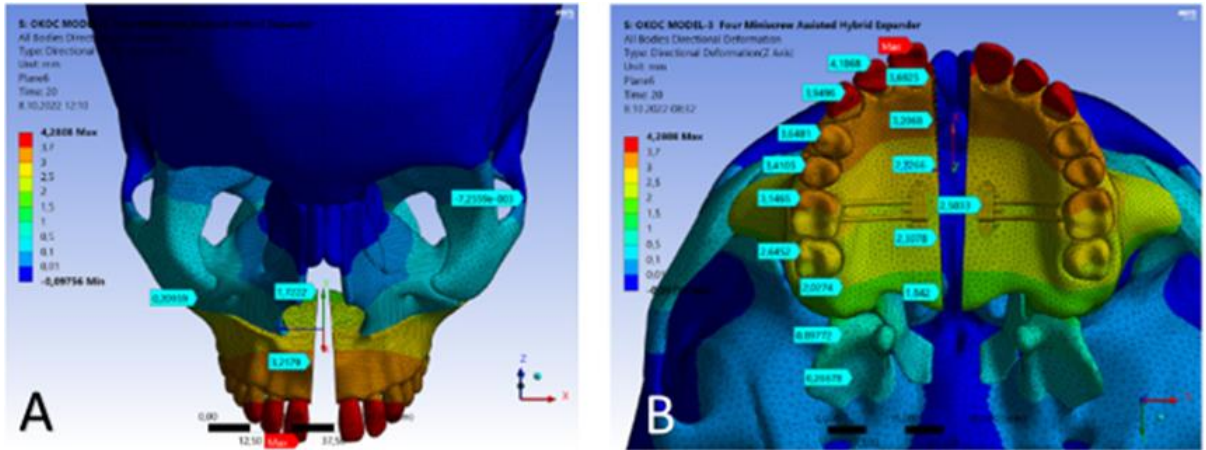


Figure 2.23 Displacement of the landmarks due to SARPE after 5 mm activation of the expander apparatus for the model simulated with median and lateral osteotomies without PMS disjunction: frontal view simulation. (A) and occlusal view simulation; (B) V – shaped opening of the mid-palatal suture can be observed (wider anteriorly than posteriorly) (Adapted from Koç & Jacob, 2022)

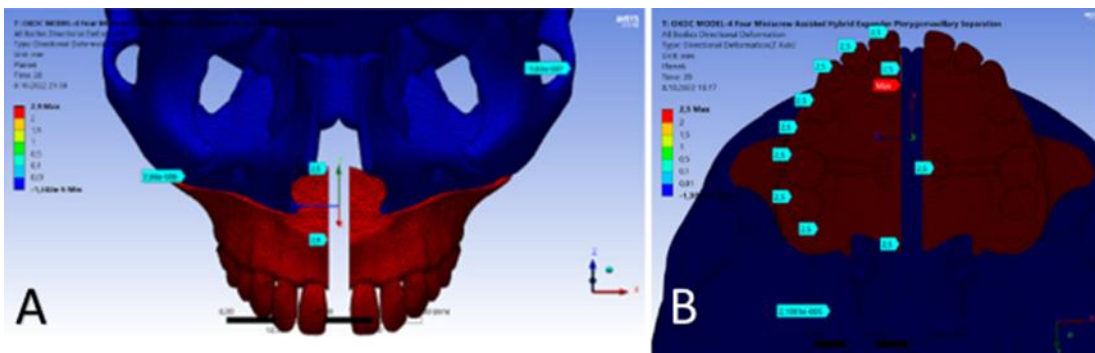


Figure 2.24 Displacement of the landmarks due to SARPE after 5 mm activation of the expander apparatus for the model simulated with median and lateral osteotomies with PMS disjunction: frontal view simulation (A) and occlusal view simulation (B). More parallel opening of the mid-palatal suture is noted (adapted from (Koç & Jacob, 2022).

It should be noted that all these investigations used a single finite element model to simulate their osteotomies, ignoring any individual variations. A more detailed analysis

of stress and displacement on models with anatomical variations is needed to evaluate the difference in response and explore clinical implications.

2.7 Significance

Although static finite element analysis assessment may not accurately represent tooth movement, however, by partitioning the geometry into its component parts and validating the assumptions made about these parts based on clinical data, the outcomes should be more representative of the clinical setups.

On an additional level, the inclusion of individual variation derived from real human material will enhance the method and bring it closer to clinical reality. The context of variability of response has not yet been addressed by any FEA investigation on surgically assisted rapid palatal expansion.

Bone property variation was not considered as a factor influencing the outcomes in prior FEA investigations. This study creates a link between digital finite element models and real clinical setups by taking into consideration changes in cortical bone thickness measured in real individuals. While earlier research assessed the stress generated by various SARPE techniques, they failed to take cortical bone thickness into account.

Earlier research incorporated information on bone properties to assess tooth movement solely, such as distalization (Ammoury et al., 2019), the impact of bone attributes like bone thickness, on skeletal response (stress and displacement) to orthopedic movements has never been researched before.

Our research further seeks to examine the mechanical impact of a mid-palatal osteotomy that is performed with minimally invasive techniques. As opposed to other studies (Han et al., 2009; Koç & Jacob, 2022; S. C. Lee et al., 2014a) where the maxilla

was split in two separate entities by simulated mid-palatal osteotomies. The latter is considered an invasive approach that calls for general anesthesia, while a less extended cut could minimize the morbidity, the burden of general anesthesia as well as the cost of the procedure.

The anatomy of the maxilla was segmented into distinct components (specified as masks) in our models, and a numerical result was generated for each part, which was not applied in previous studies, where the maxilla was evaluated as a single entity.

2.8 Specific Objectives

- 1- Evaluate the success of a minimally invasive mid-palatal sagittal osteotomy in reducing stress and allowing adequate expansion
- 2- Assess the relationship between bone thickness and the amount of stress generated on the corresponding bone structures during expansion
- 3- Assess the relationship between bone thickness and the amount of skeletal expansion in the different models/variations of osteotomies
- 4- Evaluate the relationship of stress with the amount of expansion
- 5- Investigate a potential pattern between amount of stress and expansion with respect to the bone thickness variations between the models
- 6- Define the model with the maximum amount of expansion
- 7- Assess the relationship of different types and combination of osteotomies with the amount of stress
- 8- Assess the relationship of different types and combination of osteotomies with the amount of expansion.

CHAPTER 3

MATERIALS AND METHODS

3.1 Materials

In our investigation, we adapted the 3D models of the maxillary arch made by Ammoury et al. (Ammoury, 2017). These models were created originally from a pre-treatment cranial Computed Tomography (CT) scan of an adult patient undergoing radiologic evaluation (at the Department of Radiology at the American University of Beirut Medical Center). CT scan imaging was used because it delivered high contrast quality which helps differentiate the trabecular from the cortical bone. CT scans provide better resolution and more importantly better contrast compared to the regular CBCT usually requested in clinical settings. In addition, the CT scan is a powerful non-destructive tool that allows for longitudinal diagnoses of bone properties (e.g., density). A Class I occlusion with midlines on, parallel roots, and a well-aligned full dentition were all revealed by the scan, indicating a normal occlusion and perhaps previous orthodontic treatment. Thirteen models were created using the 13 different anatomical variables associated with bone morphology. The cortical bone thickness at the incisors, premolars, and molars, which are each separated into buccal and palatal parts, varies between these models (Fig. 3.1).

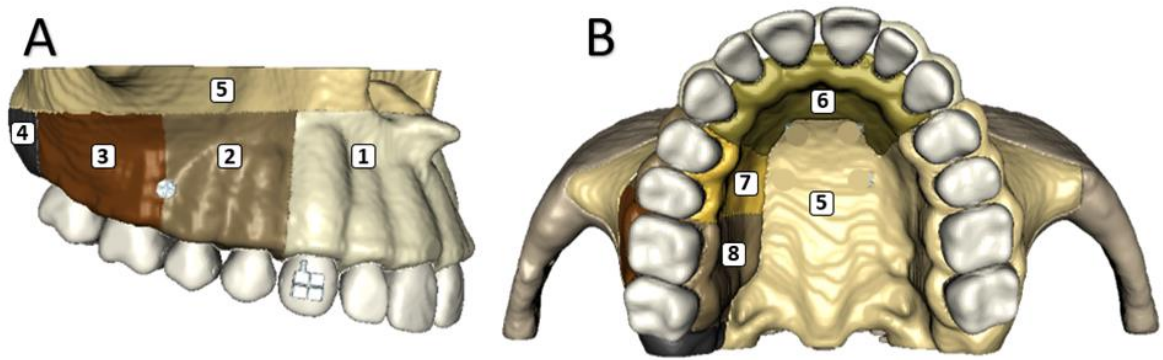


Figure 3.1 (A) Lateral view of the maxillary arch with 1- Buccal incisors region; 2- Buccal premolars region and 3- Buccal molars region; 4- Tuberosity region; 5- Maxilla. (B) Occlusal view of the maxillary arch with 6- Palatal incisors region; 7- Palatal premolars region and 8- Palatal molars region. A mini – screw is simulated between the roots of second premolar and first molar, and a bonded bracket is simulated on the buccal surface of the canine (Ammoury et al., 2019).

3.2 Methods

3.2.1 Adaptation of the model to our study

The model’s limit was extended cranially in our study: we included an additional mask called *Maxillary Extension* that represented the area extending cranially from the Maxilla mask (Fig. 3.1 A; B [5]) until the lower orbital rim on both the right and left sides (Fig 3.2). The mask was created using the “Paint with Threshold” tool with a lower value of 398 and upper value of 3,071 Hounsfield units (HU).

Smoothing filters were applied to improve the surface quality.

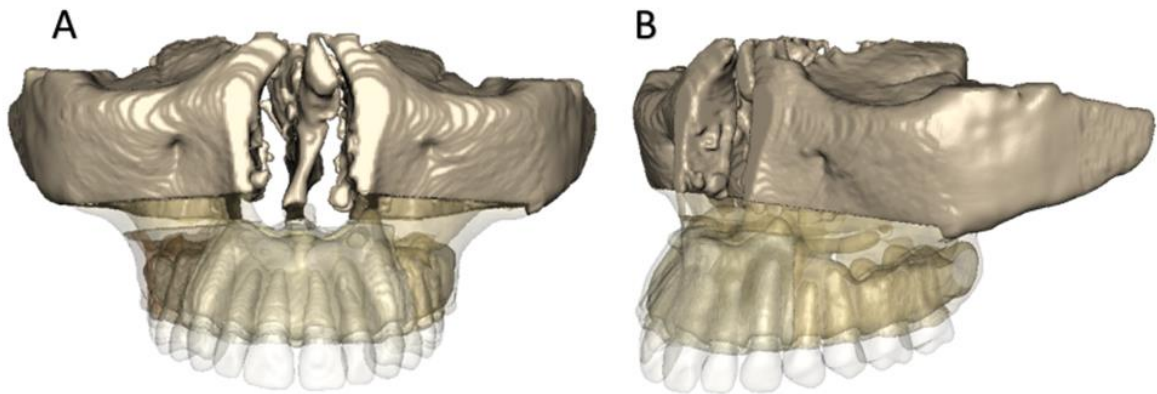


Figure 3.2 (A) Frontal view and (B) Lateral view of the model showing the “Maxillary Extension mask” in opaque color.

3.2.2 *Expansion Setups*

Five distinct setups are included in our study, each of which corresponds to a different clinical setup (Table 3.1):

1. The initial setup, in which no cuts were made, and a bone-borne expander was simulated, is referred to as our control model (Fig. 3.3).
2. The second setup incorporates a bone-borne expander and a mid-palatal sagittal osteotomy only, which is considered a minimally invasive SARPE cut. This cut is done on the mid-palatal suture extending from the incisive foramen to a point between first and second molars (Fig. 3.4).
3. The third setup includes a bone-borne expander and the mid-palatal sagittal osteotomy with an additional osteotomy at the level of the anterior nasal spine extending from ANS point to the cervical part of the central incisors between the roots (Fig. 3.5).
4. The fourth setup consists of a bone-borne expander and the mid-palatal sagittal osteotomy with an osteotomy at the level of the anterior nasal spine and lateral cuts

extended 5 mm above the apices of the teeth from the distal of the canine to the mesial of the second molar (Fig. 3.6).

5. The fifth setup includes bone-borne expander and a mid-palatal sagittal osteotomy, an osteotomy at the level of the anterior nasal spine and a Lefort cut with a pterygomaxillary disjunction (Fig. 3.7).

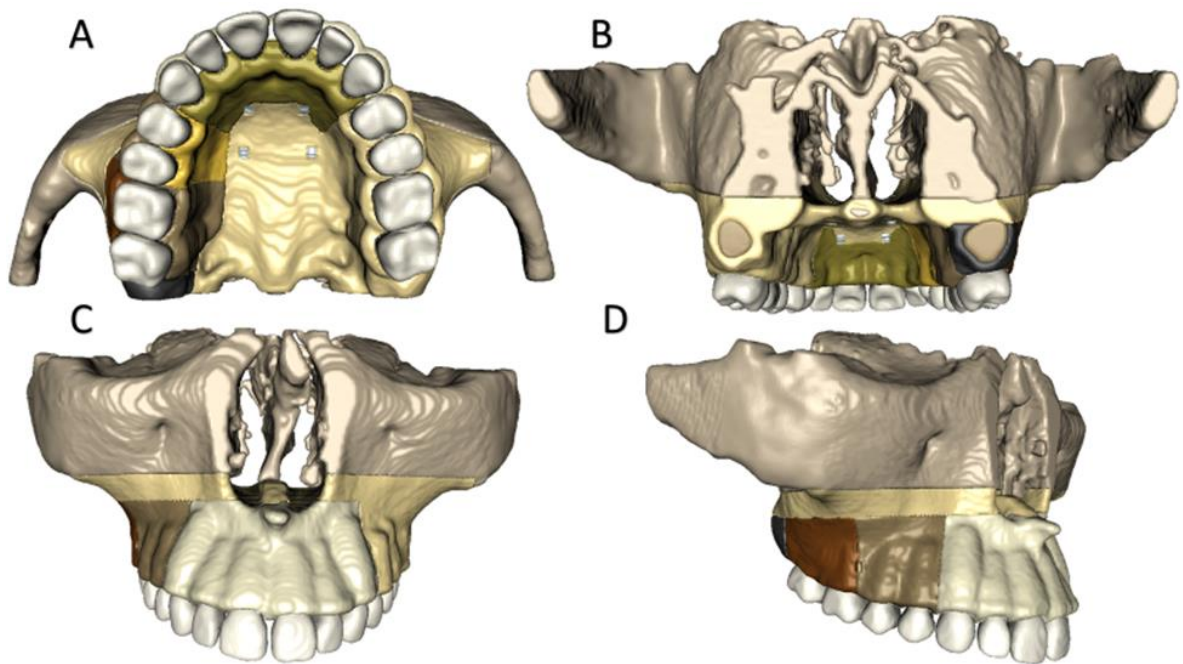


Figure 3.3 Maxillary model of setup 1 (control model): (A) Occlusal view (B) Posterior view (C) Anterior view (D) Right side lateral view

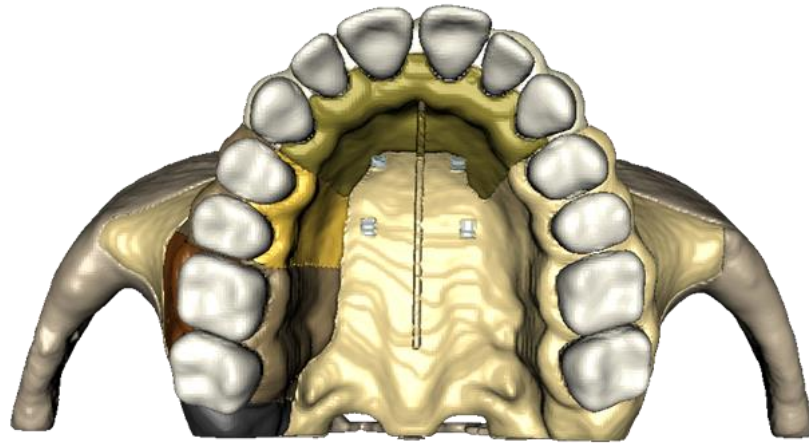


Figure 3.4 Maxillary model of setup 2: Palatal view showing the mid-palatal sagittal osteotomy

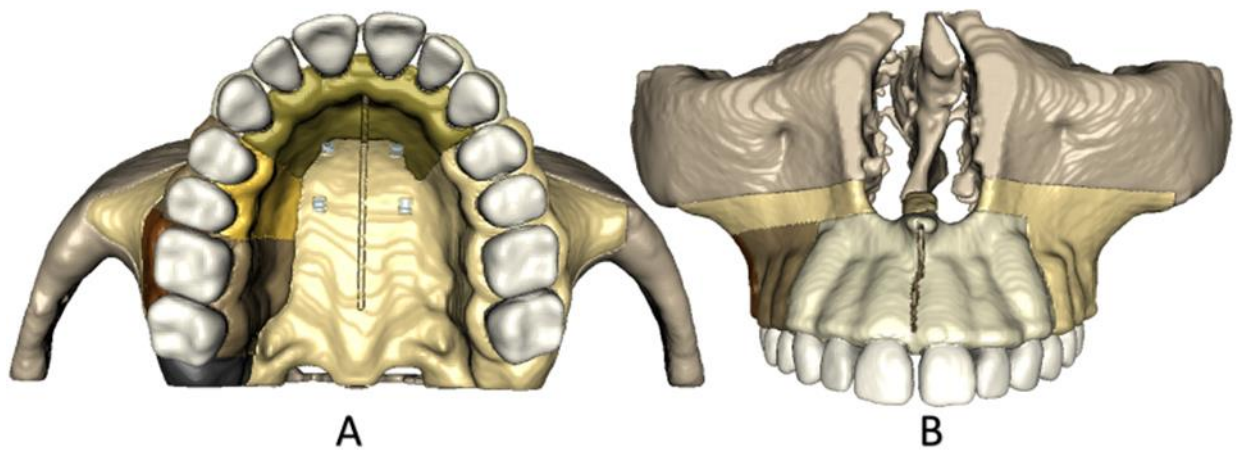


Figure 3.5 Maxillary model of setup 3: (A) Occlusal view of the maxillary model showing the mid-palatal sagittal cut; and (B) Frontal view showing the anterior maxillary cut below ANS

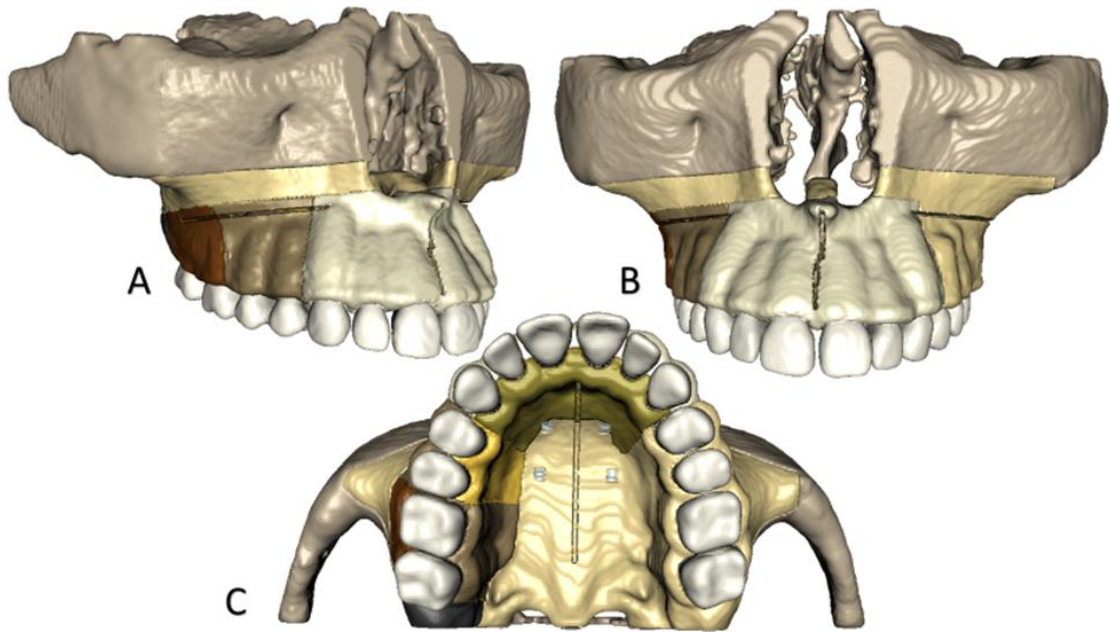


Figure 3.6 Maxillary model of setup 4: (A) Lateral view that shows the lateral and ANS osteotomy; (B) Frontal view; (C) Occlusal view that shows the mid-palatal sagittal osteotomy

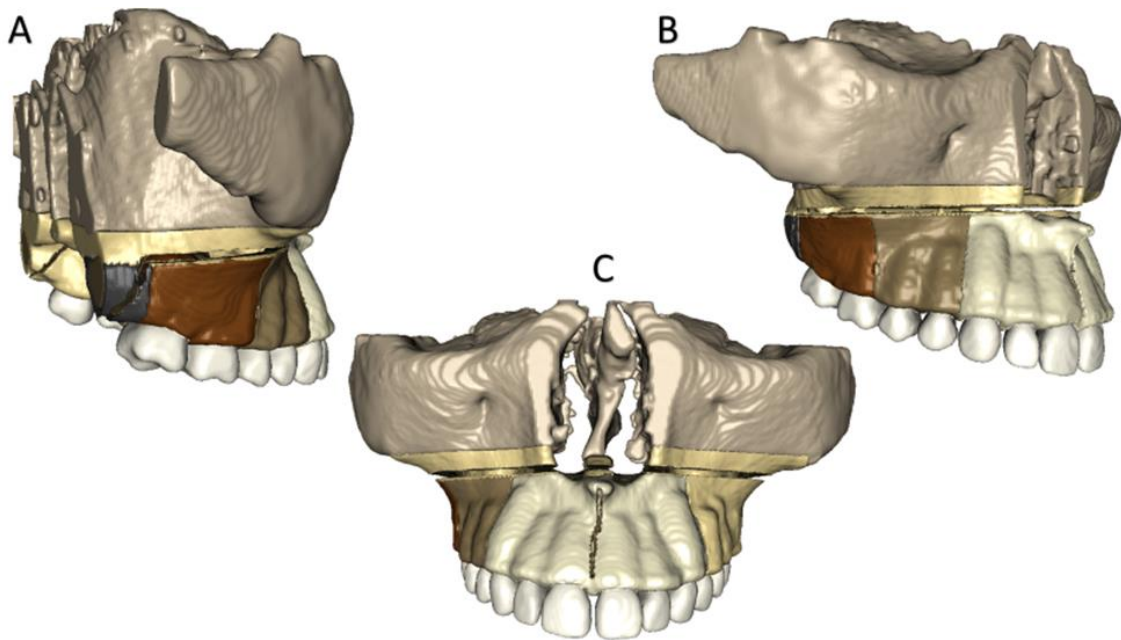


Figure 3.7 Maxillary model of setup 5: (A) Right lateral posterior view that shows the pterygomaxillary disjunction; (B) Right lateral view; (C) Frontal view

Each of the 13 models that Ammoury et al. provided were subjected to the five setups, resulting in a total of 65 distinct models that were used in our study.

Table 3.1 The different included setups

<i>Setup 1</i>	Bone – borne expander with no osteotomies (control)
<i>Setup 2</i>	Bone – borne expander + Mid-palatal sagittal osteotomy
<i>Setup 3</i>	Setup 2 + osteotomy at ANS
<i>Setup 4</i>	Setup 3 + lateral osteotomies
<i>Setup 5</i>	Setup 3 + LeFort osteotomy

Software ScanIP TM S-2021.06 Build 1266 was used to create each model. (Simpleware, Synopsys, Mountain View, CA, USA). On every model, the screw and the bracket were removed, and the surfaces were adjusted to fill any resulting cavities.

A separate mask was created using the *paint tool* with the square shaped cursor, to represent the anatomy of the osteotomies. This mask was then subtracted from the cortical and trabecular bone masks to simulate the osteotomies, using the *boolean tool*. The created osteotomies masks were imported then subtracted from the bone masks into all the models except control models, for better replicability. The osteotomies were created with specific dimensions:

1. The midpalatal sagittal osteotomy measures 1 mm in width relative to the thickness of the piezoelectric blade tip typically used for such non-invasive osteotomy and 4 mm in depth when considering the typical thickness of the

palatal bone. According to prior research, the maximum anterior palatal bone thickness was 6.5 ± 1.5 mm. Therefore, a cut depth of 4 mm is safely not interfering with the nasal cortical floor and includes the entire palatal cortical bone thickness along with a portion of the trabecular bone. (Kang et al., 2007; Poon et al., 2015) (Fig. 3.8).

2. The osteotomy at the anterior nasal spine measures 1 mm in width and 5 mm in depth (Fig. 3.9).
3. The lateral and full LeFort osteotomy have a 1 mm wide and of full depth (Figs. 3.10, Fig. 3.11).

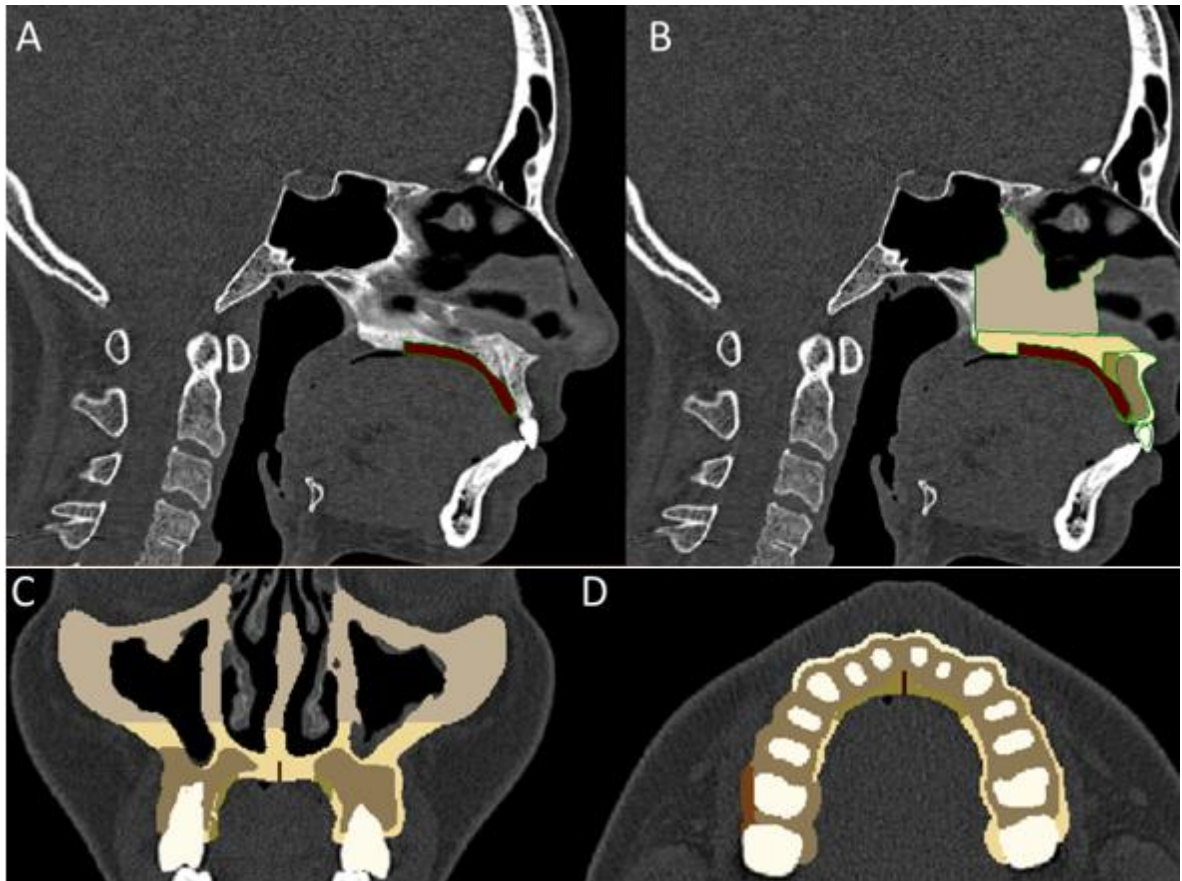


Figure 3.8 Computed Tomography of the head with multiple views of the mid-palatal sagittal osteotomy in dark brown captured from ScanIP software. (A) Sagittal view; (B) Sagittal view including the other bone masks; (C) Coronal view including other bone masks and (D) Axial view including other bone masks

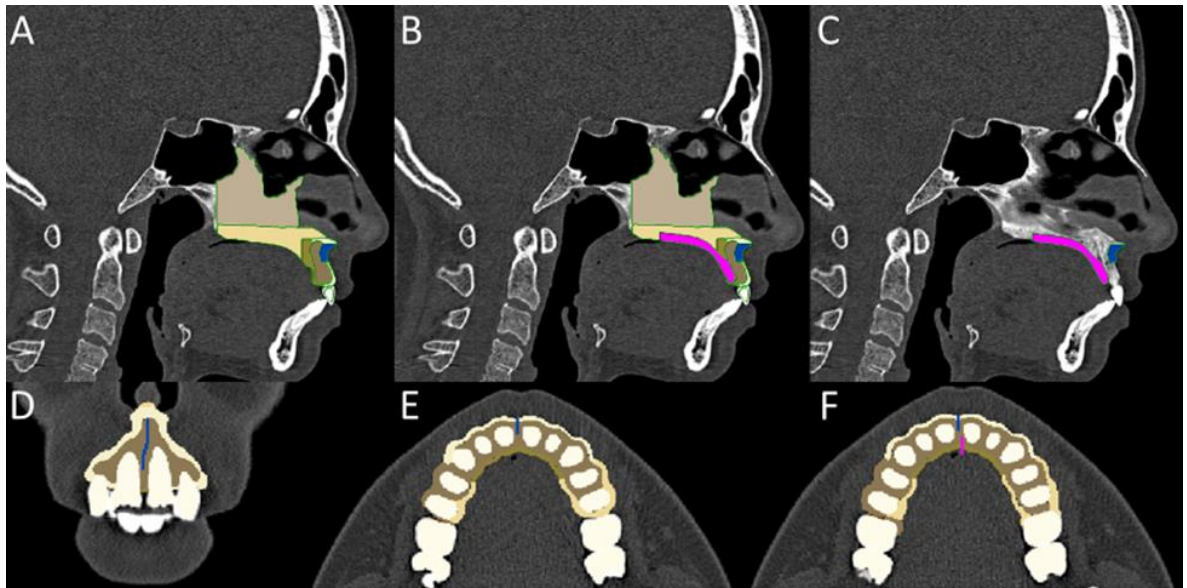


Figure 3.9 Computed Tomography of the head with multiple views of the osteotomy at the anterior nasal spine captured from ScanIP. (A) Sagittal view showing the ANS osteotomy only (in blue); (B) Sagittal view including the mid-palatal sagittal osteotomy (in purple), the osteotomy at ANS (in blue) and the other masks; (C) Sagittal view highlighting the two mid-palatal sagittal and ANS osteotomy; (D) Axial view showing the osteotomy at ANS; (E) Coronal view showing the osteotomy at ANS alone; (F) Coronal view showing the osteotomies at ANS and the midsagittal area.

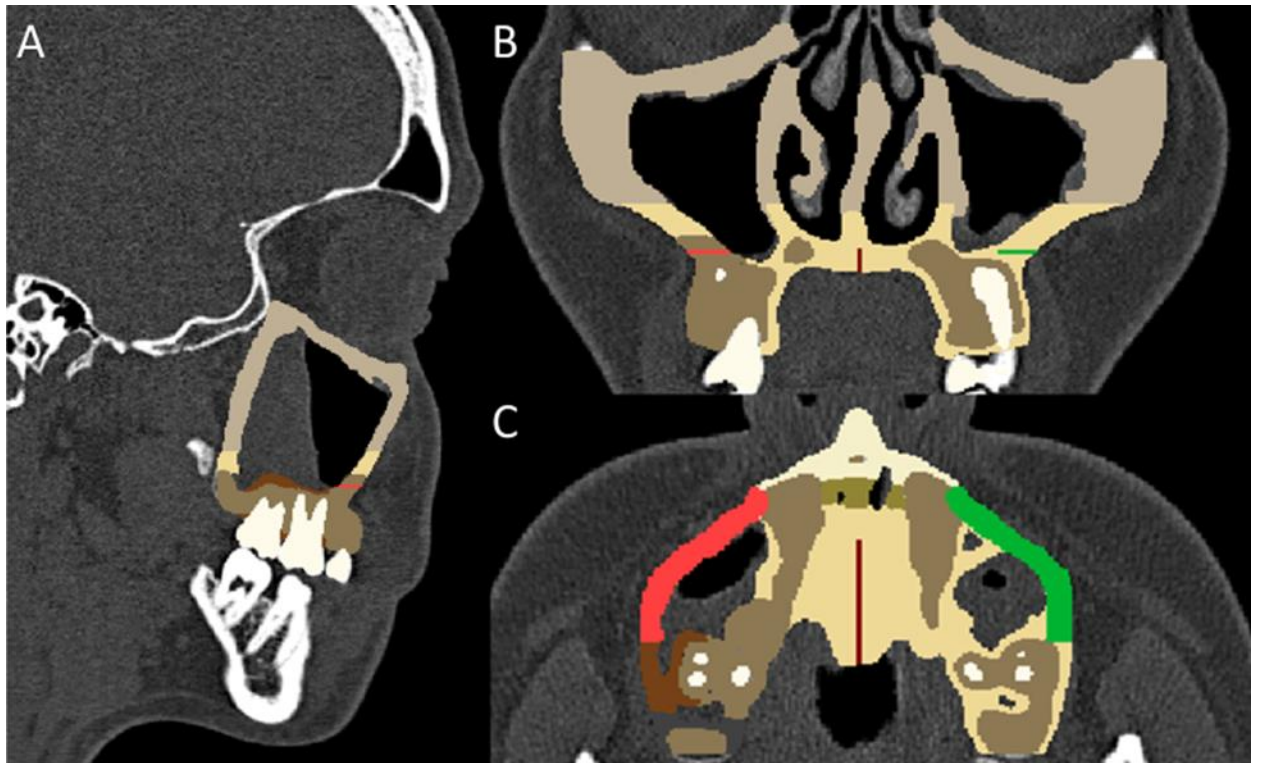


Figure 3.10 Computed Tomography of the head with multiple views of the lateral osteotomies along with the mid-palatal sagittal osteotomy. (A) Sagittal view showing the right lateral osteotomy (in red); (B) Axial view showing both the lateral and mid-palatal sagittal osteotomies; (C) Coronal view showing both the right (red) and left (green) lateral and mid-palatal sagittal osteotomies.

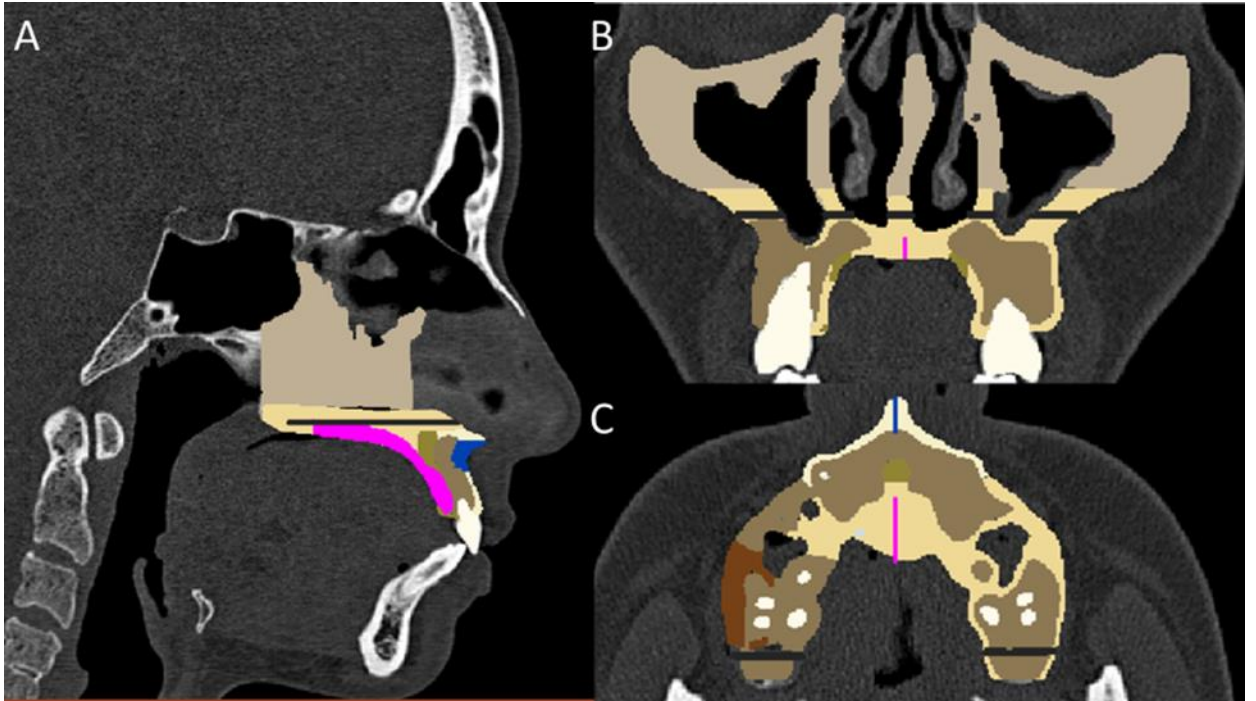


Figure 3.11 Computed Tomography of the head with multiple views displaying the LeFort osteotomy in addition to the mid-palatal sagittal and ANS osteotomies. (A) Sagittal view showing the LeFort, mid-palatal sagittal and ANS osteotomies; (B) Axial view showing the Lefort and mid-palatal sagittal osteotomies; (C) Coronal view showing the Lefort, mid-palatal sagittal and ANS osteotomies.

Four rectangular masks made with the paint tool were used to simulate the mini-screws (2 mm in length and 1 mm in width and 1 mm in height) to represent the bone-borne palatal expander (MARPE). Lateral to the mid-palatal suture, four mini screws were simulated: two anteriorly and 14 mm apart, distal to the canines, and two posteriorly, at the mesial margin of the second premolars (Fig. 3.12). For improved reproducibility, this same mask was later imported into all the corresponding 65 models.

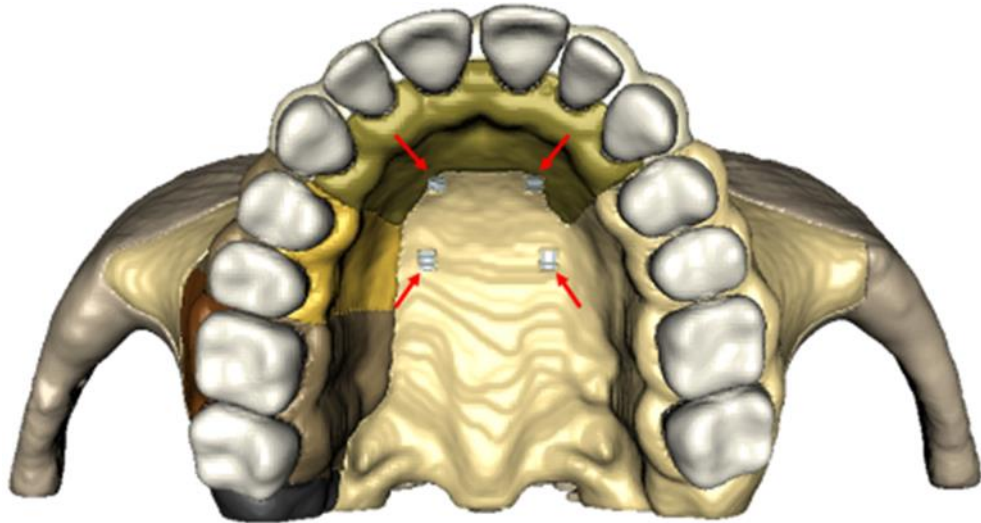


Figure 3.12 To simulate the MARPE, four rectangular spaces (pointed with red arrows) were constructed in the palatal region, where the force of expansion will be applied.

3.2.3 *Meshing*

Prior to finite element analysis, all 3D models underwent the meshing process, which involves dividing the models into elements (Fig. 3.13). Following convergence testing to identify the maximum element size at which the results of the solution are similar, the mesh size was fixed at 0.604 mm (corresponding to coarseness level of -36), as tested previously (Ammoury et al., 2019). Then, models were exported in “*inp.*” file format from ScanIP. This process resulted in 65 meshed models exported.

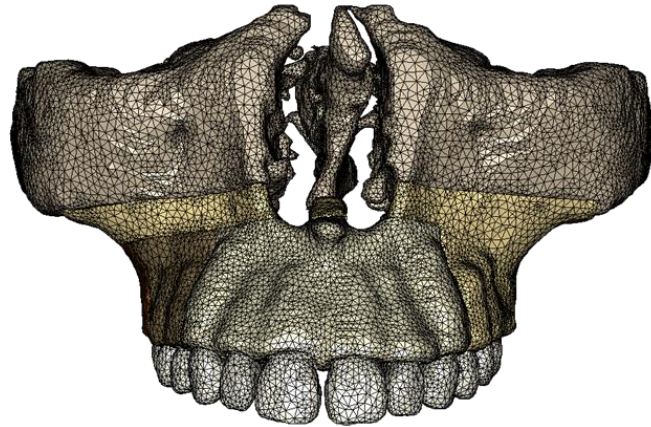


Figure 3.13 Frontal view of the meshed model of the maxilla.

3.2.4 *Finite Element Analysis*

The Finite Element FE solving software Abaqus 6.14 (Dassault Systèmes®, Vélizy-Villacoublay, France), was used to import the meshed models from the input file format and perform the finite element analysis which is detailed below.

3.2.4.1 Materials properties

The quality of the FEA findings depends on the baseline data utilized to determine the tissue response parameters (Middleton et al., 1996). Moreover, based on scientific simulations widely utilized in FEA applications in orthodontics, assumptions regarding the various skeletal elements are developed. For instance, data from the literature was used to describe the material properties (Young's Modulus of Elasticity and Poisson's ratios) of trabecular bone, teeth, and mini screws (Table 3.2). All materials were homogenous, isotropic, and linearly elastic with the exception of the cortical bone (Field et al., 2009; Lim et al., 2003).

Table 3.2 Material properties of anatomical components used in orthodontic FEA study (Field et al., 2009; Kojima et al., 2012; Lim et al., 2003).

Material	Young's Modulus (N/mm ² = MPa)	Poisson's Ratio
Stainless Steel	200,000	0.3
Tooth	20,000	0.2
Cortical Bone	13,700	0.33
Trabecular Bone	1,500	0.33
PDL	0.68	0.45

3.2.4.2 Boundary Conditions

The majority of FEA research only considered a limited portion of the maxilla surrounding the area of study. The upper and posterior parts of the maxilla have typically been regarded as totally restrained in these studies. The fact that the frontal, ethmoid, sphenoid, malar, and nasal bones (together with the maxillary bone) are fused together and constricted in all directions makes this claim believable.

To represent accurately the attachments of the maxilla to its neighboring structures, the zygomatic, palatal, and sphenoid bones, the maxilla's superior and posterior surfaces of the study's models were fully constrained in translation and rotation (Fig. 3.14).

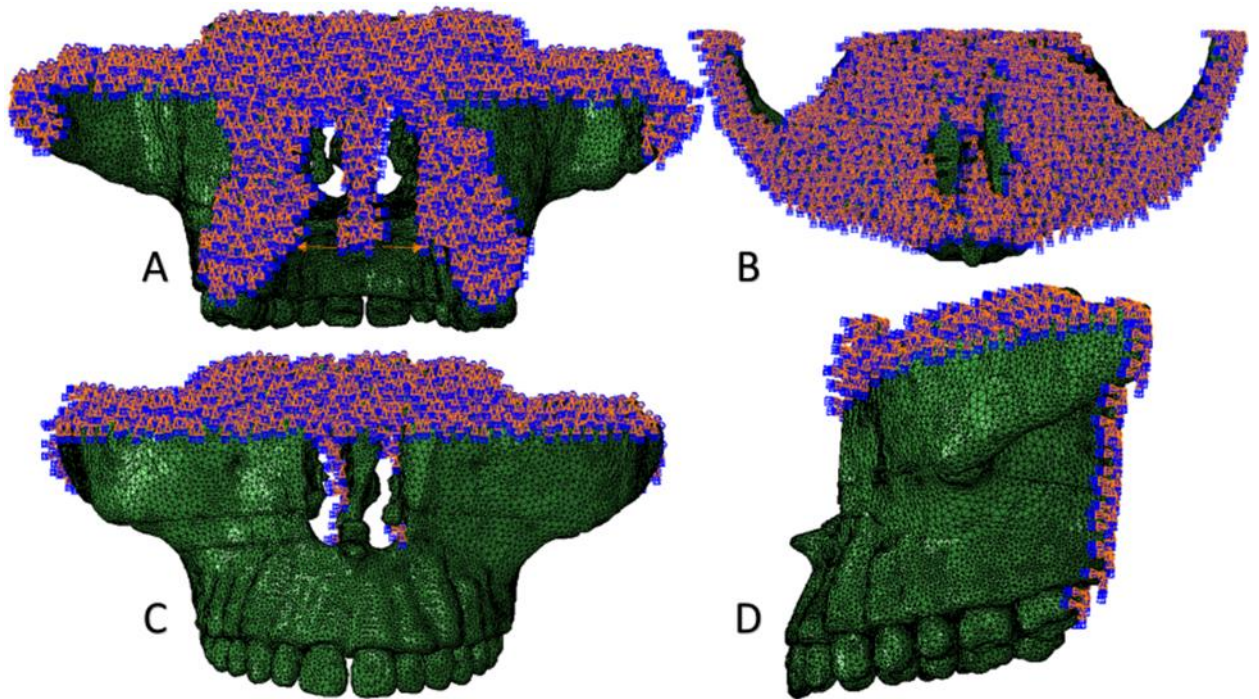


Figure 3.14 Meshed maxillary model with the boundary conditions applied (selected elements highlighted in pink and blue): models constrained from translation and rotation representing the areas of attachments of the maxilla to adjacent bones: zygomatic, palatal and sphenoid. A superior view; B, posterior view, and C, lateral view.

3.2.4.3 Expansion application

To define a precise and reproducible area of expansion application, sets were created by selecting a specific number of nodes (10 nodes) on each of the four mini – screw attachments: nodes were selected on the head of the mini-screws to form four different sets for expansion load application. Followed by applying an amount of expansion of 4 mm of displacement on each set representing a total of expansion of 8 mm (4 mm per side). Expansion was applied only on the x-axis, which is related to the transverse dimension. They were given the numbers (-4 mm) and (+4 mm) for right and left sides respectively to represent the centrifugal direction correctly resulting in palatal expansion. Consequently, the maxillary arches received an overall 8 mm of expansion (Fig. 3.15).

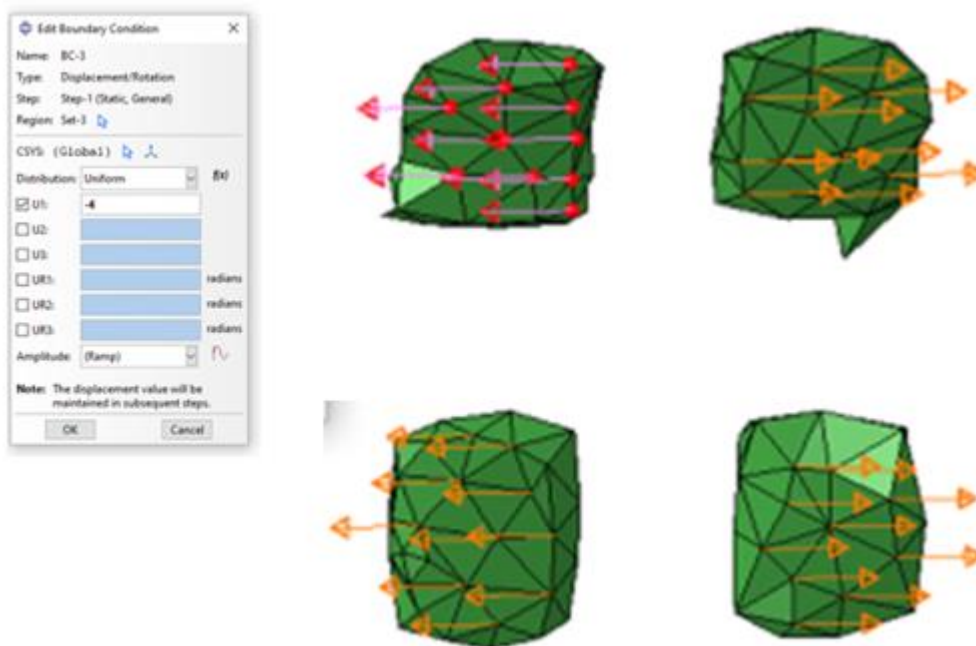


Figure 3.15 Load application: 10 nodes are selected on each mini screw and an expansion of 4 mm referred to as U1 in the x axis, is applied on each mini screw, (- 4) mm on the left and (+ 4) mm on the right.

3.2.4.4 Data collection and Export

The data were collected on the right side where the individual variations were applied because the maxilla structure is symmetrical, and the forces applied were equal on the right and left sides. Stress was measured on the whole surface of these different bone areas:

1. Central Palatal area: between the force application points and the mid-palatal suture
2. Buccal cortical plate of the incisors
3. Palatal bone of the incisors
4. Buccal bone at the molars
5. Palatal bone at the molars

6. Extension of the maxilla representing the maxillary attachment to the zygomatic and orbital bones.
7. Body of the Maxilla

The method used is detailed below:

1. First, 150-200 elements covering the entire bone surface were selected dispersedly on the whole different bone areas described previously, each element carried an independent value that represented the stress at this specific area defined by the element itself (Fig. 3.16).
2. The average of the stress values collected from the 150-200 elements was calculated to define the average stress recorded on each section.

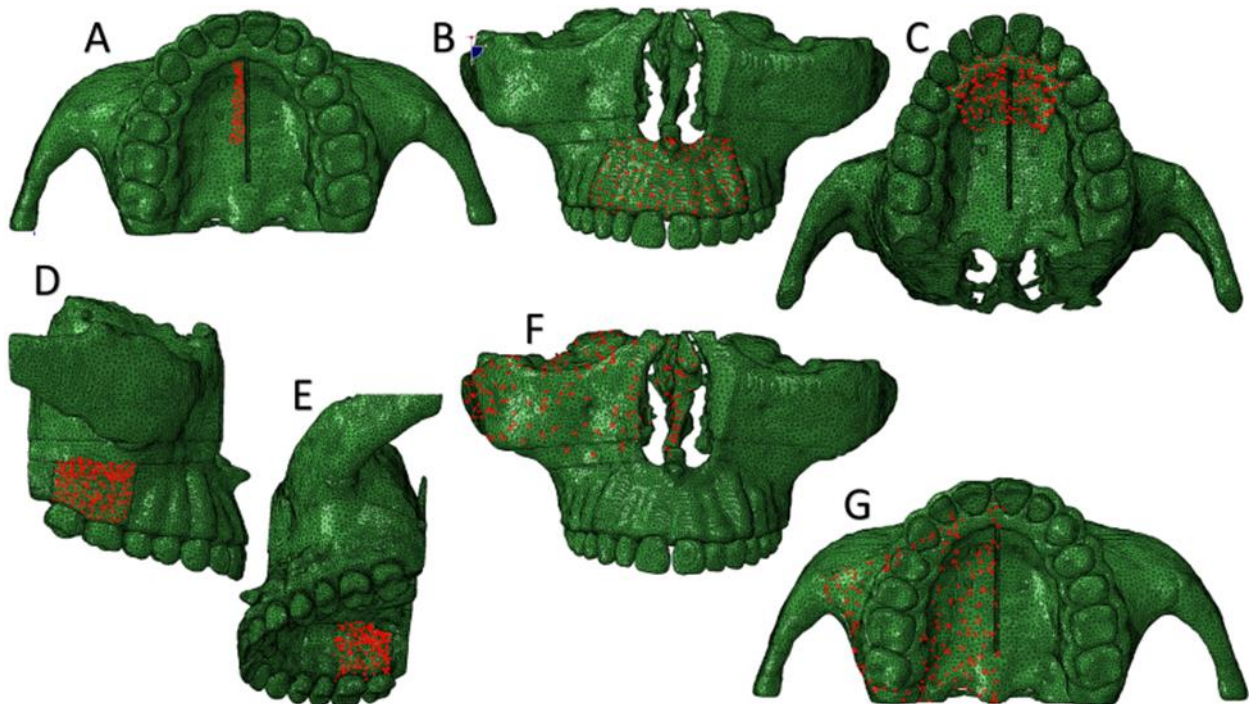


Figure 3.16 Different views of the meshed maxillary model showing the elements selection (red) in various regions. (A) Elements selected along the mid-palatal suture mesial to the force application points; (B) Elements selected on the buccal bone of the incisors mask; (C) Elements selected on the palatal bone of the incisors; (D) Elements

selected on the buccal bone of the molars; (E) Element selected on the palatal bone of the molars; (F) Elements selected on the maxillary extension; (G) Element selected on the maxilla

Additionally, about 10 nodes were selected in various regions of all the models to measure the amount of resultant skeletal expansion. The locations were chosen based on the alveolar bone's cervical region's highest convexity. Three areas were considered, which correspond to the anterior, middle, and posterior palates correspondingly and are at the level of the central incisor, canine, and first molar (Fig. 3.17).

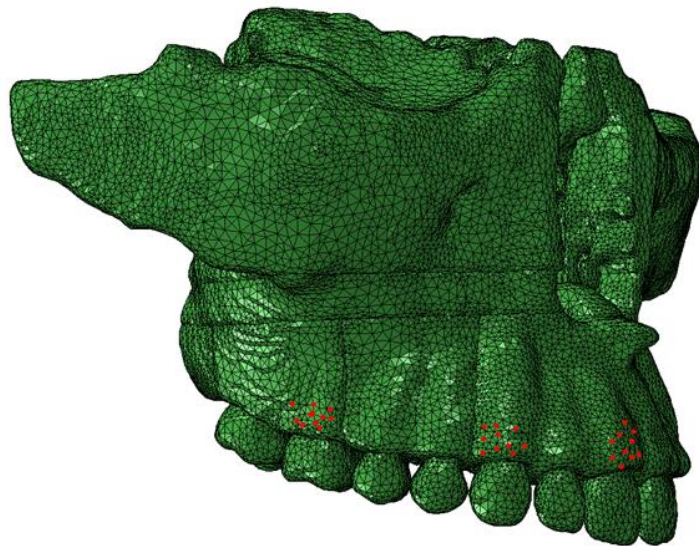


Figure 3.17 Lateral view of the right side of the model with nodes selected in the cervical part of the buccal bone of the right central incisor, canine and first molar, to measure the amount of expansion (displacement).

After running the finite element analysis, the stress results were exported as DAT files and displacement values were collected using the probing method on the

selected nodes (Fig. 3.17). The numbers were transferred into excel where the averages were calculated. Finally, the averages were inserted into final data sheet.

Color mapped representations were used as well to visually display the FE results. However, to assess individual variations, statistical analysis was applied on the numerical data collected.

3.3 Statistical analysis

Descriptive statistics (means and standard deviations) were generated for the following variables: expansion on the molars, canines, and incisors; as well as for the stresses at the mid-palatal area, at the buccal and palatal bones of the incisors, and at the buccal and palatal bones of the molars for the 5 setups.

The Shapiro-Wilk normality test was run to check if the outcome variables have a normal distribution.

The repeated measures ANOVA test, followed by the Bonferroni post-hoc test, was conducted when the data followed a normal distribution, to compare the means of the expansion and stresses variables between the different setups. The level of significance was set at 0.05.

The equivalent non-parametric test, the Friedman test, followed by pairwise comparisons using the Wilcoxon test, was used when the data did not follow a normal distribution. A Bonferroni adjusted p-value was then used to evaluate the significance of the Wilcoxon pairwise comparisons tests: $p\text{-value} = 0.005$ ($0.05/10$ Wilcoxon tests).

Furthermore, the Spearman product moment correlation coefficient was performed to test correlations between the stresses, the expansion at the different regions and bone thickness for each setup separately.

All statistical analyses were performed using SPSS statistical software.

CHAPTER 4

RESULTS

4.1 Comparison between the different setups

4.1.1 Stress

Stress at the mid-palatal area was highest in the control setup. Differences between the control and each of the experimental setups were statistically significant. Differences among the experimental setups were not statistically significant (Table 4.2). The least amount of stress was observed in the mid-palatal cut setup ($16\,331.88 \pm 2207.93$ MPa) relative to the control setup ($32\,006.54 \pm 2984.55$ MPa) (Fig. 4.1) (Table 4.1).

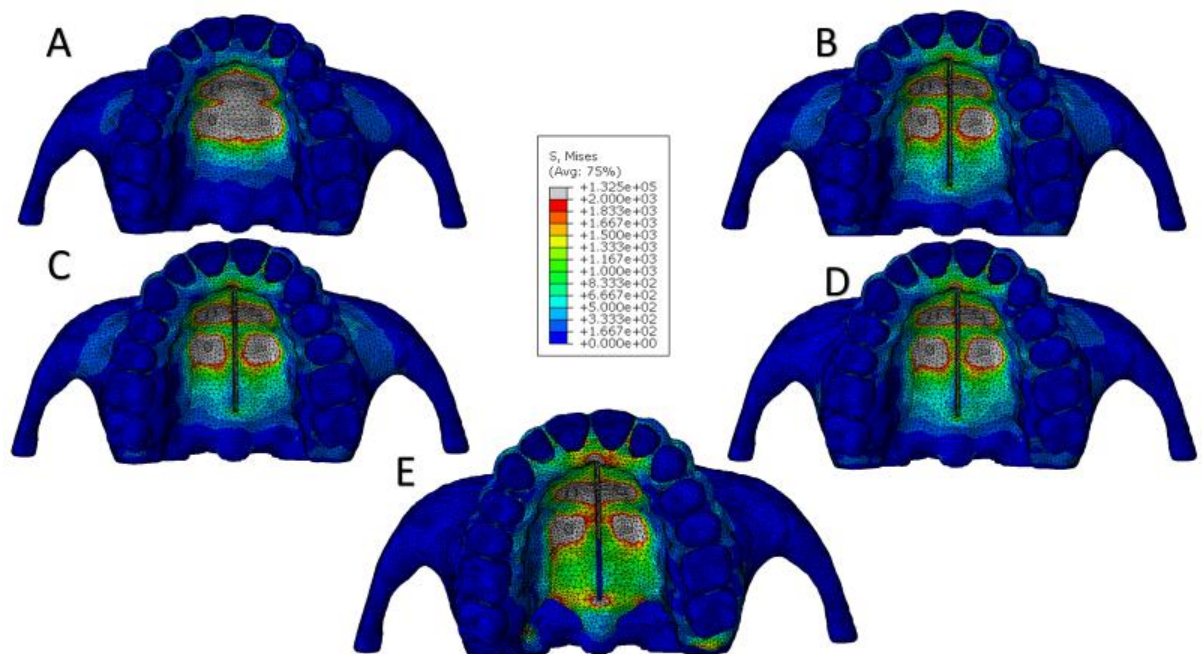


Figure 4.1 Visualization of stress distribution in the mid-palatal area. (A) Palatal view of the control setup model; (B) Palatal view of setup 2 model; (C) Palatal view of setup 3 model; (D) Palatal view of setup 4 model; (E) Palatal view of setup 5 model.

Table 4.1 Descriptive statistics for the stresses at the level of the different bone parts

Stress	Model	N models	Mean	SD
StressMidPa	1	13	3356.69	258.86
	2	13	1507.30	237.42
	3	13	1596.06	113.31
	4	13	1466.05	246.59
	5	13	1554.00	229.94
	Total	65	1896.02	768.45
StressMax	1	13	596.43	77.99
	2	13	499.08	101.64
	3	13	544.07	87.19
	4	13	489.51	98.72
	5	13	374.00	86.57
	Total	65	500.62	115.18
StressMEx	1	13	57.07	8.00
	2	13	76.06	19.38
	3	13	73.49	15.56
	4	13	67.55	15.96
	5	13	1.39	1.08
	Total	65	55.11	30.85
StressBlnc	1	13	244.37	31.38
	2	13	308.20	54.13
	3	13	314.13	38.00
	4	13	310.45	64.68
	5	13	359.38	48.37
	Total	65	307.31	59.96
StressPalnc	1	13	1171.75	226.92
	2	13	1060.08	177.85
	3	13	1129.78	152.24
	4	13	1047.45	190.41
	5	13	1121.06	184.15
	Total	65	1106.02	187.75
StressBM	1	13	94.76	17.77
	2	13	126.15	27.90
	3	13	137.62	19.95
	4	13	139.46	29.03
	5	13	157.87	36.34
	Total	65	131.17	33.57
StressPaM	1	13	106.53	27.97
	2	13	160.93	37.69
	3	13	268.23	401.03
	4	13	157.99	35.02
	5	13	334.90	87.17
	Total	65	205.72	198.18

Stress in MPa. **StressMidPa**: Stress at the mid-palatal area; **StressMax**: Stress at the maxilla; **StressMEx**: Stress at the maxillary extension; **StressBlnc**: Stress at the buccal bone of the incisors; **StressPalnc**: Stress at the palatal bone of the incisors; **StressBM**: Stress at the buccal bone of the molars; **StressPaM**: stress at the palatal bone of the molars. **StD**: standard variation.

Stress at the maxillary extension decreased to nearly zero between the control setup (57.07 ± 8.00 MPa), setup 2 (76.06 ± 19.38), setup 3 (73.49 ± 15.56), setup 4

(67.55 ± 19.38) and the experimental setup 5 in which a LeFort Osteotomy was applied, freeing the entire maxilla from the surrounding buttressing bones (Fig. 4.2) (1.39 ± 1.08) (Table 4.1; Table 4.2). Differences among the experimental setups 2,3 and 4 were not significantly different.

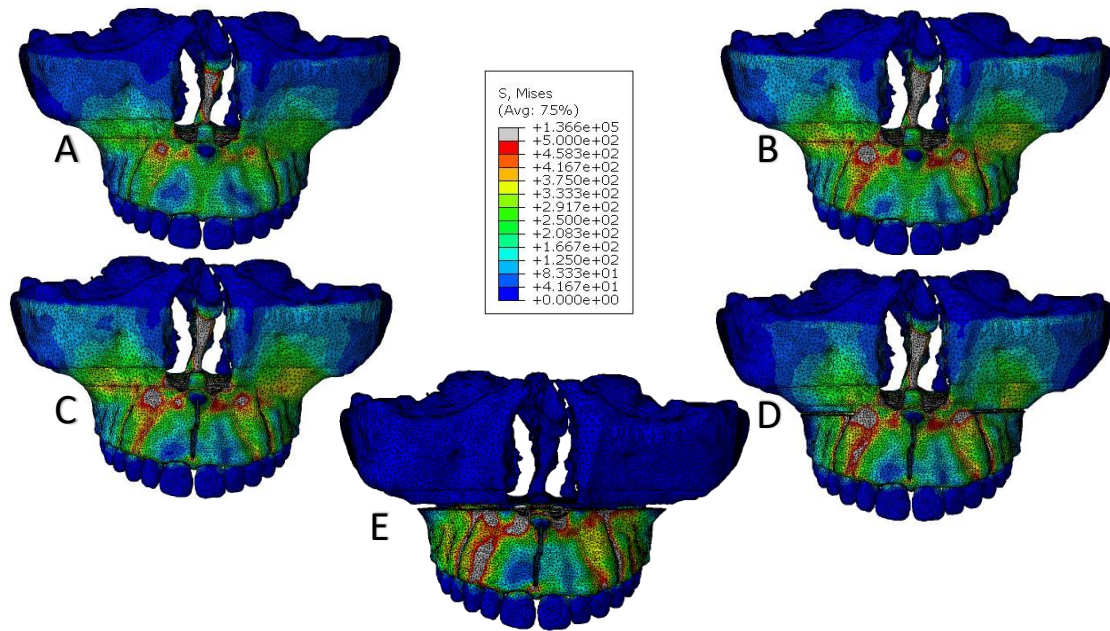


Figure 4.2 Visualization of stress distribution on the buccal bone of the incisors and the maxillary extension. (A) Frontal view of the control setup model; (B) Frontal view of the setup 2 model; (C) Frontal view of the setup 3 model; (D) Frontal view of the setup 4 model; (E) Frontal view of the setup 5 model.

At the bone buccal to the incisors, stress varied significantly between the control setup and the experimental setups 3 and 5 but not among the setups (Table 4.2). Stress values were the highest in setup 5 (359.38 ± 59.96 MPa). The LeFort osteotomy cut probably hindering the dissipation of stresses to the areas above the maxilla (Fig. 4.2).

All types of osteotomies caused a significant elevation in stress at the bone buccal to the molars relative to the control setup (Table 4.2). The maximum recorded stress was in setup 5 (157.87 ± 36.34 MPa) (Table 4.1) (Fig. 4.3).

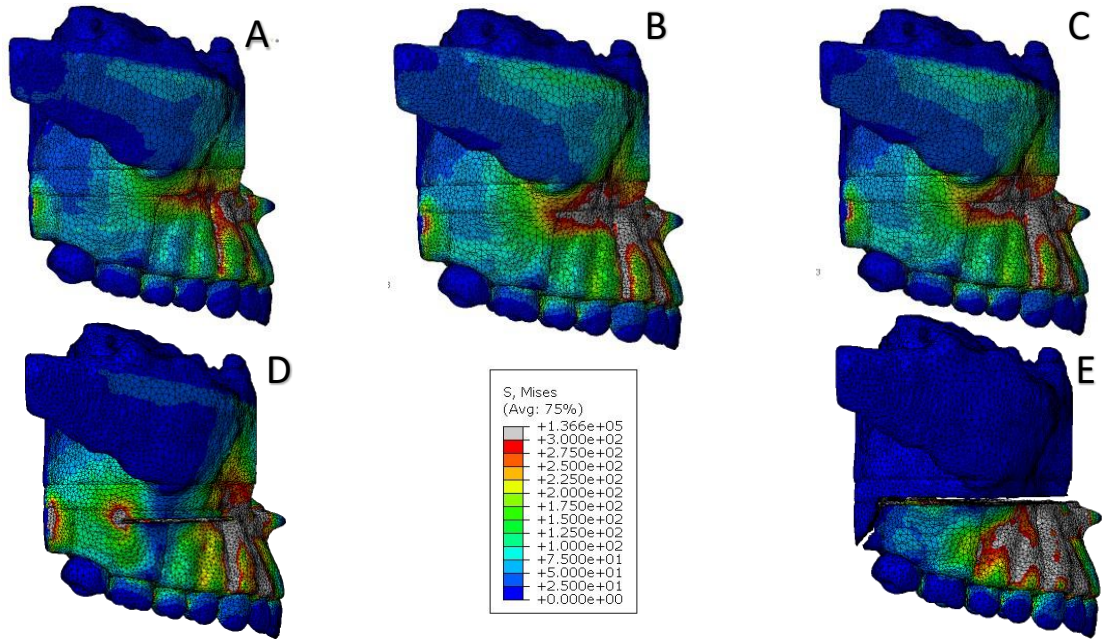


Figure 4.3 Visualization of stress distribution on the buccal bone of the molars. (A) Right side view of the model of control setup; (B) Right side view of setup 2 model; (C) Right side view of setup 3 model; (D) Right side view of setup 4 model; (E) Right side view of setup 5 model.

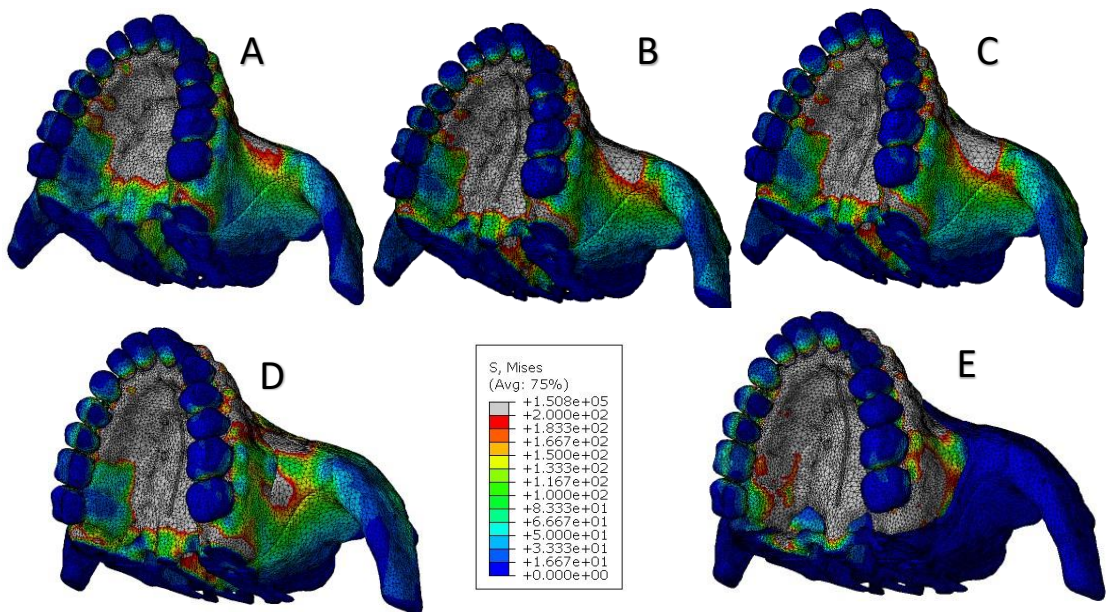


Figure 4.4 Visualization of stress distribution on the palatal bone of incisors and molars. (A) palatal view of the right side of control setup model; (B) Palatal view of the right side of setup 1 model; (C) Palatal view of the right side of setup 2 model; (D) Palatal view of the right side of setup 3 model; (E) Palatal view of the right side of setup 4 model.

Stress at the bone palatal to the molars was showed the lowest value in setup 1 (106.53 ± 27.97 MPa) and was statistically increased in this region in all the experimental setups (setup 2: 160.93 ± 37.69 MPa; setup 3: 268.23 ± 401.03 MPa and setup 4: 157.99 ± 35.02) and was maximal in setup 5 (334.90 ± 87.17) (Fig. 4.4) (Table 4.1; Table 4.2). Differences among experimental setups were not significant.

Table 4.2 Pairwise comparison of stress at the different bone parts

Pairwise comparison of setups	StressMidPa	Stress MEx	StressBlnc	StressBM	StressPM
Setup 1-2	0.001	0.009	0.005	0.000	0.003
Setup 1-3	0.001	0.009	0.001	0.000	0.001
Setup 1-4	0.001	0.064	0.007	0.001	0.003
Setup 1-5	0.001	0.001	0.003	0.000	0.001
Setup 2-3	0.196	0.807	0.463	0.918	0.917
Setup 2-4	0.463	0.249	0.972	1.000	0.861
Setup 2-5	0.196	0.001	0.075	0.184	0.522
Setup 3-4	0.075	0.152	0.753	1.000	0.600
Setup 3-5	0.807	0.001	0.075	0.602	0.023
Setup 4-5	0.345	0.001	0.064	1.000	0.020

Stress in MPa. **StressMidPa**: Stress at the mid-palatal area; **StressMEx**: Stress at the maxillary extension; **StressBlnc**: Stress at the buccal bone of the incisors; **StressPalnc**: Stress at the palatal bone of the incisors; **StressBM**: Stress at the buccal bone of the molars; **StressPM**: stress at the palatal bone of the molars. **Std**: standard variation.

4.1.2 Expansion

Expansion amount at the bone near the cervical part of the molar, canine and incisor was significantly different among all setups except between setups 2 and 3, when the lateral osteotomies were added to the mid-palatal and ANS osteotomies (Table 4.4).

Expansion increased gradually with each added osteotomy to the model and was maximal in setup 5 at all levels (molar: 3.57 ± 0.29 mm; canine: 2.85 ± 0.50 mm and incisor: 2.71 ± 0.48 mm) (Table 4.3) (View Appendix Table 6).

Expansion followed a V-shaped pattern: more anteriorly (at incisor) than posteriorly (at molar) in all setups except setup 5 where expansion was more important posteriorly (Table 4.3; Table 4.4).

Table 4.3 Descriptive statistics of the expansion at three different locations

	Setup	Number of models	Mean	SD
Exp6	1	13	0.36	0.06
	2	13	0.53	0.11
	3	13	0.56	0.07
	4	13	0.79	0.12
	5	13	3.57	0.29
	Total	65	1.16	1.23
Exp3	1	13	0.39	0.08
	2	13	0.67	0.12
	3	13	0.74	0.08
	4	13	0.89	0.13
	5	13	2.85	0.50
	Total	65	1.11	0.92
Exp1	1	13	0.99	0.21
	2	13	1.07	0.23
	3	13	1.13	0.17
	4	13	1.30	0.14
	5	13	2.71	0.48
	Total	65	1.44	0.70

Expansion in mm; **Exp6**: expansion at the first molars; **Exp3**: expansion at the canines; **Exp1**: expansion at the incisors. **SD**: standard variation

Table 4.4 Pairwise comparison of expansion at various locations

Pairwise comparison of setups	Exp6	Exp3	Exp1
Setup 1-2	0.002	0.000	0.003
Setup 1-3	0.001	0.000	0.001
Setup 1-4	0.001	0.000	0.001
Setup 1-5	0.001	0.000	0.001
Setup 2-3	0.033	0.140	0.009
Setup 2-4	0.001	0.001	0.001
Setup 2-5	0.001	0.000	0.001
Setup 3-4	0.001	0.000	0.002
Setup 3-5	0.001	0.000	0.001
Setup 4-5	0.001	0.000	0.001

Expansion in mm; **Exp6**: expansion at the first molars; **Exp3**: expansion at the canines; **Exp1**: expansion at the incisors.

4.1.3 Cortical bone thickness variations across the model

The greatest mean thickness value was observed at the side of the bone buccal to the incisors (2.46 ± 1.68 mm). The lowest value was at the palatal side of the molars (1.74 ± 0.58 mm) (Table 4.5).

Table 4.5 Mean of cortical bone thickness at the first molars and incisors level

	Number of Models	Mean	StD
BT6B	65	2,07	0,90
BT6P	65	1,97	0,92
BTIncB	65	2,46	1,62
BTIncP	65	1,74	0,56

Cortical bone thickness means in mm: **BT6B**: buccal bone thickness at first molars; **BT6P**: palatal bone thickness at first molars; **BTIncB**: buccal bone thickness at the incisors; **BTIncP**: palatal bone thickness at the incisors. **StD**: Standard deviation

4.2 Correlations

4.2.1 Setup 1

When adjunct osteotomies were not applied during expansion, strong positive correlations were observed between the stress generated at the bone buccal and palatal to the molars and the displacement measured at the level of the canines ($r = 0.706$ and $r = 0.830$, respectively). When the expansion at the incisors increased, the stress at the corresponding buccal bone increased ($r = 0.790$).

Palatal bone thickness at the incisors correlated positively with expansion at all levels, especially at the incisors ($r = 0.818$), (Table 4.6).

Thickness of the bone palatal to the incisors correlated strongly with stress the bone buccal to the incisors ($r = 0.874$), and thickness of the bone buccal to the incisors correlated with stress at the bone palatal to the incisors ($r = 0.764$).

4.2.2 Setup 2

When a mid-palatal sagittal osteotomy was added to the model, more expansion at the level of the molars was accompanied with an increase in stress at the bone buccal and palatal to the molars ($r = 0.790$ and $r = 0.831$ respectively). Also, bone thickness at the bone palatal to the incisors correlated strongly and positively with stress at the bone buccal and palatal to the molars ($r = 0.709$ and $r = 0.736$ respectively) (Appendix Table 2).

4.2.3 Setup 3

In setup 3, the combined osteotomies at mid-palate and the anterior nasal spine resulted in a strong association between the expansion at the incisors level and buccal and palatal bone thickness at the incisors ($r = 0.720$ and $r = 0.775$ respectively). Stress at the bone buccal to the incisors increased with expansion at this level ($r = 0.753$) (Appendix Table 3).

4.2.4 Setup 4

In setup 4, when introducing the lateral osteotomies, no strong correlations were noted between stress and bone thickness with the amount of expansion at the different bone parts. However, the bone palatal to the incisors thickness was strongly correlated with stress the bone buccal to the molars (Appendix Table 4).

4.2.5 Setup 5

Setup 5 comprised the least number of correlations: bone thickness did not affect expansion at all after introducing the Lefort osteotomy. Bone thickness was faintly correlated to stress in some areas like the maxillary extension and the mid-palatal area. However, a strong negative correlation was noted between stress at the bone palatal to the incisors and expansion at the molars.

Table 4.6 Table of correlations between stress, expansion, and cortical bone thickness of setup 1

		Exp6	Exp3	Exp1	StressMidPa	StressMax	StressMEx	StressBlnc	Stressalnc	StressBM	StressPaM	BT6B	BT6P	BTIncB	BTIncP
Exp6	Correlation	1	.758**	.807**	0.218	0.502	0.232	.670*	0.27	0.549	0.549	0.417	0.24	0.226	.588*
	Sig. (2-tailed)	.	0.003	0.001	0.474	0.08	0.446	0.012	0.372	0.052	0.052	0.157	0.43	0.457	0.035
Exp3	Correlation		1	.771**	0.43	.734**	0.284	0.491	0.086	.706**	.830**	0.483	0.466	0.041	.657*
	Sig. (2-tailed)		.	0.002	0.142	0.004	0.347	0.088	0.781	0.007	0	0.095	0.108	0.893	0.015
Exp1	Correlation			1	0.166	0.497	0.276	.790**	0.541	.613*	0.436	0.442	0.254	0.436	.818**
	Sig. (2-tailed)			.	0.588	0.084	0.361	0.001	0.056	0.026	0.136	0.13	0.402	0.136	0.001
Stress	Correlation				1	0.11	.709**	0.242	-0.049	0.357	0.396	0.522	0.385	-0.286	0.055
	Sig. (2-tailed)				.	0.721	0.007	0.426	0.873	0.231	0.181	0.067	0.194	0.344	0.859
Stress	Correlation					1	0.088	0.346	0.066	0.308	.632*	0.385	0.247	0.033	0.467
	Sig. (2-tailed)					.	0.775	0.247	0.831	0.306	0.021	0.194	0.415	0.915	0.108
Stress	Correlation						1	0.516	0.352	0.286	0.187	.808**	.560*	0.071	0.291
	Sig. (2-tailed)						.	0.071	0.239	0.344	0.541	0.001	0.046	0.817	0.334
StressB	Correlation							1	.753**	0.527	0.231	.593*	0.335	.610*	.764**
	Sig. (2-tailed)							.	0.003	0.064	0.448	0.033	0.263	0.027	0.002
StressP	Correlation								1	0.214	-0.148	0.418	-0.027	.874**	0.505
	Sig. (2-tailed)								.	0.482	0.629	0.156	0.929	0	0.078
StressB	Correlation									1	.703**	0.269	0.533	0.099	.626*
	Sig. (2-tailed)									.	0.007	0.374	0.061	0.748	0.022
StressP	Correlation										1	0.264	0.335	-0.203	0.39
	Sig. (2-tailed)										.	0.384	0.263	0.505	0.188
BT6B	Correlation											1	.654*	0.357	0.538
	Sig. (2-tailed)											.	0.015	0.231	0.058
BT6P	Correlation												1	0.016	.582*
	Sig. (2-tailed)												.	0.957	0.037
BTIncB	Correlation													1	0.549
	Sig. (2-tailed)													.	0.052
BTIncP	Correlation														1
	Sig. (2-tailed)														.

StressMidPa: Stress at the mid-palatal area; **StressMax:** Stress at the maxilla; **StressMEx:** Stress at the maxillary extension; **StressBlnc:** Stress at the buccal bone of the incisors; **StressPalnc:** Stress at the palatal bone of the incisors; **StressBM:** Stress at the buccal bone of the molars; **StressPaM:** stress at the palatal bone of the molars; ; **Exp6:** expansion at the first molars; **Exp3:** expansion at the canines; **Exp1:** expansion at the incisors; **BT6B:** buccal bone thickness at first molars; **BT6P:** palatal bone thickness at first molars; **BTIncB:** buccal bone thickness at the incisors; **BTIncP:** palatal bone thickness at the incisors **StD:** standard variation. ** Correlation is significant at the 0.01; * Correlation is significant at the 0.05 level (2-tailed).

CHAPTER 5

DISCUSSION

In this research, we have established methods not used or recorded previously. In this chapter, we consider the strengths of the study, comparisons with previous studies, the significance of the computed correlations, clinical considerations, limitations and future research.

5.1 Strengths

The novelty of our approach related to the introduction of a potential mid-palatal osteotomy that would not require general anesthesia or extended surgery, thus providing less morbidity. Moreover, the incorporation of individual variation, which has been applied earlier to tooth movement, was applied for the first time to bony response in a combined orthodontic/orthopedic model.

5.1.1 *Limited osteotomy*

Our research focused on the mechanical impact of a simulated mid-palatal osteotomy that is considered minimally invasive in comparison with current surgical applications whereby the maxilla is completely split in two symmetrical parts (Zawiślak et al., 2020) (Fig 5.1). In addition to the assumption that the applied limited osteotomy would require only local anesthesia, the morbidity of the procedure would be significantly reduced, notwithstanding the advantage of a reduced cost.

5.1.2 Individual variation

Our research team pioneered in earlier research the incorporation of individual information on bone properties to assess tooth movement (Ammoury et al., 2019). This study is the first to include such variations in bone thickness on skeletal response (stress and displacement) to orthopedic movements.

Most FEA studies used in engineering provided conclusions and readings based on a single mathematical solution, which was equivalent to a single setup or simplified elements of anatomy that represent a fractioned clinical setting. Yet, individual variation in the medical and dentistry is the basis for personalized treatment (Ghafari, 2015). Varied outcomes may result from the same treatment, necessitating the analysis of larger samples to identify central tendencies and possible outliers.

Accordingly, we have incorporated variations in cortical bone thickness replicating the data from studies on human cadavers safely presumed to simulate variations among living patients. This strategy is the most effective to date at creating a connection between virtual finite element models and actual variation in anatomy and clinical settings. This strategy allowed the statistical analysis that revealed the impact of biological variations, resulting in the generation of comparisons among methods and the formulation of new hypotheses.

5.1.3 Effect of bone characteristics on skeletal expansion

Although FEA does not address physiology and metabolism, it has proven to be appropriate to evaluate anatomical differences and their capacity to influence bone movement particularly that the system can control for material properties and boundaries. Whereas some studies differentiated between cortical and cancellous bone

(N. Kaya et al., 2023; Koç & Bolat Gumus, 2023; S. C. Lee et al., 2014b; Möhlhenrich et al., 2017; Zawiślak et al., 2020), the impact of cortical bone in tooth movement has been shown to be primary (Ghafari et al., 2020). Moreover, anatomical variations to cortical bone thickness were not accounted for in those studies. This distinction may impact the outcome of various studies considering the reported variation in palatal cortical bone thickness at 3 mm and 6 mm from the mid-palatal suture, gauged in a study of 223 CBCT images of different patients, conducted for the placement of mini-implants in palatal expansion with MARPE.

5.1.4 Anatomic representation from 3D model

To produce an accurate and comprehensive FE model, much effort at extended time is required, otherwise the modeling of the researched structures may be compromised. In a few studies, the FE models were generated on a plastic skull rather than radiographic images, consequently presenting many anatomical flaws (Han et al., 2009; Holberg et al., 2007). In contrast, our model was built from a patient's CT scan in which data on bone thickness from individual cadavers were incorporated to reproduce individual variations.

Moreover, and unlike published studies in which the maxilla was evaluated as a single entity, we segmented the anatomy of the maxilla into distinct components (specified as masks), generating a numerical result for component. This strategy should be more representative of the clinical settings.

5.1.5 Comparison with FEA expansion studies

FE modeling has provided valuable information in studies of SARPE through the evaluation of complex stress distributions and displacement patterns in the facial skeleton model. Our study was distinctive compared to other studies in several ways, including variations on the SARPE cuts, model construction, collection of data, and consequently outcomes.

5.1.6 Development of the model

As an experimental model built on assumptions, the output of FE modeling reflects the closeness of such assumptions to real anatomy and associated physiology. In this section, we compare the model setups related to maxillary expansion among published studies and the present investigation.

5.1.6.1 Material properties

Material properties were assigned to the evaluated maxillofacial structures based on the data used and tested by previous studies (Ammoury et al., 2019; Field et al., 2009; Lim et al., 2003). The assumption that the mid-palatal suture had the same material properties as the adjacent cortical bone (Poisson's ratio, elastic modulus (Table 3.2) was adopted in previous studies (S. C. Lee et al., 2014b; Nowak et al., 2021; Shi et al., 2020). Inherent in this assumption is the consideration of the mid-palatal suture as entirely fused in skeletally mature individuals and as part of the surrounding bone. Accordingly, surgically assisted rapid palatal expansion is indicated. We considered the mid-palatal suture as a linear elastic, homogeneous isotropic material, based on the

premise that a linear elastic assumption for suture behavior provides a reasonable prediction of maxillary displacements and suture stresses or strains for a time period shortly after a single appliance activation.

5.1.6.2 Boundary conditions

The maxilla was fixed in all planes of space at the upper and posterior limits because of the absence of any mobile joints. However, several variations have been used in other studies.

Some authors fixed the contact between the pterygoid process and the maxilla when not in the osteotomy region, as also applied to all surfaces subjected to osteotomy, avoiding friction or contact, even though the movement was limited to the simulated osteotomy gap (de Assis et al., 2014). Some studies defined frictional contact between the contacting surfaces in models with pterygomaxillary suture disjunction (friction coefficient 0.3). They set boundary conditions at the surfaces in contact with the sphenoid bone of the lower part of the maxilla, separated by lateral osteotomy, thus this part moved as a single unit, with no separation or sliding of the faces and edges (Koç & Bolat Gumus, 2023).

Other investigators defined boundaries only at the upper limit of the model. The cranial boundaries of the segmented region were located at approximately half the height of the orbital cavities, where all nodes at this demarcation were rigidly fixed to constrain the model in all spatial directions (Dalband et al., 2015; Möhlhenrich et al., 2017). In more extended models, the foramen magnum, which formed the base of the model, was constrained in its displacement by the X, Y, and Z direction (Holberg et al., 2007; S. C. Lee et al., 2014b; Zawiślak et al., 2020).

5.1.6.3 Load application

We applied the load by defining a displacement of 4 mm on each side (total of 8mm) to simulate the effect of the expander when the jackscrew is activated. This approach was employed in other studies with various openings: 0.5 mm (Möhlhenrich et al., 2017; Zawisłak et al., 2020), 2.5 mm (Koç & Bolat Gumus, 2023; S. C. Lee et al., 2014b), and 1 mm (de Assis et al., 2014). Other protocols applied a force in Newton: 100 N (Dalband et al., 2015; N. Kaya et al., 2023) or in grams: 6000g (Han et al., 2009). The amount of expansion applied in our study simulated the total expansion produced by the expansion appliance, which is more representative of the clinical situation.

Applying the load as displacement simulates the palatal expander effect more accurately since the screw opens to a specific distance that cannot be surpassed, whereas the force in newton or kg has a continuous effect which might exaggerate the results. Also, different types of screws can generate different amount of forces in newtons: approximately 22 kg on the A2620 expander, about 20.5 kg on the Hyrax expander, and about 17.5 kg on Palatal Split Screw (Camporesi et al., 2013). As a result, quantifying the expansion in mm reduces the possibility of variation.

5.1.6.4 Extent of the mid-palatal osteotomy

Minimally invasive surgery reduces the effects of conventional surgery (AlAsseri & Swennen, 2018) and is more acceptable by patients, especially those fearful of general anesthesia, post-surgical effects and longer recovery. The goals of orthognathic surgery are to achieve stability, function, and esthetics in the orofacial region.

Piezoelectric devices (piezoelectric osteotomes, for example, Piezotome) have proven to be more precise in cutting bone. Because of the cavitation effect and

micromovement, they enable soft tissue preservation, more precision and control, and the capacity to create a dry operation field. By combining piezosurgery and local anesthesia, the mid-palatal sagittal osteotomy would provide an ideal approach to reduce cost and morbidity.

Rapid maxillary expansion assisted with mid-palatal cortex osteotomy to correct maxillary transverse deficiency was investigated in 14 young adults with a mean age of 20.4 ± 3.5 years old (Luxi et al., 2017). Under local anesthesia and using a ball drill, the osteotomy was performed along the mid-palatal suture from the incisive canal to the posterior limit of the bony palate. The authors concluded that the procedure was an effective micro-invasive method to expand the maxillary basal bone and arch in young adult patients with maxillary transverse deficiency.

A main aim of the present study was to simulate the less invasive method. Thus, we compared the mid-palatal sagittal osteotomy with more extensive cuts. The osteotomy was extended from the incisive foramen to the distal level of the first molars, with a width of 1 mm and a depth of 4 mm. This approach was less invasive than those described in previous FEA studies that separated the maxilla in two independent parts through the incisive foramen (Koç & Bolat Gumus, 2023; S. C. Lee et al., 2014b; Möhlhenrich et al., 2017; Zawisłak et al., 2020) (Fig. 5.1).

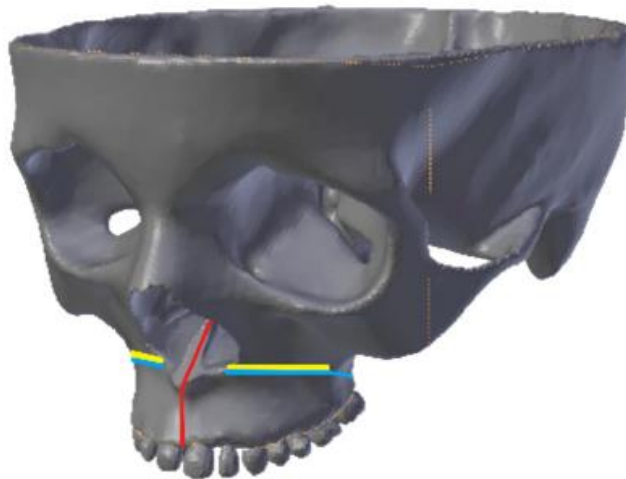


Fig. 5.1. Schematic representation of the osteotomy line on the 3D finite element model of facial skeleton. Red color marked-sagittal osteotomy (adapted from Zawisłak et al., 2020).

Even when the integrity of the foramen was respected in some investigations, the mid-palatal osteotomy was not evaluated independently in conjunction with the expansion (Dalband et al., 2015; Han et al., 2009; Holberg et al., 2007). Thus, conclusions could not be formulated about the efficacy of this procedure.

Mid-palatal suture cortico-punctures and LeFort I cortico-puncture have been evaluated recently as other less invasive procedures (N. Kaya et al., 2023). However, the mid-palatal suture cortico-punctures were not compared to a full mid-palatal osteotomy. Research is needed for such comparison to sort out differences in efficacy and morbidity.

5.1.7 Findings

5.1.7.1 Stress

A major decrease in stress (nearly by half) was observed at the mid-palatal area following the mid-palatal sagittal osteotomy. Stresses were increased at the maxillary

extension, the buccal bone of the incisors, and mostly on the buccal bone of the molars. These findings suggest that an effective expansion occurred with release of the stress in the palatal area and resistance by the buccal and more cranial bones.

The degree of stress in the mid-palatal suture area was greater than in the other areas in the control model, compared with all expansion modalities subjected to the surgical cuts. Considering the position of the mid-palatal suture as the closest region to the applied transverse forces, the mid-palatal osteotomy yielded nearly half of the highest stress values (3356.69 MPa) computed in the control model. Similar findings were reported by Zawisłak et al (2020), whereby the osteotomy of the palatal suture decreased stresses in the hard palate and increased them in the higher cranial structures (arcus superciliaris region). In comparisons among a single mid-palatal and its combination with lateral cuts involving or avoiding pterygomaxillary separation, Mõhlhenrich et al. (2017) concluded that each additional osteotomy resulted in a decrease in stress at the mid-palatal suture. Unlike our findings, they observed that the lateral osteotomy had the greatest influence on stress reduction. The difference in findings is likely related to the difference in setting the boundaries at the pterygoid plate in our study.

Only after freeing the entire maxilla from the surrounding buttressing bones through the LeFort osteotomy combined with the mid-palatal and anterior nasal spine osteotomies, stress decreased at the maxillary extension significantly relative to the control model. When this additional invasive osteotomy was applied, the stresses recorded at the level of the buccal bone of the incisors and the palatal bone of the molars were maximal. This finding suggests that this extensive cut prevented the

dissipation of stress to the facial skeleton; most of the tension was focused buccal to the incisors and palatal to the molars.

Although different regions are studied by different authors, similar results were reported by Zawisłak et al (2020) who found that the highest stresses within the facial skeleton were recorded in the models without osteotomy, with Le Fort I osteotomy, and with Le Fort I and PMJ separation. The authors reported highest stress values in the anterior region of the hard palate. As in our study, they also found unfavorable stress redistribution below the osteotomy line following Le Fort I and PMJ separation, and a favorable decrease in stress below the osteotomy line following Le Fort I osteotomy with an incision in the palatal suture without separation in PMJ, along with a significant reduction in stress in the orbital regions and the entire midface to values of 4.4 MPa maximally.

Stress was not statistically significantly different between applying the mid-palatal osteotomy alone, with the anterior nasal spine osteotomy, or with additional lateral osteotomies. When lateral osteotomies were added, we reported general stresses in our defined maxillary extension like the descriptions of Holberg et al. (2007) who contributed more details including less stress at the infraorbital foramen, the supraorbital margin, the zygomaticoalveolar crest, and other midfacial structures.

Moreover, the authors described an exception at the anterior wall of the maxillary sinus wherein von Mises stresses increased from 20.1 MPa (without surgery) to 180.8 MPa (with conventional surgery) after surgical weakening of the lateral maxillary sinus wall. However, the authors compared the application of lateral osteotomies to the control setup with no surgery and not to surgical approaches.

5.1.7.2 Expansion

Expansion at the cervical level of the first molars was increased significantly after the mid-palatal sagittal osteotomy (View Appendix Table 6). However, the differences between setups 2 and 3 were not statistically significant, highlighting the efficiency of the osteotomy. Zawis´lak et al (2020) also reported an increase in transverse dimensions in the variants with palatal osteotomy but more anteriorly than posteriorly. They observed that to increase the lateral dimensions of the maxilla, osteotomy of the palatal suture produced a satisfactory effect with a moderate increase in stress in the facial skeleton. These findings were concomitant with our observations. Also consistent with the findings on the maxillary extension in our study was the report by Lee et al. (2014) of higher stresses in the zygomatic arch with the single mid-palatal cut, compared with the osteotomies combined with lateral cuts and pterygomaxillary disjunction. Nevertheless, Lee et al. did not find significant differences between the evaluated surgical modalities in which the amounts of stress were low and similar. The disparity in the findings could be explained by low amounts of loading Lee et al exerted on the anatomic structures after separation of the mid-palatal suture; they applied an initial expansion of only 0.5-mm compared to 4mm in our study.

All types of osteotomies caused a significant elevation in stress at the buccal bone of the molars relative to the control model. The values were significantly higher after adding the Lefort osteotomy suggesting that the dissipation of the molar buccal area stress was no longer possible after adding the lateral cuts.

In comparison to the control and other experimental models, a considerable increase in expansion was revealed at the level of molars, canines and incisors when the LeFort osteotomy was introduced. The maximal value was recorded at the first molars

level (View Appendix Table 6). In contrast with the results of Zawisłak et al, who noted that the expansion of the anterior and lateral teeth was similar, thus producing parallel expansion (Zawisłak et al., 2020). Han et al. (2009) found that displacement in the x-axis gradually increased from the control setup to that including only LeFort with separation at pterygomaxillary junction and that the expansion increased almost twice, especially in the posterior region, after adding a paramedian osteotomy. Similarly, Dalband et al. (2015) described displacement in the X axis gradually increasing from the control the combined LeFort osteotomy with pterygomaxillary separation, with maximal expansion when a para-sagittal osteotomy was added. Coincident with our findings, the increase was observed mainly in the posterior maxillary region, indicating that a favorable maxillary expansion in the posterior maxilla would require all three osteotomies.

Also, relative to having the mid-palatal cut alone, adding a cut at the anterior nasal spine or adding lateral cuts did not make a significant difference. However, more expansion is achieved at all three areas relative to the control model when adding lateral cuts to the mid-palatal and anterior nasal spine osteotomies.

Except for setup 5, expansion in the incisors region was greater than that in the first molar region in our study. The Lefort 1 osteotomy resulted in significantly greater expansion at the cervical bone of the first molars relative to the incisors (View Appendix Table 6). Similarly, Kaya et al. (2023) observed more displacement with LeFort combined with PMJ separation in the molar area compared to the premolar areas in the bone-borne modality. However, Zawisłak et al. (2020) reported similar expansion in the anterior and lateral teeth, and greater expansion in the anterior maxillary region. Mołhlenrich et al. (2017) reported that when combining a mid-

palatal and lateral cuts with pterygomaxillary separation, the lateral opening of the median gap was relatively uniform, whereas the models with only median osteotomy showed proportionally larger opening in the anterior region relative to the posterior region of the same model. Lee et al. (2014) stated that using a bone-borne expander with all types of osteotomies led to more anterior than posterior alveolar bone displacement. They related this finding to the decreased resistance in the anterior area that resulted from the surgical approaches.

5.2 Correlations

5.2.1 *Correlation between stress and displacement*

The correlations between stress and displacement reveal that the more osteotomies are included in the expansion setup, the less correlations are present between the stress and amount of expansion. In the control model, more expansion at the canines level was observed with an increase in stress at the buccal and palatal bone of the molars and more expansion at the incisors is noted with more stress at the bone buccal to the incisors, which could be explained by more tension on the bone caused by more displacement, due to the absence of osteotomies to help release the stress (Appendix Table 1). More expansion anteriorly (at incisors level) was accompanied by more stress buccal to the incisors. After introducing the mid-palatal cut, stress at the bone buccal and palatal to the molars started correlating positively with the expansion posteriorly at the molar's level. Moreover, after the addition of the ANS and lateral cuts, an increase in stress buccal to the incisors was associated with an increase in expansion anteriorly, meaning that the presence of the osteotomy did not help reduce stress at this region following more expansion. Finally, after applying the most invasive SARPE

osteotomy, the stresses were no longer affected by the amounts of expansion, probably because the skeletal parts moved more freely with less constraints. However, the stress decreased at the bone palatal to the incisors with more expansion at the molar.

5.2.2 Correlation between bone thickness and displacement

In the control setup, thickness of the bone palatal to the incisors correlated with expansion at all levels, especially anteriorly because this area is the closest to the force application areas. After adding the anterior nasal spine osteotomy, expansion anteriorly was affected by the thickness of the bone buccal and palatal to the incisors, due to the position of the osteotomy in the anterior area: more bone thickness was associated with more expansion in this case, therefore applying the osteotomy would be more effective in thicker bone. No correlations were found between bone thickness and displacement in setup 5, moreover, bone thickness variable does not affect the amount of expansion when more extensive cuts are applied (Appendix Table 5).

5.2.3 Correlation between bone thickness and stress

Before incorporating any osteotomy to the expansion models, bone thickness at the buccal side of the incisors correlated the most with the stress at the bone palatal to the incisors and bone thickness at the palatal side of the incisors correlated with stress at the bone buccal to the incisors. The greater the thickness, the more stress was generated. However, when simulating the mid-palatal sagittal osteotomy, the stress at the bone palatal to the incisors started correlating positively with stress posteriorly at the bone buccal and palatal to the molars. Hypothetically, these associations could be related to the extension of the mid-palatal osteotomy from distal of the incisors to distal of the molars, therefore thickness of the bone anteriorly could affect displacement posteriorly.

After adding Lefort osteotomy, the thickness of the bone correlated moderately with stress, since the extensive cut did not allow bone properties such as thickness to affect the stress generated.

5.3 Clinical implications

The findings suggest several clinical implications, some of which supporting our hypothesis.

1. The mid-palatal area exhibited the highest stress during bone-borne expansion without surgical cuts. The addition of mid-palatal sagittal osteotomy reduced the stress by half in this area. The further additions of various osteotomies did not generate greater stress. Therefore, the mid-palatal osteotomy seems sufficient to reduce stress significantly.
2. Expansion assumed a V-shaped pattern, greater anteriorly than posteriorly, except in model 4 with the most extended osteotomies, when the widening was greater posteriorly. Therefore, a more invasive osteotomy would be required if more posterior is sought. However, a mid-palatal osteotomy could avoid the more morbid SARPE if more expansion is sought anteriorly and a moderate one posteriorly.
3. Expansion increases in all areas with each added osteotomy to the surgical protocol, but the addition of the lateral osteotomies to the mid-palatal and anterior nasal spine osteotomies does not yield added value to the outcome. Thus, these additional cuts would not be necessary, reducing the morbidity of the surgical intervention.
4. The increased stress in the maxillary extension areas was correlated with the decreased stress in the suture area. If boundaries were not set around the surrounding extensions of the maxilla, the stress would have dissipated in the structures bound

within this extension. Accordingly, such distribution should be expected in the clinical setting.

5. The thickness of trabecular and cortical bones can be differentiated by their density using cone-beam computed tomography imaging, which has been observed to vary significantly on this type of imaging (Ghafari & Ammouy, 2020). The use of this additional diagnostic tool will allow a mapping of individual bone topography and the development of a surgical treatment plan with the choice of the adequate osteotomy for each case. As the osteotomies included are more invasive, individual variation such as bone thickness correlates less with the stress and expansion amounts.
6. The stresses recorded at the palatal bone of the incisors were not statistically significantly different among all experimental setups except with the control setup. This finding indicates that any adjunct osteotomy combined with RPE in skeletally mature patients is more efficient than the MARPE alone. Accordingly, the limitations of MARPE should be known to the orthodontist before its application.

5.4 Limitations and research considerations

Our results may not correspond to those obtained in clinical settings because our study included mathematical modeling based on radiographic imaging of a skull, even though the inclusion of individual variation of cortical bone anatomy moved the investigation closer to clinical reality than single FEA models.

The results depend on the patient's level of bone maturity; in the present research setting, the material properties represent adult morphology but must be seen within the parameters and limitations of the experimental setup. Influencing factors are variable,

including shape of the palate and other anatomic structures, maturity of the suture, and bone density, all potentially affecting the biomechanical expression of the maxillary expansion. Thus, the non-invasive FE modeling provides trends and may not translate in firm clinical guidelines until preferably time-dependent FEA is investigated, ideally in tandem with clinical treatment. The addition of the palatal (and other) soft tissues to the model might improve the accuracy of the simulation.

In the foreseen investigations, the addition of creep strain to the finite element model and the application of cycles of force over time may produce a better resemblance to the clinical scenario.

As in most FE simulations, we based ours on an optimized model that comprises ideal properties (elastic moduli and Poisson's ratios). However, the measured stresses are at best approximations allowing for some systematic error. We did not include the intra-bony part of the mini-screw, modeling only its head for force application. This simplification is acceptable for the study aims that did not include the assessment of differences in the shapes and sizes of the anchoring devices.

With the necessity of establishing boundary conditions, we opted to fix the posterior section of the maxilla in all planes of space, even in setup 4, in which the surgical cut required the cut of the pterygomaxillary junction. This distinction may have represented a limitation as the results may have been influenced, possibly preventing additional expansion, which was nevertheless greatest posteriorly in this setup.

CHAPTER 6

CONCLUSIONS

1. The minimally invasive mid-palatal cut performed during surgically assisted rapid palatal expansion is the most efficient at reducing stress in the area showing the maximal stress values: the mid-palatal suture area.
2. A re-distribution of this stress in the entire facial skeleton causes an increase in stress numbers at the areas farther from the suture
3. Expansion anteriorly and posteriorly improves significantly when performing a mid-palatal osteotomy alone. However, in order to obtain maximal expansion, a Lefort osteotomy is needed. Adding anterior nasal spine and lateral osteotomies to the mid-palatal cut will not increase the displacement significantly.
4. Expansion occurs in a V-shape, more anteriorly than posteriorly in all modalities, however, when more expansion is needed posteriorly than anteriorly, a more invasive osteotomy is necessary.
5. The amount of expansion is less likely to be affected by bone thickness when applying the most invasive osteotomy (Lefort I), a less extensive approach, such as incorporating a mid-palatal cut will leave more room for individual variations to affect the result, therefore in this case a cone-beam computed tomography imaging is necessary diagnostic tool to evaluate the indication of this osteotomy.

APPENDIX

Table of contents of the appendix:

Table 1: Table of correlations between stress, expansion, and cortical bone thickness for the control setup.

Table 2: Table of correlations between stress, expansion, and cortical bone thickness for setup 1

Table 3: Table of correlations between stress, expansion, and cortical bone thickness for setup 2

Table 4: Table of correlations between stress, expansion, and cortical bone thickness for setup 3

Table 5: Table of correlations between stress, expansion, and cortical bone thickness for setup 4

Table 6: Table of correlations between stress, expansion, and cortical bone thickness for setup 5

Figure 1: Percentage of displacement at molar, canine and incisor region in each setup

Table 1: Table of correlations between stress, expansion, and cortical bone thickness for the control setup

		Exp6	Exp3	Exp1	StressMidPa	StressMax	StressMEx	StressBlnc	Stressalnc	StressBM	StressPaM	BT6B	BT6P	BTIncb	BTIncP
Exp6	Correlation	1	.758**	.807**	0.218	0.502	0.232	.670*	0.27	0.549	0.549	0.417	0.24	0.226	.588*
	Sig. (2-tailed)	.	0.003	0.001	0.474	0.08	0.446	0.012	0.372	0.052	0.052	0.157	0.43	0.457	0.035
Exp3	Correlation		1	.771**	0.43	.734**	0.284	0.491	0.086	.706**	.830**	0.483	0.466	0.041	.657*
	Sig. (2-tailed)		.	0.002	0.142	0.004	0.347	0.088	0.781	0.007	0	0.095	0.108	0.893	0.015
Exp1	Correlation			1	0.166	0.497	0.276	.790**	0.541	.613*	0.436	0.442	0.254	0.436	.818**
	Sig. (2-tailed)			.	0.588	0.084	0.361	0.001	0.056	0.026	0.136	0.13	0.402	0.136	0.001
Stress	Correlation				1	0.11	.709**	0.242	-0.049	0.357	0.396	0.522	0.385	-0.286	0.055
	Sig. (2-tailed)				.	0.721	0.007	0.426	0.873	0.231	0.181	0.067	0.194	0.344	0.859
Stress	Correlation					1	0.088	0.346	0.066	0.308	.632*	0.385	0.247	0.033	0.467
	Sig. (2-tailed)					.	0.775	0.247	0.831	0.306	0.021	0.194	0.415	0.915	0.108
Stress	Correlation						1	0.516	0.352	0.286	0.187	.808**	.560*	0.071	0.291
	Sig. (2-tailed)						.	0.071	0.239	0.344	0.541	0.001	0.046	0.817	0.334
StressB	Correlation							1	.753**	0.527	0.231	.593*	0.335	.610*	.764**
	Sig. (2-tailed)							.	0.003	0.064	0.448	0.033	0.263	0.027	0.002
StressP	Correlation								1	0.214	-0.148	0.418	-0.027	.874**	0.505
	Sig. (2-tailed)								.	0.482	0.629	0.156	0.929	0	0.078
StressB	Correlation									1	.703**	0.269	0.533	0.099	.626*
	Sig. (2-tailed)									.	0.007	0.374	0.061	0.748	0.022
StressP	Correlation										1	0.264	0.335	-0.203	0.39
	Sig. (2-tailed)										.	0.384	0.263	0.505	0.188
BT6B	Correlation											1	.654*	0.357	0.538
	Sig. (2-tailed)											.	0.015	0.231	0.058
BT6P	Correlation												1	0.016	.582*
	Sig. (2-tailed)												.	0.957	0.037
BTIncb	Correlation													1	0.549
	Sig. (2-tailed)													.	0.052
BTIncP	Correlation														1
	Sig. (2-tailed)														.

StressMidPa: Stress at the mid-palatal area; **StressMax:** Stress at the maxilla; **StressMEx:** Stress at the maxillary extension; **StressBlnc:** Stress at the buccal bone of the incisors; **StressPalnc:** Stress at the palatal bone of the incisors; **StressBM:** Stress at the buccal bone of the molars; **StressPaM:** stress at the palatal bone of the molars; ; **Exp6:** expansion at the first molars; **Exp3:** expansion at the canines; **Exp1:** expansion at the incisors; **BT6B:** buccal bone thickness at first molars; **BT6P:** palatal bone thickness at first molars; **BTIncb:** buccal bone thickness at the incisors; **BTIncP:** palatal bone thickness at the incisors **StD:** standard variation. ** Correlation is significant at the 0.01; * Correlation is significant at the 0.05 level (2-tailed).

Table 2: Table of correlations between stress, expansion, and cortical bone thickness for setup 2

		Exp6	Exp3	Exp1	StressMidPa	StressMax	StressMEx	StressBlnc	Stressalnc	StressBM	StressPaM	BT6B	BT6P	BTIncb	BTIncP
Exp6	Correlation	1	0.314	.616*	.583*	0.36	0.41	.655*	0.396	.790**	.831**	.600*	0.377	0.316	.680*
	Sig. (2-tailed)	.	0.296	0.025	0.036	0.226	0.164	0.015	0.18	0.001	0	0.03	0.204	0.292	0.011
Exp3	Correlation		1	0.352	0.217	0.545	0.297	0.113	0.201	0.429	0.377	0.162	0.245	-0.143	0.234
	Sig. (2-tailed)		.	0.238	0.476	0.054	0.324	0.714	0.511	0.143	0.204	0.596	0.42	0.641	0.442
Exp1	Correlation			1	-0.049	0.209	0.253	.725**	.692**	0.533	0.516	0.214	-0.077	0.544	.588*
	Sig. (2-tailed)			.	0.873	0.494	0.405	0.005	0.009	0.061	0.071	0.482	0.803	0.055	0.035
Stress	Correlation				1	0.247	0.522	0.242	0.099	0.467	.588*	0.484	0.544	0.148	0.33
	Sig. (2-tailed)				.	0.415	0.067	0.426	0.748	0.108	0.035	0.094	0.055	0.629	0.271
Stress	Correlation					1	0.099	0.055	-0.126	0.533	0.214	-0.099	0.335	-0.352	0.308
	Sig. (2-tailed)					.	0.748	0.859	0.681	0.061	0.482	0.748	0.263	0.239	0.306
Stress	Correlation						1	0.357	0.429	0.418	0.401	0.379	0.412	0.495	0.473
	Sig. (2-tailed)						.	0.231	0.144	0.156	0.174	0.201	0.162	0.086	0.103
StressB	Correlation							1	.764**	0.335	0.527	0.44	0.038	.720**	0.516
	Sig. (2-tailed)							.	0.002	0.263	0.064	0.133	0.901	0.006	0.071
StressP	Correlation								1	0.049	0.33	0.478	-0.049	.648*	0.275
	Sig. (2-tailed)								.	0.873	0.271	0.098	0.873	0.017	0.364
StressB	Correlation									1	.648*	0.258	0.407	0.231	.709**
	Sig. (2-tailed)									.	0.017	0.394	0.168	0.448	0.007
StressP	Correlation										1	.582*	0.302	0.401	.736**
	Sig. (2-tailed)										.	0.037	0.316	0.174	0.004
BT6B	Correlation											1	.654*	0.357	0.538
	Sig. (2-tailed)											.	0.015	0.231	0.058
BT6P	Correlation												1	0.016	.582*
	Sig. (2-tailed)												.	0.957	0.037
BTIncb	Correlation													1	0.549
	Sig. (2-tailed)													.	0.052
BTIncP	Correlation														1
	Sig. (2-tailed)														.

StressMidPa: Stress at the mid-palatal area; **StressMax:** Stress at the maxilla; **StressMEx:** Stress at the maxillary extension; **StressBlnc:** Stress at the buccal bone of the incisors; **StressPalnc:** Stress at the palatal bone of the incisors; **StressBM:** Stress at the buccal bone of the molars; **StressPaM:** stress at the palatal bone of the molars; ; **Exp6:** expansion at the first molars; **Exp3:** expansion at the canines; **Exp1:** expansion at the incisors; **BT6B:** buccal bone thickness at first molars; **BT6P:** palatal bone thickness at first molars; **BTIncb:** buccal bone thickness at the incisors; **BTIncP:** palatal bone thickness at the incisors **StD:** standard variation. ** Correlation is significant at the 0.01; * Correlation is significant at the 0.05 level (2-tailed).

Table 3: Table of correlations between stress, expansion, and cortical bone thickness for setup 3

		Exp6	Exp3	Exp1	StressMidPa	StressMax	StressMEx	StressBlnc	Stressalnc	StressBM	StressPaM	BT6B	BT6P	BTInCB	BTInCP
Exp6	Correlation	1	0.309	.623*	0.534	0.14	0.072	.672*	0.146	0.24	0.275	0.331	0.143	0.201	0.466
	Sig. (2-tailed)	.	0.304	0.023	0.06	0.647	0.816	0.012	0.634	0.43	0.362	0.27	0.641	0.51	0.109
Exp3	Correlation		1	0.38	0.196	-0.256	0.124	0.289	-0.35	0.245	0.449	0.036	0.284	-0.099	0.306
	Sig. (2-tailed)		.	0.2	0.522	0.398	0.687	0.338	0.241	0.419	0.124	0.908	0.347	0.747	0.31
Exp1	Correlation			1	0.115	-0.154	0.126	.753**	0.192	0.06	0.473	0.423	0.121	.720**	.775**
	Sig. (2-tailed)			.	0.707	0.616	0.681	0.003	0.529	0.845	0.103	0.15	0.694	0.006	0.002
Stress	Correlation				1	0.291	0	0.28	0.264	0.176	-0.115	0.467	0.198	-0.077	0.033
	Sig. (2-tailed)				.	0.334	1	0.354	0.384	0.566	0.707	0.108	0.517	0.803	0.915
Stress	Correlation					1	-0.198	0.132	0.313	0.06	-0.242	-0.165	-0.044	0	-0.06
	Sig. (2-tailed)					.	0.517	0.668	0.297	0.845	0.426	0.59	0.887	1	0.845
Stress	Correlation						1	0.308	-0.357	0.527	0.17	0.126	0.346	-0.126	0.379
	Sig. (2-tailed)						.	0.306	0.231	0.064	0.578	0.681	0.247	0.681	0.201
StressB	Correlation							1	0.099	0.258	0.33	.610*	0.434	0.451	.775**
	Sig. (2-tailed)							.	0.748	0.394	0.271	0.027	0.138	0.122	0.002
StressP	Correlation								1	0.154	0.148	0.308	-0.06	0.478	0.143
	Sig. (2-tailed)								.	0.616	0.629	0.306	0.845	0.098	0.642
StressB	Correlation									1	.720**	0.236	.632*	-0.137	.555*
	Sig. (2-tailed)									.	0.006	0.437	0.021	0.655	0.049
StressP	Correlation										1	0.269	0.527	0.22	.775**
	Sig. (2-tailed)										.	0.374	0.064	0.471	0.002
BT6B	Correlation											1	.654*	0.357	0.538
	Sig. (2-tailed)											.	0.015	0.231	0.058
BT6P	Correlation												1	0.016	.582*
	Sig. (2-tailed)												.	0.957	0.037
BTInCB	Correlation													1	0.549
	Sig. (2-tailed)													.	0.052
BTInCP	Correlation														1
	Sig. (2-tailed)														.

StressMidPa: Stress at the mid-palatal area; **StressMax:** Stress at the maxilla; **StressMEx:** Stress at the maxillary extension; **StressBlnc:** Stress at the buccal bone of the incisors; **StressPalnc:** Stress at the palatal bone of the incisors; **StressBM:** Stress at the buccal bone of the molars; **StressPaM:** stress at the palatal bone of the molars; ; **Exp6:** expansion at the first molars; **Exp3:** expansion at the canines; **Exp1:** expansion at the incisors; **BT6B:** buccal bone thickness at first molars; **BT6P:** palatal bone thickness at first molars; **BTInCB:** buccal bone thickness at the incisors; **BTInCP:** palatal bone thickness at the incisors **StD:** standard variation. ** Correlation is significant at the 0.01; * Correlation is significant at the 0.05 level (2-tailed).

Table 4: Table of correlations between stress, expansion, and cortical bone thickness for setup 4

		Exp6	Exp3	Exp1	StressMidPa	StressMax	StressMEx	StressBlnc	Stressalnc	StressBM	StressPaM	BT6B	BT6P	BTInCB	BTInCP
Exp6	Correlation	1	0.435	.586*	0.33	0.088	0.234	0.371	-0.366	0.484	0.283	0.184	0.187	0.066	0.517
	Sig. (2-tailed)	.	0.137	0.035	0.271	0.775	0.442	0.212	0.219	0.094	0.348	0.547	0.541	0.83	0.07
Exp3	Correlation		1	0.223	0.415	.633*	0.022	-0.074	-0.44	0.446	0.322	0.27	0.415	-0.14	0.36
	Sig. (2-tailed)		.	0.464	0.158	0.02	0.943	0.809	0.132	0.127	0.284	0.373	0.158	0.648	0.226
Exp1	Correlation			1	-0.082	-0.192	0.275	0.137	-0.236	0.28	0.445	0.192	0.005	.687**	.643*
	Sig. (2-tailed)			.	0.789	0.529	0.364	0.655	0.437	0.354	0.128	0.529	0.986	0.01	0.018
Stress	Correlation				1	.665*	0.5	.626*	0.044	.566*	0.478	.593*	0.478	-0.143	0.242
	Sig. (2-tailed)				.	0.013	0.082	0.022	0.887	0.044	0.098	0.033	0.098	0.642	0.426
Stress	Correlation					1	0.187	0.335	0.005	0.451	0.308	0.297	0.33	-0.324	0.148
	Sig. (2-tailed)					.	0.541	0.263	0.986	0.122	0.306	0.325	0.271	0.28	0.629
Stress	Correlation						1	.637*	0.418	.604*	.588*	0.401	0.363	0.247	0.324
	Sig. (2-tailed)						.	0.019	0.156	0.029	0.035	0.174	0.223	0.415	0.28
StressB	Correlation							1	0.319	.720**	.588*	0.412	0.313	0.121	0.418
	Sig. (2-tailed)							.	0.289	0.006	0.035	0.162	0.297	0.694	0.156
StressP	Correlation								1	0.192	0.302	0.28	0	0.159	-0.027
	Sig. (2-tailed)								.	0.529	0.316	0.354	1	0.603	0.929
StressB	Correlation									1	.835**	0.527	0.538	0.159	.709**
	Sig. (2-tailed)									.	0	0.064	0.058	0.603	0.007
StressP	Correlation										1	.659*	0.291	0.451	.615*
	Sig. (2-tailed)										.	0.014	0.334	0.122	0.025
BT6B	Correlation											1	.654*	0.357	0.538
	Sig. (2-tailed)											.	0.015	0.231	0.058
BT6P	Correlation												1	0.016	.582*
	Sig. (2-tailed)												.	0.957	0.037
BTInCB	Correlation													1	0.549
	Sig. (2-tailed)													.	0.052
BTInCP	Correlation														1
	Sig. (2-tailed)														.

StressMidPa: Stress at the mid-palatal area; **StressMax:** Stress at the maxilla; **StressMEx:** Stress at the maxillary extension; **StressBlnc:** Stress at the buccal bone of the incisors; **StressPalnc:** Stress at the palatal bone of the incisors; **StressBM:** Stress at the buccal bone of the molars; **StressPaM:** stress at the palatal bone of the molars; ; **Exp6:** expansion at the first molars; **Exp3:** expansion at the canines; **Exp1:** expansion at the incisors; **BT6B:** buccal bone thickness at first molars; **BT6P:** palatal bone thickness at first molars; **BTInCB:** buccal bone thickness at the incisors; **BTInCP:** palatal bone thickness at the incisors **Std:** standard variation. ** Correlation is significant at the 0.01; * Correlation is significant at the 0.05 level (2-tailed).

Table 5: Table of correlations between stress, expansion, and cortical bone thickness for setup 5

		Exp6	Exp3	Exp1	StressMidPa	StressMax	StressMEx	StressBlnc	Stressalnc	StressBM	StressPaM	BT6B	BT6P	BTIncb	BTIncP
Exp6	Correlation	1	0.41	0.248	-0.292	0.028	0.179	-0.256	-.765**	0.069	-.652*	0.003	0.099	0.36	0.179
	Sig. (2-tailed)	.	0.164	0.415	0.334	0.929	0.559	0.399	0.002	0.823	0.016	0.993	0.748	0.226	0.559
Exp3	Correlation		1	.687**	-0.093	-0.044	0.077	-0.22	-0.412	0.231	-0.313	-0.17	0.176	0.104	0.456
	Sig. (2-tailed)		.	0.01	0.762	0.887	0.803	0.471	0.162	0.448	0.297	0.578	0.566	0.734	0.117
Exp1	Correlation			1	0.071	0.148	0.033	-0.176	-0.264	.621*	-0.181	-0.143	0.275	0.379	0.478
	Sig. (2-tailed)			.	0.817	0.629	0.915	0.566	0.384	0.024	0.553	0.642	0.364	0.201	0.098
Stress	Correlation				1	0.456	-0.214	.593*	0.209	.566*	0.538	0.143	.582*	-0.522	-0.082
	Sig. (2-tailed)				.	0.117	0.482	0.033	0.494	0.044	0.058	0.642	0.037	0.067	0.789
Stress	Correlation					13	13	13	13	13	13	13	13	13	13
	Sig. (2-tailed)					1	-.604*	0.379	0.198	.626*	0.302	-0.363	-0.082	-0.247	-0.352
Stress	Correlation					.	0.029	0.201	0.517	0.022	0.316	0.223	0.789	0.415	0.239
	Sig. (2-tailed)						1	-0.055	-0.407	-0.379	-0.214	.566*	0.286	.555*	.670*
StressB	Correlation						.	0.859	0.168	0.201	0.482	0.044	0.344	0.049	0.012
	Sig. (2-tailed)							1	0.253	0.313	0.291	0.297	0.39	-0.462	0.077
StressP	Correlation							.	0.405	0.297	0.334	0.325	0.188	0.112	0.803
	Sig. (2-tailed)								1	0.154	0.538	-0.071	-0.22	-0.286	-0.313
StressB	Correlation								.	0.616	0.058	0.817	0.471	0.344	0.297
	Sig. (2-tailed)									1	0.049	-0.082	0.462	-0.06	0.099
StressP	Correlation								.	0.873	0.789	0.112	0.845	0.748	
	Sig. (2-tailed)									1	-0.203	-0.242	-0.456	-0.456	
BT6B	Correlation										.	0.505	0.426	0.117	0.117
	Sig. (2-tailed)											1	.654*	0.357	0.538
BT6P	Correlation											.	0.015	0.231	0.058
	Sig. (2-tailed)												1	0.016	.582*
BTIncb	Correlation												.	0.957	0.037
	Sig. (2-tailed)													1	0.549
BTIncP	Correlation													.	0.052
	Sig. (2-tailed)														1

StressMidPa: Stress at the mid-palatal area; **StressMax:** Stress at the maxilla; **StressMEx:** Stress at the maxillary extension; **StressBlnc:** Stress at the buccal bone of the incisors; **StressPalnc:** Stress at the palatal bone of the incisors; **StressBM:** Stress at the buccal bone of the molars; **StressPaM:** stress at the palatal bone of the molars; ; **Exp6:** expansion at the first molars; **Exp3:** expansion at the canines; **Exp1:** expansion at the incisors; **BT6B:** buccal bone thickness at first molars; **BT6P:** palatal bone thickness at first molars; **BTIncb:** buccal bone thickness at the incisors; **BTIncP:** palatal bone thickness at the incisors **Std:** standard variation. ** Correlation is significant at the 0.01; * Correlation is significant at the 0.05 level (2-tailed).

Table 6: Percentage of displacement at molar, canine and incisor regions in each setup

	Expansion at molar	Expansion at canine	Expansion at incisor
Setup 1	10.18	13.60	36.49
Setup 2	14.72	23.66	39.30
Setup 3	15.63	26.04	41.68
Setup 4	22.12	31.17	47.75
Setup 5	100.00	100.00	100.00

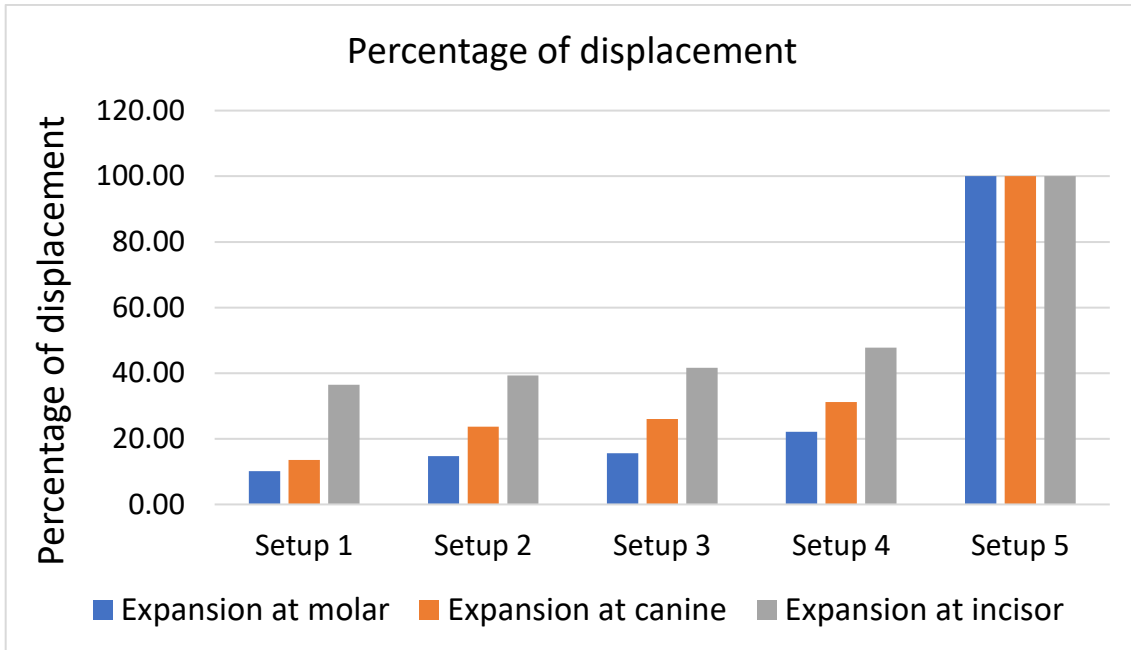


Figure 1: Graphic representation of data in Table 6.

REFERENCES

- Agarwal, A. (2010). Maxillary Expansion. *International Journal of Clinical Pediatric Dentistry*, 3(3), 139–146. <https://doi.org/10.5005/jp-journals-10005-1069>
- AlAsseri, N., & Swennen, G. (2018). Minimally invasive orthognathic surgery: A systematic review. *International Journal of Oral and Maxillofacial Surgery*, 47(10), 1299–1310. <https://doi.org/10.1016/j.ijom.2018.04.017>
- Aloise, A. C., Pereira, M. D., Hino, C. T., Filho, A. G., & Ferreira, L. M. (2007). Stability of the Transverse Dimension of the Maxilla After Surgically Assisted Rapid Expansion. *Journal of Craniofacial Surgery*, 18(4), 860. <https://doi.org/10.1097/scs.0b013e3180a77237>
- Ammoury, M. J., Mustapha, S., Dechow, P. C., & Ghafari, J. G. (2019). Two distalization methods compared in a novel patient-specific finite element analysis. *American Journal of Orthodontics and Dentofacial Orthopedics*, 156(3), 326–336. <https://doi.org/10.1016/j.ajodo.2018.09.017>
- Angelieri, F., Cevidanes, L. H. S., Franchi, L., Gonçalves, J. R., Benavides, E., & McNamara, J. A. (2013). Midpalatal suture maturation: Classification method for individual assessment before rapid maxillary expansion. *American Journal of Orthodontics and Dentofacial Orthopedics: Official Publication of the American Association of Orthodontists, Its Constituent Societies, and the American Board of Orthodontics*, 144(5), 759–769. <https://doi.org/10.1016/j.ajodo.2013.04.022>
- Angelieri, F., Franchi, L., Cevidanes, L. H. S., Gonçalves, J. R., Nieri, M., Wolford, L. M., & McNamara, J. A. (2017). Cone beam computed tomography evaluation of midpalatal suture maturation in adults. *International Journal of Oral and Maxillofacial Surgery*, 46(12), 1557–1561. <https://doi.org/10.1016/j.ijom.2017.06.021>
- Baccetti, T., Franchi, L., Cameron, C. G., & McNamara, J. A., Jr. (2001). Treatment Timing for Rapid Maxillary Expansion. *The Angle Orthodontist*, 71(5), 343–350. [https://doi.org/10.1043/0003-3219\(2001\)071<0343:TTFRME>2.0.CO;2](https://doi.org/10.1043/0003-3219(2001)071<0343:TTFRME>2.0.CO;2)
- Barbosa, V., Maganzini, A. L., & Nieberg, L. G. (2005). Dento-skeletal implications of Klippel-Feil syndrome [a case report]. *The New York State Dental Journal*, 71(1), 48–51.
- Barone, T. R., Cahali, M. B., Vasconcelos, C., & Barone, J. R. (2020). A comparison of tooth-borne and bone-anchored expansion devices in SARME. *Oral and Maxillofacial Surgery*, 24(2), 181–187. <https://doi.org/10.1007/s10006-020-00837-8>
- Bays, R. A., & Greco, J. M. (1992). Surgically assisted rapid palatal expansion: An outpatient technique with long-term stability. *Journal of Oral and Maxillofacial Surgery: Official Journal of the American Association of Oral and Maxillofacial Surgeons*, 50(2), 110–113; discussion 114–115. [https://doi.org/10.1016/0278-2391\(92\)90352-z](https://doi.org/10.1016/0278-2391(92)90352-z)
- Bell, W. H., & Jacobs, J. D. (1979). Surgical-orthodontic correction of horizontal maxillary deficiency. *Journal of Oral Surgery (American Dental Association: 1965)*, 37(12), 897–902.
- Betts, N. J. (2016). Surgically Assisted Maxillary Expansion. *Atlas of the Oral and Maxillofacial Surgery Clinics*, 24(1), 67–77. <https://doi.org/10.1016/j.cxom.2015.10.003>

- Betts, N. J., Vanarsdall, R. L., Barber, H. D., Higgins-Barber, K., & Fonseca, R. J. (1995). Diagnosis and treatment of transverse maxillary deficiency. *The International Journal of Adult Orthodontics and Orthognathic Surgery*, *10*(2), 75–96.
- Bierenbroodspot, F., Wering, P. C., Kuijpers-Jagtman, A. M., & Stoelinga, P. J. W. (2002). [Surgically assisted rapid maxillary expansion: A retrospective study]. *Nederlands Tijdschrift Voor Tandheelkunde*, *109*(8), 299–302.
- Bin Dakhil, N., & Bin Salamah, F. (n.d.). The Diagnosis Methods and Management Modalities of Maxillary Transverse Discrepancy. *Cureus*, *13*(12), e20482. <https://doi.org/10.7759/cureus.20482>
- Bin Dakhil, N., & Bin Salamah, F. (2023). The Diagnosis Methods and Management Modalities of Maxillary Transverse Discrepancy. *Cureus*, *13*(12), Article 12. <https://doi.org/10.7759/cureus.20482>
- Björk, A., & Helm, S. (1967). Prediction of the age of maximum puberal growth in body height. *The Angle Orthodontist*, *37*(2), 134–143. [https://doi.org/10.1043/0003-3219\(1967\)037<0134:POTAOM>2.0.CO;2](https://doi.org/10.1043/0003-3219(1967)037<0134:POTAOM>2.0.CO;2)
- Byloff, F. K., & Mossaz, C. F. (2004). Skeletal and dental changes following surgically assisted rapid palatal expansion. *European Journal of Orthodontics*, *26*(4), 403–409. <https://doi.org/10.1093/ejo/26.4.403>
- Camporesi, M., Franchi, L., Doldo, T., & Defraia, E. (2013). Evaluation of mechanical properties of three different screws for rapid maxillary expansion. *BioMedical Engineering OnLine*, *12*, 128. <https://doi.org/10.1186/1475-925X-12-128>
- Camps-Perepérez, I., Guijarro-Martínez, R., da Rosa, B. M., Haas Jr., O. L., & Hernández-Alfaro, F. (2023). Three-dimensional dentoskeletal changes following minimally invasive surgically assisted rapid palatal expansion: A prospective study. *International Journal of Oral and Maxillofacial Surgery*, *52*(4), 460–467. <https://doi.org/10.1016/j.ijom.2022.07.004>
- Capelozza Filho, L., Cardoso Neto, J., da Silva Filho, O. G., & Ursi, W. J. (1996). Non-surgically assisted rapid maxillary expansion in adults. *The International Journal of Adult Orthodontics and Orthognathic Surgery*, *11*(1), 57–66; discussion 67-70.
- Carvalho, P. H. A., Moura, L. B., Trento, G. S., Holzinger, D., Gabrielli, M. A. C., Gabrielli, M. F. R., & Pereira Filho, V. A. (2020). Surgically assisted rapid maxillary expansion: A systematic review of complications. *International Journal of Oral and Maxillofacial Surgery*, *49*(3), 325–332. <https://doi.org/10.1016/j.ijom.2019.08.011>
- Chamberland, S., & Proffit, W. R. (2011). Short-term and long-term stability of surgically assisted rapid palatal expansion revisited. *American Journal of Orthodontics and Dentofacial Orthopedics*, *139*(6), 815-822.e1. <https://doi.org/10.1016/j.ajodo.2010.04.032>
- Choi, T.-H., Kim, B.-I., Chung, C. J., Kim, H.-J., Baik, H.-S., Park, Y.-C., & Lee, K.-J. (2015). Assessment of masticatory function in patients with non-sagittal occlusal discrepancies. *Journal of Oral Rehabilitation*, *42*(1), 2–9. <https://doi.org/10.1111/joor.12227>

- Converse, J. M., & Horowitz, S. L. (1969). The surgical-orthodontic approach to the treatment of dentofacial deformities. *American Journal of Orthodontics*, 55(3), 217–243. [https://doi.org/10.1016/0002-9416\(69\)90104-3](https://doi.org/10.1016/0002-9416(69)90104-3)
- Cortella, S., Shofer, F. S., & Ghafari, J. (1997). Transverse development of the jaws: Norms for the posteroanterior cephalometric analysis. *American Journal of Orthodontics and Dentofacial Orthopedics*, 112(5), 519–522. [https://doi.org/10.1016/S0889-5406\(97\)70079-9](https://doi.org/10.1016/S0889-5406(97)70079-9)
- Dalband, M., Kashani, J., & Hashemzahi, H. (2015). Three-Dimensional Finite Element Analysis of Stress Distribution and Displacement of the Maxilla Following Surgically Assisted Rapid Maxillary Expansion with Tooth- and Bone-Borne Devices. *Journal of Dentistry (Tehran, Iran)*, 12(4), 298–306.
- de Assis, D. S. F. R., Xavier, T. A., Noritomi, P. Y., & Gonçalves, E. S. (2014). Finite element analysis of bone stress after SARPE. *Journal of Oral and Maxillofacial Surgery: Official Journal of the American Association of Oral and Maxillofacial Surgeons*, 72(1), 167.e1-7. <https://doi.org/10.1016/j.joms.2013.06.210>
- Field, C., Ichim, I., Swain, M. V., Chan, E., Darendeliler, M. A., Li, W., & Li, Q. (2009). Mechanical responses to orthodontic loading: A 3-dimensional finite element multi-tooth model. *American Journal of Orthodontics and Dentofacial Orthopedics*, 135(2), 174–181. <https://doi.org/10.1016/j.ajodo.2007.03.032>
- Ghafari, J. G. (2015). Centennial inventory: The changing face of orthodontics. *American Journal of Orthodontics and Dentofacial Orthopedics: Official Publication of the American Association of Orthodontists, Its Constituent Societies, and the American Board of Orthodontics*, 148(5), 732–739. <https://doi.org/10.1016/j.ajodo.2015.08.011>
- Ghafari, J. G., Macari, A. T., Zeno, K. G., & Haddad, R. V. (2020). Potential and limitations of orthodontic biomechanics: Recognizing the gaps between knowledge and practice. *Journal of the World Federation of Orthodontists*, 9(3), S31–S39. <https://doi.org/10.1016/j.ejwf.2020.08.008>
- Glassman, A. S., Nahigian, S. J., Medway, J. M., & Aronowitz, H. I. (1984). Conservative surgical orthodontic adult rapid palatal expansion: Sixteen cases. *American Journal of Orthodontics*, 86(3), 207–213. [https://doi.org/10.1016/0002-9416\(84\)90372-5](https://doi.org/10.1016/0002-9416(84)90372-5)
- Gogna, N., Johal, A. S., & Sharma, P. k. (2020). The stability of surgically assisted rapid maxillary expansion (SARME): A systematic review. *Journal of Cranio-Maxillofacial Surgery*, 48(9), 845–852. <https://doi.org/10.1016/j.jcms.2020.07.003>
- Haas, A. J. (1961). Rapid Expansion Of The Maxillary Dental Arch And Nasal Cavity By Opening The Midpalatal Suture. *The Angle Orthodontist*, 31(2), 73–90. [https://doi.org/10.1043/0003-3219\(1961\)031<0073:REOTMD>2.0.CO;2](https://doi.org/10.1043/0003-3219(1961)031<0073:REOTMD>2.0.CO;2)
- Haas, A. J. (1970). Palatal expansion: Just the beginning of dentofacial orthopedics. *American Journal of Orthodontics*, 57(3), 219–255. [https://doi.org/10.1016/0002-9416\(70\)90241-1](https://doi.org/10.1016/0002-9416(70)90241-1)

- Haas Junior, O. L., Matje, P. R. B., Rosa, B. M., Rojo-Sanchis, C., Guijarro-Martínez, R., Valls-Ontañón, A., Menezes, L. M., Hernández-Alfaro, F., & de Oliveira, R. B. (2022). Minimally invasive surgical and miniscrew-assisted rapid palatal expansion (MISMARPE) in adult patients. *Journal of Cranio-Maxillofacial Surgery*, 50(3), 211–217. <https://doi.org/10.1016/j.jcms.2021.12.011>
- Han, U. A., Kim, Y., & Park, J. U. (2009). Three-dimensional finite element analysis of stress distribution and displacement of the maxilla following surgically assisted rapid maxillary expansion. *Journal of Cranio-Maxillo-Facial Surgery: Official Publication of the European Association for Cranio-Maxillo-Facial Surgery*, 37(3), 145–154. <https://doi.org/10.1016/j.jcms.2008.10.002>
- Hernández-Alfaro, F., & Guijarro-Martínez, R. (2013). “Twist Technique” for Pterygomaxillary Dysjunction in Minimally Invasive Le Fort I Osteotomy. *Journal of Oral and Maxillofacial Surgery*, 71(2), 389–392. <https://doi.org/10.1016/j.joms.2012.04.032>
- Hernandez-Alfaro, F., Mareque Bueno, J., Diaz, A., & Pagés, C. M. (2010). Minimally Invasive Surgically Assisted Rapid Palatal Expansion With Limited Approach Under Sedation: A Report of 283 Consecutive Cases. *Journal of Oral and Maxillofacial Surgery*, 68(9), 2154–2158. <https://doi.org/10.1016/j.joms.2009.09.080>
- Hernández-Alfaro, F., & Valls-Ontañón, A. (2021). SARPE and MARPE. In M. R. Stevens, S. Ghasemi, & R. Tabrizi (Eds.), *Innovative Perspectives in Oral and Maxillofacial Surgery* (pp. 321–325). Springer International Publishing. https://doi.org/10.1007/978-3-030-75750-2_35
- Holberg, C., Steinhäuser, S., & Rudzki, I. (2007). Surgically assisted rapid maxillary expansion: Midfacial and cranial stress distribution. *American Journal of Orthodontics and Dentofacial Orthopedics: Official Publication of the American Association of Orthodontists, Its Constituent Societies, and the American Board of Orthodontics*, 132(6), 776–782. <https://doi.org/10.1016/j.ajodo.2005.12.036>
- Ishikawa, H., Nakamura, S., Misaki, K., Kudoh, M., Fukuda, H., & Yoshida, S. (1998). Scar tissue distribution on palates and its relation to maxillary dental arch form. *The Cleft Palate-Craniofacial Journal: Official Publication of the American Cleft Palate-Craniofacial Association*, 35(4), 313–319. https://doi.org/10.1597/1545-1569_1998_035_0313_stdopa_2.3.co_2
- Jensen, T., Johannesen, L. H., & Rodrigo-Domingo, M. (2015). Periodontal changes after surgically assisted rapid maxillary expansion (SARME). *Oral and Maxillofacial Surgery*, 19(4), 381–386. <https://doi.org/10.1007/s10006-015-0506-5>
- Kang, S., Lee, S.-J., Ahn, S.-J., Heo, M.-S., & Kim, T.-W. (2007). Bone thickness of the palate for orthodontic mini-implant anchorage in adults. *American Journal of Orthodontics and Dentofacial Orthopedics*, 131(4, Supplement), S74–S81. <https://doi.org/10.1016/j.ajodo.2005.09.029>
- Karp, N. S., McCarthy, J. G., Schreiber, J. S., Sissons, H. A., & Thorne, C. H. (1992). Membranous bone lengthening: A serial histological study. *Annals of Plastic Surgery*, 29(1), 2–7. <https://doi.org/10.1097/00000637-199207000-00002>

- Kaya, D., Kocadereli, I., Kan, B., & Tasar, F. (2011). Effects of facemask treatment anchored with miniplates after alternate rapid maxillary expansions and constrictions; A pilot study. *The Angle Orthodontist*, *81*(4), 639–646. <https://doi.org/10.2319/081010-473.1>
- Kaya, N., Seker, E. D., & Yücesoy, T. (2023). Comparison of the effects of different rapid maxillary expansion techniques on craniofacial structures: A finite element analysis study. *Progress in Orthodontics*, *24*(1), 7. <https://doi.org/10.1186/s40510-023-00459-2>
- Kennedy, J. W., Bell, W. H., Kimbrough, O. L., & James, W. B. (1976). Osteotomy as an adjunct to rapid maxillary expansion. *American Journal of Orthodontics*, *70*(2), 123–137. [https://doi.org/10.1016/s0002-9416\(76\)90313-4](https://doi.org/10.1016/s0002-9416(76)90313-4)
- Kim, T., Ishikawa, H., Chu, S., Handa, A., Iida, J., & Yoshida, S. (2002). Constriction of the maxillary dental arch by mucoperiosteal denudation of the palate. *The Cleft Palate-Craniofacial Journal: Official Publication of the American Cleft Palate-Craniofacial Association*, *39*(4), 425–431. https://doi.org/10.1597/1545-1569_2002_039_0425_cotmda_2.0.co_2
- King, L., Harris, E. F., & Tolley, E. A. (1993). Heritability of cephalometric and occlusal variables as assessed from siblings with overt malocclusions. *American Journal of Orthodontics and Dentofacial Orthopedics: Official Publication of the American Association of Orthodontists, Its Constituent Societies, and the American Board of Orthodontics*, *104*(2), 121–131. [https://doi.org/10.1016/S0889-5406\(05\)81001-7](https://doi.org/10.1016/S0889-5406(05)81001-7)
- Koç, O., & Bolat Gumus, E. (2023). Effects of different distractor positions on the formation of expansion, stress and displacement patterns in surgically assisted rapid maxillary expansion without pterygomaxillary disjunction: A finite element analysis study. *Computer Methods in Biomechanics and Biomedical Engineering*, *0*(0), 1–11. <https://doi.org/10.1080/10255842.2023.2170712>
- Koç, O., & Jacob, H. B. (2022). Surgically assisted rapid palatal expansion: Is the pterygomaxillary disjunction necessary? A finite element study. *Seminars in Orthodontics*, *28*(3), 227–242. <https://doi.org/10.1053/j.sodo.2022.10.017>
- Kole, H. (1959). Surgical operations on the alveolar ridge to correct occlusal abnormalities. *Oral Surgery, Oral Medicine, and Oral Pathology*, *12*(5), 515-529 concl. [https://doi.org/10.1016/0030-4220\(59\)90153-7](https://doi.org/10.1016/0030-4220(59)90153-7)
- Koudstaal, M. J., van der Wal, K. G. H., Wolvius, E. B., & Schulten, A. J. M. (2006). The Rotterdam Palatal Distractor: Introduction of the new bone-borne device and report of the pilot study. *International Journal of Oral and Maxillofacial Surgery*, *35*(1), 31–35. <https://doi.org/10.1016/j.ijom.2005.07.002>
- Kraut, R. A. (1984). Surgically assisted rapid maxillary expansion by opening the midpalatal suture. *Journal of Oral and Maxillofacial Surgery: Official Journal of the American Association of Oral and Maxillofacial Surgeons*, *42*(10), 651–655. [https://doi.org/10.1016/0278-2391\(84\)90207-6](https://doi.org/10.1016/0278-2391(84)90207-6)
- Lee, K.-J., Choi, S.-H., Choi, T.-H., Shi, K.-K., & Keum, B.-T. (2018). Maxillary transverse expansion in adults: Rationale, appliance design, and treatment outcomes. *Seminars in Orthodontics*, *24*(1), Article 1. <https://doi.org/10.1053/j.sodo.2018.01.006>

- Lee, S. C., Park, J. H., Bayome, M., Kim, K. B., Araujo, E. A., & Kook, Y.-A. (2014a). Effect of bone-borne rapid maxillary expanders with and without surgical assistance on the craniofacial structures using finite element analysis. *American Journal of Orthodontics and Dentofacial Orthopedics: Official Publication of the American Association of Orthodontists, Its Constituent Societies, and the American Board of Orthodontics*, 145(5), 638–648. <https://doi.org/10.1016/j.ajodo.2013.12.029>
- Lee, S. C., Park, J. H., Bayome, M., Kim, K. B., Araujo, E. A., & Kook, Y.-A. (2014b). Effect of bone-borne rapid maxillary expanders with and without surgical assistance on the craniofacial structures using finite element analysis. *American Journal of Orthodontics and Dentofacial Orthopedics*, 145(5), 638–648. <https://doi.org/10.1016/j.ajodo.2013.12.029>
- Lehman, J. A., Haas, A. J., Haas, D. G., & Lehman, J. A. (1984). Surgical Orthodontic Correction of Transverse Maxillary Deficiency: A Simplified Approach. *Plastic and Reconstructive Surgery*, 73(1), 62–66. <https://doi.org/10.1097/00006534-198401000-00013>
- Lim, J.-W., Kim, W.-S., Kim, I.-K., Son, C.-Y., & Byun, H.-I. (2003). Three dimensional finite element method for stress distribution on the length and diameter of orthodontic miniscrew and cortical bone thickness. *The korean journal of orthodontics*, 33(1), 11–20.
- Lines, P. A. (1975). Adult rapid maxillary expansion with corticotomy. *American Journal of Orthodontics*, 67(1), 44–56. [https://doi.org/10.1016/0002-9416\(75\)90128-1](https://doi.org/10.1016/0002-9416(75)90128-1)
- Luxi, W., Xiaojia, S., Juan, L. I., Pengruofeng, L., & Jun, L. (2017). Midpalatal cortex osteotomy assisted rapid maxillary expansion for correction of maxillary transverse deficiency in young adults. *Zhejiang Da Xue Xue Bao. Yi Xue Ban = Journal of Zhejiang University. Medical Sciences*, 46, 198–205. <https://doi.org/10.3785/j.issn.1008-9292.2017.04.13>
- Marchetti, C., Pironi, M., Bianchi, A., & Musci, A. (2009). Surgically assisted rapid palatal expansion vs. segmental Le Fort I osteotomy: Transverse stability over a 2-year period. *Journal of Cranio-Maxillofacial Surgery*, 37(2), 74–78. <https://doi.org/10.1016/j.jcms.2008.08.006>
- Marshall, S. D., Southard, K. A., & Southard, T. E. (2005). Early Transverse Treatment. *Seminars in Orthodontics*, 11(3), 130–139. <https://doi.org/10.1053/j.sodo.2005.04.006>
- McNamara, J. A., Sigler, L. M., Franchi, L., Guest, S. S., & Baccetti, T. (2010). Changes in Occlusal Relationships in Mixed Dentition Patients Treated with Rapid Maxillary Expansion: A Prospective Clinical Study. *The Angle Orthodontist*, 80(2), 230–238. <https://doi.org/10.2319/040309-192.1>
- Melsen, B. (1975). Palatal growth studied on human autopsy material. A histologic microradiographic study. *American Journal of Orthodontics*, 68(1), 42–54. [https://doi.org/10.1016/0002-9416\(75\)90158-x](https://doi.org/10.1016/0002-9416(75)90158-x)
- Menon, S., Manerikar, R., & Sinha, R. (2010). Surgical Management of Transverse Maxillary Deficiency in Adults. *Journal of Maxillofacial and Oral Surgery*, 9(3), Article 3. <https://doi.org/10.1007/s12663-010-0034-7>

- Middleton, J., Jones, M., & Wilson, A. (1996). The role of the periodontal ligament in bone modeling: The initial development of a time-dependent finite element model. *American Journal of Orthodontics and Dentofacial Orthopedics*, *109*(2), 155–162. [https://doi.org/10.1016/S0889-5406\(96\)70176-2](https://doi.org/10.1016/S0889-5406(96)70176-2)
- Möhlhenrich, S. C., Modabber, A., Kniha, K., Peters, F., Steiner, T., Hölzle, F., Fritz, U., & Raith, S. (2017). Simulation of three surgical techniques combined with two different bone-borne forces for surgically assisted rapid palatal expansion of the maxillofacial complex: A finite element analysis. *International Journal of Oral and Maxillofacial Surgery*, *46*(10), 1306–1314. <https://doi.org/10.1016/j.ijom.2017.05.015>
- Mommaerts, M. Y. (1999). Transpalatal distraction as a method of maxillary expansion. *The British Journal of Oral & Maxillofacial Surgery*, *37*(4), 268–272. <https://doi.org/10.1054/bjom.1999.0127>
- Northway, W. M., & Meade, J. B. (1997). Surgically assisted rapid maxillary expansion: A comparison of technique, response, and stability. *The Angle Orthodontist*, *67*(4), 309–320. [https://doi.org/10.1043/0003-3219\(1997\)067<0309:SARMEA>2.3.CO;2](https://doi.org/10.1043/0003-3219(1997)067<0309:SARMEA>2.3.CO;2)
- Nowak, R., Olejnik, A., Gerber, H., Frątczak, R., & Zawisłak, E. (2021). Comparison of Tooth- and Bone-Borne Appliances on the Stress Distributions and Displacement Patterns in the Facial Skeleton in Surgically Assisted Rapid Maxillary Expansion—A Finite Element Analysis (FEA) Study. *Materials*, *14*(5), Article 5. <https://doi.org/10.3390/ma14051152>
- Oliveira De Felipe, N. L., Da Silveira, A. C., Viana, G., Kusnoto, B., Smith, B., & Evans, C. A. (2008). Relationship between rapid maxillary expansion and nasal cavity size and airway resistance: Short- and long-term effects. *American Journal of Orthodontics and Dentofacial Orthopedics: Official Publication of the American Association of Orthodontists, Its Constituent Societies, and the American Board of Orthodontics*, *134*(3), 370–382. <https://doi.org/10.1016/j.ajodo.2006.10.034>
- Oulis, C. J., Vadiakas, G. P., Ekonomides, J., & Dratsa, J. (1994). The effect of hypertrophic adenoids and tonsils on the development of posterior crossbite and oral habits. *The Journal of Clinical Pediatric Dentistry*, *18*(3), 197–201.
- Persson, M., & Thilander, B. (1977). Palatal suture closure in man from 15 to 35 years of age. *American Journal of Orthodontics*, *72*(1), 42–52. [https://doi.org/10.1016/0002-9416\(77\)90123-3](https://doi.org/10.1016/0002-9416(77)90123-3)
- Pogrel, M. A., Kaban, L. B., Vargervik, K., & Baumrind, S. (1992). Surgically assisted rapid maxillary expansion in adults. *The International Journal of Adult Orthodontics and Orthognathic Surgery*, *7*(1), Article 1.
- Poon, Y.-C., Chang, H.-P., Tseng, Y.-C., Chou, S.-T., Cheng, J.-H., Liu, P.-H., & Pan, C.-Y. (2015). Palatal bone thickness and associated factors in adult miniscrew placements: A cone-beam computed tomography study. *The Kaohsiung Journal of Medical Sciences*, *31*(5), 265–270. <https://doi.org/10.1016/j.kjms.2015.02.002>
- Prado, G. P. R., Furtado, F., Aloise, A. C., Biló, J. P. R., Masako Ferreira, L., & Pereira, M. D. (2014). Stability of surgically assisted rapid palatal expansion with and without retention analyzed by 3-dimensional imaging. *American Journal of Orthodontics and Dentofacial Orthopedics*, *145*(5), 610–616. <https://doi.org/10.1016/j.ajodo.2013.12.026>

- Proffit, W. R., Jr, H. W. F., & Sarver, D. M. (2006). *Contemporary Orthodontics*. Elsevier Health Sciences.
- Proffit, W. R., & White, R. P. (1990). Who needs surgical-orthodontic treatment? *The International Journal of Adult Orthodontics and Orthognathic Surgery*, 5(2), 81–89.
- Rakosi, T., Jonas, I., & Graber, T. M. (1993). *Orthodontic Diagnosis*. G. Thieme Verlag.
- Reyneke, J. P., & Conley, R. S. (2020a). Surgical/Orthodontic Correction of Transverse Maxillary Discrepancies. *Oral and Maxillofacial Surgery Clinics of North America*, 32(1), Article 1. <https://doi.org/10.1016/j.coms.2019.08.007>
- Reyneke, J. P., & Conley, R. S. (2020b). Surgical/Orthodontic Correction of Transverse Maxillary Discrepancies. *Oral and Maxillofacial Surgery Clinics of North America*, 32(1), 53–69. <https://doi.org/10.1016/j.coms.2019.08.007>
- Rice, D. P. C., Rice, R., & Thesleff, I. (2003). Molecular mechanisms in calvarial bone and suture development, and their relation to craniosynostosis. *European Journal of Orthodontics*, 25(2), 139–148. <https://doi.org/10.1093/ejo/25.2.139>
- Ricketts, R. M. (1981). Perspectives in the clinical application of cephalometrics. The first fifty years. *The Angle Orthodontist*, 51(2), 115–150. [https://doi.org/10.1043/0003-3219\(1981\)051<0115:PITCAO>2.0.CO;2](https://doi.org/10.1043/0003-3219(1981)051<0115:PITCAO>2.0.CO;2)
- Schimming, R., Feller, K. U., Herzmann, K., & Eckelt, U. (2000). Surgical and orthodontic rapid palatal expansion in adults using Glassman’s technique: Retrospective study. *The British Journal of Oral & Maxillofacial Surgery*, 38(1), 66–69. <https://doi.org/10.1054/bjom.1999.0274>
- Shayani, A., Sandoval Vidal, P., Garay Carrasco, I., & Merino Gerlach, M. (2022). Midpalatal Suture Maturation Method for the Assessment of Maturation before Maxillary Expansion: A Systematic Review. *Diagnostics*, 12(11), 2774. <https://doi.org/10.3390/diagnostics12112774>
- Shi, Y., Zhu, C.-N., & Xie, Z. (2020). Displacement and stress distribution of the maxilla under different surgical conditions in three typical models with bone-borne distraction: A three-dimensional finite element analysis. *Journal of Orofacial Orthopedics = Fortschritte Der Kieferorthopädie: Organ/Official Journal Deutsche Gesellschaft Fur Kieferorthopädie*, 81(6), 385–395. <https://doi.org/10.1007/s00056-020-00251-5>
- Starch-Jensen, T., & Blæhr, T. L. (2016). Transverse Expansion and Stability after Segmental Le Fort I Osteotomy versus Surgically Assisted Rapid Maxillary Expansion: A Systematic Review. *Journal of Oral & Maxillofacial Research*, 7(4), e1. <https://doi.org/10.5037/jomr.2016.7401>
- Suri, L., & Taneja, P. (2008). Surgically assisted rapid palatal expansion: A literature review. *American Journal of Orthodontics and Dentofacial Orthopedics*, 133(2), Article 2. <https://doi.org/10.1016/j.ajodo.2007.01.021>
- Susami, T., Kuroda, T., & Amagasa, T. (1996). Orthodontic treatment of a cleft palate patient with surgically assisted rapid maxillary expansion. *The Cleft Palate-Craniofacial Journal: Official Publication of the American Cleft Palate-Craniofacial Association*, 33(5), 445–449. https://doi.org/10.1597/1545-1569_1996_033_0445_otoacp_2.3.co_2

- Sygouros, A., Motro, M., Ugurlu, F., & Acar, A. (2014). Surgically assisted rapid maxillary expansion: Cone-beam computed tomography evaluation of different surgical techniques and their effects on the maxillary dentoskeletal complex. *American Journal of Orthodontics and Dentofacial Orthopedics*, *146*(6), 748–757. <https://doi.org/10.1016/j.ajodo.2014.08.013>
- Symons, A. L., Townsend, G. C., & Hughes, T. E. (2002). Dental characteristics of patients with Duchenne muscular dystrophy. *ASDC Journal of Dentistry for Children*, *69*(3), 277–283, 234.
- Timms, D. J., & Vero, D. (1981). The relationship of rapid maxillary expansion to surgery with special reference to midpalatal synostosis. *The British Journal of Oral Surgery*, *19*(3), 180–196. [https://doi.org/10.1016/0007-117x\(81\)90003-2](https://doi.org/10.1016/0007-117x(81)90003-2)
- Verstraaten, J., Kuijpers-Jagtman, A. M., Mommaerts, M. Y., Bergé, S. J., Nada, R. M., & Schols, J. G. J. H. (2010). A systematic review of the effects of bone-borne surgical assisted rapid maxillary expansion. *Journal of Cranio-Maxillofacial Surgery*, *38*(3), 166–174. <https://doi.org/10.1016/j.jcms.2009.06.006>
- Westling, L., & Mohlin, B. (1996). Palatal dimensions and some inherited factors (body height and metacarpal index). *Swedish Dental Journal*, *20*(4), 141–149.
- Zai, B. A., Khan, A. S., & Mehboob, H. (2015). *FINITE ELEMENT METHOD ANALYSIS OF A JAW STRUCTURE UPON SURGICALLY ASSISTED RAPID MAXILLARY EXPANSION WITH VARIOUS SURGICAL PROCEDURES*. *24*(02).
- Zawiślak, E., Olejnik, A., Frątczak, R., & Nowak, R. (2020). Impact of Osteotomy in Surgically Assisted Rapid Maxillary Expansion Using Tooth-Borne Appliance on the Formation of Stresses and Displacement Patterns in the Facial Skeleton—A Study Using Finite Element Analysis (FEA). *Applied Sciences*, *10*(22), Article 22. <https://doi.org/10.3390/app10228261>
- Zhu, J. F., Crevoisier, R., King, D. L., Henry, R., & Mills, C. M. (1996). Posterior crossbites in children. *Compendium of Continuing Education in Dentistry (Jamesburg, N.J.: 1995)*, *17*(11), 1051–1054, 1056, 1058.